VOLUME CHANGES OF ALASKA GLACIERS: CONTRIBUTIONS TO RISING SEA LEVEL AND LINKS TO CHANGING CLIMATE

A

THESIS

Presented to the Faculty

of the University of Alaska Fairbanks

in Partial Fulfillment of the Requirements

for the Degree of

DOCTOR OF PHILOSOPHY

By

Anthony A. Arendt, B.S., M.S.

Fairbanks, Alaska

May 2006

Abstract

We have used airborne altimetry to measure surface elevations along the central flowline of 86 glaciers in Alaska, Yukon Territory and northwestern British Columbia (northwestern North America). Comparison of these elevations with contours on maps derived from 1950s to 1970s aerial photography yields elevation and volume changes over a 30 to 45 year period. Approximately one-third of glaciers have been re-profiled 3 to 5 years after the earlier profile, providing a measure of short-timescale elevation and volume changes for comparison with the earlier period. We have used these measurements to estimate the total contribution of glaciers in northwestern North America to rising sea level, and to quantify the magnitude of climate changes in these regions. We found that glaciers in northwestern North America have contributed to about 10% of the rate of global sea level rise during the last half-century and that the rate of mass loss has approximately doubled during the past decade. During this time, summer and winter air temperatures at low elevation climate stations increased by 0.2 ± 0.1 and $0.4\pm0.2^{\circ}$C $(\text{decade})^{-1}$ respectively. There was also a weak trend of increasing precipitation and an overall lengthening of the summer melt season. We modeled regional changes in glacier mass balance with climate station data and were able to reproduce altimetry measurements to within reported errors. We conclude that summer temperature increases have been the main driver of the increased rates of glacier mass loss, but winter warming might also be affecting the glaciers through enhanced melt at low elevations and a change in precipitation from snow to rain, especially in maritime regions. Uncertainties in our calculations are large, owing to the inaccuracies of the maps used to provide baseline elevations, the sparsity of accurate climate data, and the complex and dynamic nature of glaciers in these regions. Tidewater, surging, and lake-terminating glaciers have dynamical cycles that are not linked in a simple way to climate variability. We found that regional volume losses can depend on one or several large and dynamic glaciers. These glaciers should be treated separately when extrapolating altimetry data to an entire region.

Table of Contents

List of Figures

List of Tables

List of Appendices

Acknowledgements

This work was supported by the NASA Cryospheric Sciences Program and Solid Earth and Natural Hazards Program, the NOAA Climate Change Detection and Attribution Project, the NASA Interdisciplinary Sciences Program, NSF Arctic Natural Sciences grants (NAG5-12914, NAG5-13760, NAGW-3727, NNG04GH64G, NA86GP0470, OPP-987-6421, OPP-032-7067) and a Center for Global Change student research grant.

I would like to thank my committee members for their guidance and support. Keith Echelmeyer, my supervisor, has been a mentor and friend. He not only taught me a great deal about glaciology, but also introduced me to the adventures of Alaska. I will always remember that a single brownie *can* sustain a person through a full day of grueling hiking in the Brooks Range. Will Harrison taught me to be a careful and meticulous scientist, and was always around to advise on anything from glacier timescales to car repairs. Martin Truffer provided valuable insights into my work, and never let me say no to another round of lab coffee. Craig Lingle, Roman Motyka and John Walsh each provided many ideas and feedback throughout my studies.

The success of the altimetry project is the result of many people's efforts. Keith Echelmeyer, Will Harrison, Jim Mitchell, Kevin Abnett, Dale Pomraning, Carl Bakken and Chris Larsen came up with the idea of small aircraft altimetry in the early 1990s and designed and tested the early system. Guðfinna Aðalgeirsdóttir, Bernhard Rabus, Joe Sapiano and Dan Elsberg were students who operated the system and interpreted and published early results. Wendy Seider, Laurence Sombardier, Patty Del Vecchio, Jennette DeMallie, By Valentine and Sandy Zirnheld were technicians who performed the often thankless job of reducing the mountains of data. By and Sandy deserve special thanks for taking the lead on fieldwork and data reduction. Craig Lingle took over field operations in 2003 and has been instrumental in expanding the project. This has included the development of an updated altimetry system spearheaded by Chris Larsen, who has also made significant contributions to the analysis of results. Paul Claus became our pilot a few years ago and his interest and enthusiasm for the project has gone beyond that of just another "hired hand". We are especially grateful for the opportunity to stay at his Ultima Thule lodge during some of our field operations, and we appreciate the comfortable accommodations provided by his family, Donna, Eleanor, and John Claus. Brent Ritchie, Matthew Drucken-

miller and Sandy Zirnheld collected the 2004-2005 altimetry data.

Two trips abroad gave me new insights and helped provide motivation in completing my degree. Thanks to Charlie Raymond, Al Rasmussen, Ed Waddington and the entire glaciology group at the University of Washington for the chance to share and develop ideas. Thanks to Judy and Keith Love who gave me a place to stay during my visit to Seattle. Regine Hock and the glaciology group at the University of Stockholm also gave me valuable feedback on my thesis. Special thanks to Regine for helping to organize a productive and enjoyable trip in Europe.

Friends made my time in Alaska truly memorable. Adam Bucki, Leif Cox, Andy Mahoney and Alain Burgisser have been my close companions as we discovered the mountains of Alaska. Leif and Adam taught me that a former vegetarian from the big city could learn to hunt and fish. Andy has been my "best mate" from the start. Lars, Sharon, and the entire crew at Belfair always had a warm place to share time with friends on a cold winter day. We only wish that Karoline could be there to join us. I am thankful for warm conversations with Amanda and Sebastien, European adventures with Tina and Alain, fondue dinners at Martin and Dana's, Mt. Wrangell fieldwork with Tinu, Swiss-chocolate-sampling with Elsbeth, Sunday saunas with Inari, Jason and Tanja, afternoon skiing with Ellie and hunting trips with Pat. Special thanks to Leslie for sharing many adventures with me, and for helping me when times were tough.

Finally I thank my family for their continued support. Mum and Dad in Edmonton, Nicole and Chris on Vancouver Island, and Chris in New Jersey always had a room ready (complete with running water) whenever I needed to get away from cabin life and the darkness of the Alaska winter.

Chapter 1
Introduction

Alaska and northwestern Canada are covered by nearly 90,000 km^2 of glacier ice. It has long been suspected that these glaciers play an important role in Earth's hydrological cycle because they are sensitive to climate and can make potentially large contributions to rising sea level [*Meier*, 1984]. Until recently, it has not been possible to measure the changes of these glaciers because of their remoteness. Early estimates of the contribution of these glaciers to rising sea level had to rely on a small handful of glacier routinely monitored using conventional mass balance methods [*Rabus et al.*, 1995; *March*, 2003].

In 1992 a team of scientists led by Keith Echelmeyer at the University of Alaska, Fairbanks Geophysical Institute developed a small, inexpensive system for measuring the volume changes of glaciers. They interfaced a rangefinder with a gyroscope, compass, Global Positioning System (GPS) and computer, and installed the equipment in the back of a small aircraft. Elevations were measured on nearly 100 glaciers between 1993 and 1998, for comparison with elevations determined from contours on US Geological Survey maps from the 1950s [*Echelmeyer et al.*, 1996]. Differencing these elevations and extrapolating them to the entire glacier, they obtained a measure of the glacier volume change. Repeat measurements were obtained on about one third of these glacier beginning in 1998. Investigations were carried out on subsets of glaciers on the Kenai Penninsula [*Aðalgeirsdóttir et al.*, 1998], Brooks Range [*Rabus and Echelmeyer*, 1998] and the nine glaciers measured during the International Geophysical Year [*Sapiano et al.*, 1998].

In 2000 we began compiling the extensive dataset of glacier volume changes in order to assess the total contribution of Alaska glaciers to rising sea level. We divided Alaska into seven regions based on mountain ranges, and developed a method for extrapolating the glacier measurements to other unmeasured glaciers. This method involved taking averages of glacier thickness changes across elevations, accounting for the variability in glacier changes and surface area with elevation. We arrived at two estimates for the contribution of these glaciers to rising sea level, one for the period during the 1950s to early 1990s, based on 67 glaciers, and one for the more recent period of mid-1990s to 2000/2001, based on 28 glaciers. We observed more rapid rates of mass loss than estimated in previous studies. These results were published in Science [*Arendt et al.*, 2002] which is reproduced here as

Chapter 2.

After obtaining a broad picture of the patterns of glacier change in Alaska, we were left with two important, unsolved problems. The first was to improve upon our methods for extrapolating to unmeasured glaciers, and the second was to understand the measured changes in terms of climatic variations. Concerning the extrapolation problem, ours was the first study to take measurements of elevation changes and assume these represent changes at the same elevation on adjacent, unmeasured glaciers. Such an assumption is theoretically flawed, because thickness changes occur both due to surface mass exchanges driven by climate and due to the flow of the glacier through time. It is probably reasonable to assume that patterns in the climate (for example, the magnitude of summer air temperatures) can be extrapolated over regions. The glacier flow, however, is driven by the unique geometry of each glacier, such as its surface slope and ice thickness. We investigated this problem for glaciers of the Western Chugach Mountains. We chose this region because in 2004, we obtained measurements of 21 glaciers in this area providing us with the best spatial resolution of any region previously sampled. We had measurements of large and small glaciers, and those terminating in the ocean, lakes or on land. This variety of glaciers helped remove biases present in other glacier mass balance datasets. With the large sample size we were able to use simple statistical methods to compare extrapolation techniques. The results of this study are given in Chapter 3 [*Arendt et al.*, in press], which is in press in the Journal of Geophysical Research.

The second issue concerning the altimetry measurements was to determine the extent to which they could be related to climate changes in northwestern North America. Glacier thinning and retreat is commonly identified as a signal of global climate change. While it is true that in nearly all cases glacier mass loss is triggered by some kind of change in climate, there are many complexities regarding the timing of that change, its magnitude and type (eg: changes in temperature, solar radiation, or solid precipitation), and the role of glacier dynamics in determining the glacier response to that change. In northwestern North America there are many tidewater, lake terminating and surge-type glaciers which complicate any comparison of their changes to climate. Furthermore, there is a paucity of climate data in these areas; those stations with long-term records are generally located at low elevations near human settlements, generally far away from mountainous regions.

Despite these issues, we used as much information as we could obtain to build a climatic database for comparison with our altimetry measurements. We assembled surface temperature and precipitation data and upper air reanalysis model output of temperature and geopotential heights. We then used simple mass balance models to simulate changes in glacier balance. Modeled balances were compared with measured balances on a regional basis to determine how well the climate measurements represented the glacier changes. The findings of this work are in Chapter 4, which is in preparation for submission to the Journal of Applied Meteorology.

Chapter 5 summarizes our key findings and places them in the context of recent glacier changes measured in other regions on Earth. Appendicies A, B and C contain detailed information on the error budgets determined for the papers in Chapters 2, 3 and 4 respectively. Each Appendix has appeared or been submitted as supplemental online information to accompany the publications.

Bibliography

Aðalgeirsdóttir, G., K. Echelmeyer, and W. Harrison (1998), Elevation and volume changes on the Harding Icefield, Alaska, *Journal of Glaciology*, *44*(148), 570–582.

Arendt, A. A., K. A. Echelmeyer, W. D. Harrison, C. S. Lingle, and V. B. Valentine (2002), Rapid wastage of Alaska glaciers and their contribution to rising sea level, *Science*, *297*, 382–386.

Arendt, A., K. Echelmeyer, W. Harrison, C. Lingle, S. Zirnheld, V. Valentine, B. Ritchie, M. Druckenmiller (in press), Updated estimates of glacier volume changes in the Western Chugach Mountains, Alaska, USA and a comparison of regional extrapolation methods, *Journal of Geophysical Research*.

Echelmeyer, K., W. Harrison, C. Larsen, J. Sapiano, J. Mitchell, J. DeMallie, B. Rabus, G. Aðalgeirsdóttir, and L. Sombardier (1996), Airborne surface profiling of glaciers: A case-study in Alaska, *Journal of Glaciology*, *42*(142), 538–547.

March, R. (2003), Mass balance, meteorology, area altitude distribution, glacier-surface altitude, ice motion, terminus position, and runoff at Gulkana Glacier, Alaska, 1996 balance year, *Tech. rep.*, USGS.

Meier, M. (1984), Contribution of small glaciers to global sea level, *Science*, *226*(4681), 1418–1421.

Rabus, B., and K. Echelmeyer (1998), The mass balance of McCall Glacier, Brooks Range, Alaska, U.S.A.; its regional revelance and implications for climate change in the Arctic, *Journal of Glaciology*, *44*(147), 333–351.

Rabus, B., K. Echelmeyer, D. Trabant, and C. Benson (1995), Recent changes of McCall glacier, alaska, *Annals of Glaciology*, *21*, 231–239.

Sapiano, J., W. Harrison, and K. Echelmeyer (1998), Elevation, volume and terminus changes of nine glaciers in North America, *Journal of Glaciology*, *44*(146), 119–135.

Chapter 2

Rapid Wastage of Alaska Glaciers and their Contribution to Rising Sea Level[1]

2.1 Abstract

We have used airborne laser altimetry to estimate volume changes of 67 glaciers in Alaska from the mid-1950s to the mid-1990s. The average rate of thickness change of these glaciers was -0.52 m/year. Extrapolation to all glaciers in Alaska yields an estimated total annual volume change of -52$\pm$15 km^3/year (water equivalent), equivalent to a rise in sea level (SLE) of 0.14$\pm$0.04 mm/year. Repeat measurements of 28 glaciers from the mid-1990s to 2000-2001 suggest an increased average rate of thinning, -1.8 m/year. This leads to an extrapolated annual volume loss from Alaska glaciers equal to -96$\pm$35 km^3/year, or 0.27$\pm$0.10 mm/year SLE, during the last decade. These recent losses are nearly double the estimated annual loss from the entire Greenland Ice Sheet during the same time period, and are much higher than previously published loss estimates for Alaska glaciers. They form the largest glaciological contribution to rising sea level yet measured.

2.2 Introduction

Mountain glaciers (glaciers other than those of Greenland and Antarctica) comprise only about 3% of the glacierized area on Earth, but are important because they may be melting rapidly under present climatic conditions and may therefore make large contributions to rising sea level. Previous studies estimate the contribution of all mountain glaciers to rising sea level during the last century to be 0.2 to 0.4 mm/year, based on observations and model simulations of glacier mass balance [1, 2, 3, 4, 5, 6]. The range of uncertainty is large, and it stems from insufficient measurements of glacier mass balance: conventional mass balance programs are too costly and difficult to sample adequately the >160 000 glaciers on Earth. At present, there are only about 40 glaciers worldwide with continuous balance measurements spanning more than 20 years [7]. High latitude glaciers, which are particularly important because predicted climate warming may be greatest there [6], receive even less attention due to their remote locations. Glaciers that are monitored routinely are often chosen more for their ease of access and manageable size than for how well they rep-

[1]Published as Arendt, A.A. and Echelmeyer, K.A. and Harrison, W.D. and Lingle, C.S. and Valentine, V.B. (2002) Rapid Wastage of Alaska Glaciers and their Contribution to Rising Sea Level. Science 297, 382-386.

resent a given region, or how large a contribution they might make to changing sea level. As a result, global mass balance data are biased toward small glaciers (<20 km^2) rather than those that contain the most ice (>100 km^2). Also, large cumulative errors can result from using only a few point measurements to estimate glacier-wide mass balances on an individual glacier.

Glaciers in Alaska and neighboring Canada (labelled "Alaska" glaciers herein) cover 90 000 km^2 [8], or about 13% of the mountain glacier area on Earth [9], and include some of the largest ice masses outside of Greenland and Antarctica. Additionally, many of these glaciers have high rates of mass turnover. However, they are under-represented by conventional mass balance studies, which include only three to four long-term programs on relatively small glaciers. Dyurgerov and Meier [4], by necessity, extrapolated the data from these few small glaciers to estimate the contribution of all Alaska glaciers to sea-level change, and they specifically pointed to the need for further data in this region, especially on the larger glaciers. In the present study we use airborne laser altimetry to address this problem. We have measured volume and area changes on 67 glaciers, representing about 20% of the glacierized area in Alaska and neighboring Canada, and we use these data to develop new estimates of the total contribution of Alaska glaciers to rising sea level.

2.3 Data and Methods

Our altimetry system consists of a nadir-pointing laser rangefinder mounted in a small aircraft and a gyro to measure the orientation of the ranger, and uses kinematic global positioning system (GPS) methods for continuous measurement of aircraft position [10]. Profiles are flown along centerlines of the main trunk and major tributaries of a particular glacier at altitudes of 50 to 300 m above the surface; in some cases, more than one profile is flown to determine cross-glacier variations in elevation change. These profiles are compared to contours on 15-minute U.S. Geological Survey (USGS) and Canadian Department of Energy, Mines and Resources topographic maps made from aerial photographs acquired in the 1950s to early 1970s (depending on location). Differences in elevation are calculated at profile/contour line intersection points. If more than one profile is flown along a given glacier, averages are taken at each elevation and applied to the appropriate areas. Digital elevation models (DEMs) derived from the 15-minute maps are used to

determine the area-altitude distribution of each glacier at the time of mapping. We calculate volume changes by assuming that our measured elevation changes apply over the entire area within the corresponding elevation band. These changes are then integrated over the original area-altitude distribution of the glacier. When converting to water equivalent volume changes, we assume all measured changes in elevation are due to losses of ice (density = 900 kg/m^3) and make no seasonal corrections for snow cover. Glacier-wide average thickness changes are found by dividing the total volume change by the average of the old and new glacier areas. We define the area of a glacier as its ice extent within its hydrologic basin, except for the very large Bering/Bagley (BER) and Malaspina/Seward (MAL) glaciers, where we limit the volume change calculations to the measured elevation ranges (about 1500 m and 2300 m, respectively; see Fig. S2). Changes in glacier length (and area) are determined by comparing the mapped terminus with that determined from our measurements. We have estimated volume and area changes during the period ca. 1950s to 1993-96 (the "early period") for the 67 glaciers, which we have categorized into seven geographic regions (Figure 2.1). Our sample includes 12 tidewater, 5 lake-terminating and 50 land-terminating glaciers (Table 2.1). Three of the land-terminating glaciers historically exhibited surge behavior. Since 1999, we have re-profiled 28 glaciers that were first profiled during 1993-96, covering about 13% of the glacierized area in Alaska. Re-profiling involves flying the aircraft along the path of an earlier profile, repeatable to within a transverse distance of $\pm$15-25 m, using differential GPS navigation. We try repeat the profiles at the same time in the season as they were originally flown (usually within the same week). Comparisons are then made at the crossing points between the old and the new profiles, providing measurements of glacier change during the intervening five to seven years (the "recent period"). Crossing points between the old and new profiles are determined in three steps: (1) a single elevation measurement (Z_1) on the old profile is selected; (2) elevation measurements from the new profile which fall within a 20-60 by 3 m (transverse by longitudinal) rectangular window centered on this old profile data point are designated as crossing points, and are averaged to a single new elevation (Z_2); (3) the elevation change is calculated as $Z_2 - Z_1$. Steps 1-3 are repeated for all elevation measurements on the old profile. Typically we find $1 - 2 \times 10^4$ crossing points distributed over the elevation of a glacier. This method assumes that transverse variations in elevation change are small within the

averaging window.

Some of the sources of error in our results have been discussed previously [10, 11, 12, 13]. For early period comparisons, the primary errors are those in the topographic maps. These errors can be large, especially in accumulation areas where photogrammetric contrast is poor, or in locations with poor geodetic control. Errors in the recent period measurements are dominated by errors in the areal-extrapolation of one or a few altimetry profiles across an entire glacier surface. Altimetry system errors, which depend on the orientation of the aircraft relative to the glacier surface, are generally small. We have quantified the random component of map, areal-extrapolation and altimetry system errors for each glacier in our sample (Table 2.1). Systematic offsets may substantially increase these errors in some cases, but they are difficult to quantify for each glacier. Substantial early period measurement errors may also occur because we do not always know the precise dates at which the aerial photographs, used to create the maps, were acquired, and we have not always included corrections for seasonal effects due to flying at different times of the year. A detailed description of our error analysis is in Appendix A.

2.4 Results and Discussion

Most glaciers in our sample thinned over most of their lengths during both the early and recent periods (Figure 2.2), while fewer than 5% thickened. Some thinned dramatically, in particular rapidly retreating tidewater glaciers such as Columbia Glacier (COL), which, near the terminus, thinned 300 m during the early period and 150 m during the last five years. Note that lower Columbia Glacier actually thinned significantly more than shown in Fig. 2B because ice was removed from below sea level, but we do not show these changes because they do not contribute to sea level change. Tazlina (TAZ) and Turquoise (TUR) glaciers are more representative of typical valley glaciers; these thinned at the terminus by 100 to 150 m during the early period, and about 20 m during the ca. 1995 to 2001 period.

These thickness changes translate to volume changes by integration over the area-altitude distribution, which describes the total glacier area in each elevation bin (typical area-altitude distributions are shown in Figure 2.3). The glacier-wide average rate of thickness change (Table 1.1) is the volume change divided by the area, and is directly comparable with annual mass balance measurements from conventional measurement programs

(here we use ice equivalent units instead of the conventional water equivalent units, since we have directly measured changes in ice thickness). We found that most glaciers during the early and recent periods had negative thickness changes, indicating overall surface lowering (Figure 2.4). Comparing only those glaciers with both early and recent period measurements shows that, during the past five to seven years, glacier thinning was almost three times as fast (-1.8 m/year) as that measured on the same glaciers from the mid-1950s to the mid-1990s (-0.7 m/year). This increase in average thinning rate exceeds our error limits, and is significantly larger than typical variations in five year averages of long-term mass balance records of Alaska glaciers. Some conventional mass balance studies have also shown a similar trend toward more negative balances over the last decade [14].

To estimate the contribution of Alaska glaciers to rising sea level, we extrapolated our measured thickness changes within each region to all unmeasured glaciers in that region. Extrapolations were made using a single thickness change profile for a region (solid black curves in Figure 2.3), calculated by averaging the thickness changes of all measured glaciers at each elevation band within that region. The total extrapolated volume change was found by integrating the average measured thickness changes over the area-altitude distribution of all unmeasured glaciers in that region (solid blue curves in Fig. S1). Both the early and recent period total volume change estimates are an average of two values, one obtained from area-weighted average thickness changes, and one which does not include a correction for area. This extrapolated value was then added to the measured changes to give a total volume change in each region. Columbia, LeConte (LEC), Hubbard (HUB) and Taku (TAK) glaciers were considered as separate "regions" because they have recently been subject to tidewater glacier dynamics, characterized by large instabilities. An estimate of the error in this extrapolation was obtained by considering the total of the errors for each measured glacier (Table 2.1), the scatter of the measured changes within each elevation band in a given region (gray bars in Figure 2.3), and the differences between two methods of performing the extrapolation, one which weights the average thickness changes by area, and one which does not. We have included these possible extrapolation errors, along with those determined for the measured glaciers, and an estimate of systematic errors, in our final error analysis (supporting online text).

We estimated the total annual volume change of Alaska glaciers for the early and recent

periods to be -52±15 km^3/year and -96±35 km^3/year water equivalent, equivalent to a rise in sea level (SLE) of 0.14±0.04 and 0.27±0.10 mm/year, respectively. Glaciers bordering the Gulf of Alaska in the Chugach and St. Elias Mountains and Coast Ranges made the largest contribution of all Alaska glaciers. These glaciers are large and they have very high rates of mass turnover due to their maritime environment. It is interesting to note that about 75% of the total measured volume changes over both periods is accounted for by a few large and dynamic glaciers (such as Columbia, Malaspina, Bering, LeConte, and Kaskawulsh Glaciers). Note that although the measured glaciers had a rate of thickness change during the recent period that was nearly three times the rate measured during the early period, the increase in the rate of loss is smaller when we extrapolate to all glaciers because of the regional area-altitude extrapolation methods used. Also, the uncertainty in the recent period extrapolation is larger than for the early period because there are fewer measured glaciers during the recent period.

Our estimates of the contribution from Alaska glaciers to rising sea level (0.14±0.04 mm/year) are seven times larger than the 0.02 mm/year estimated by Dyurgerov and Meier [4] for the period from 1961 to 1990. This is not surprising because these authors used only data from Wolverine Glacier to represent the glaciers bordering the Gulf of Alaska; Dyurgerov and Meier suspected that their estimates for the Alaska contribution to rising sea level were too small because of the lack of data on larger glaciers.. The USGS mass balance program reported an average thickness change of -0.18 m/year (ice equivalent) for Wolverine Glacier, but most of the Gulf of Alaska glaciers which we measured had thinning rates that were much larger than this. Also, Dyurgerov and Meier used a slightly smaller value (75 000 km^2) for the total area of glacier ice in Alaska.

Our ca. 1995 to 2001 estimated annual volume loss is nearly twice that estimated for the entire Greenland Ice Sheet during the same period (-51 km^3/year or 0.14 mm/year SLE [15]). Our results indicate that Alaska glaciers contributed about 9% of the observed rate of sea-level rise (1.5±0.5 mm/year [6]) over the last fifty years and about 8% or more of the increased rate of sea level rise (possibly as large as 3.2 mm/year [16]) over the last decade or so.

Most (but not all) glaciers in our sample retreated. Over the early period there was a 0.8% (131 km^2) decrease in the total area of the measured glaciers, and a 0.4% decrease

during the last five to seven years (Table 2.1). It is sometimes assumed that such changes in glacier length and area can be used to infer changes in glacier mass balance and response to climate, with retreat indicating an overall loss in glacier volume. However, we have found that during both the early and recent periods, about 10% of the sampled glaciers either advanced while simultaneously thinning, or retreated while thickening during the early period (Table 2.1). Even for those glaciers with the more "normal" response of retreat while thinning, we found a very low correlation between the rate of length change and the rate of thickness change. This indicates that flow dynamics must be taken into consideration when examining changes in glacier length (and area) at time scales of $\sim$10 to 40 years. In the approximation that glacier response to a change in climate can be characterized by a single time constant [17, 18], our results suggest that the response times of most glaciers in our sample are greater than $\sim$40 years. Caution is evidently required when making inferences about mass balance from changes in glacier length (or area) alone.

The large standard deviation of the average rates of thickness change within some regions (Figure 2.3) indicates that a number of factors must control glacier mass balance, including local climate and glacier geometry. Our geographical classification of glacier regions does not consider regional climatic zones. For instance, we examined recent period changes of a subset of five glaciers in the southern Alaska Range. These glaciers are located within a radius of 30 km, and if they were to experience similar climate conditions, then their mean thickness changes would be dictated by their area-altitude distributions alone, at least over time periods which are short relative to mass redistribution by flow. For these glaciers, the average thickness change showed no significant correlation with the area-weighted mean elevation. This suggests that climate variability occurs on a small spatial scale, such as with distance from the coast. In contrast, Rabus and Echelmeyer [13] found that, in a similar-sized region, elevation changes on one glacier in the Brooks Range (McCall Glacier) were representative of other glaciers.

Our observations of rapid glacier wastage during the early period, with increased rates of thinning during the recent period, may be linked to climate warming during the past several decades [6], but other factors are involved. The large rates of thinning we observed for some tidewater glaciers are due to their unstable dynamics of rapid retreat and slow advance, and are not simply linked to climate warming, although retreat is likely

initiated by negative mass balance. Periodic thickness changes characteristic of surge-type glaciers are also not simply linked to climate warming. For example, there was a large downglacier ice flux during the 1993-95 surge of Bering Glacier, leading to a thickening on the eastern segment of the piedmont lobe, but overall the glacier thinned from 1972 to 1995. A few glaciers in our sample thickened, and in most cases these were located near other glaciers that thinned; almost all of these anomalous glaciers are tidewater or paleo-tidewater (eg: Hubbard and Taku Glaciers), and are probably in a stage of advance associated with unstable tidewater glacier dynamics. Nevertheless, nearly all of the measured glaciers experienced increased thinning rates during ca. 1995 to 2001 relative to the ca. 1950 to 1995 period. This is consistent with the results of conventional mass balance studies on Gulkana and Wolverine [19], McCall [13], Taku [20], and Lemon Creek [21] Glaciers, which show increased negative balances during the last decade.

Compared with the estimated inputs from the Greenland Ice Sheet [15] and other sources [1, 6], Alaska glaciers have, over the past 50 years, made the largest single glaciological contribution to rising sea level yet measured. We suggest that other glacierized regions, with the possible exceptions of West Antarctica and Patagonia, may lack sufficient ice mass and/or mass turnover to produce sea level contributions of equivalent magnitude during these time periods. Mountain glaciers may be contributing a substantial fraction of the increased rate of sea-level rise suggested by satellite observations during 1993 to 1998 [16]. And while we note that the large glaciers bordering the Gulf of Alaska are the most important in determining the sea level contribution, the different rates of thinning observed in the various Alaska regions may be important in characterizing patterns of climate change.

Bibliography

1. M. Meier, *Science* **226**, 1418 (1984).

2. M. F. Meier, *Ice, climate and sea level; do we know what is happening?* (Springer-Verlag, 1993), pp. 141–160.

3. Z. Zuo, J. Oerlemans, *Climate Dynamics* **13**, 835 (1997).

4. M. Dyurgerov, M. Meier, *Arctic and Alpine Research* **29**, 392 (1997).

5. J. Gregory, J. Oerlemans, *Nature* **391**, 474 (1998).

6. J. Houghton, *et al.*, *Projections of Future Climate Change*, Climate change 2001; the scientific basis (Cambridge University Press, 2001), pp. 525–582.

7. M. Dyurgerov, M. Meier, *Arctic and Alpine Research* **29**, 379 (1997).

8. Alaska Department of Natural Resources, Land Records Information Section, *Glaciers, 1:2,000,000. 1990* (www.asgdc.state.ak.us/metadata/vector/physical/glacier/glcr2mil.html).

9. W. Haeberli, H. Bösch, K. Scherler, G. strem, C. Wallén, *World Glacier Inventory* (IAHS(ICSI)-UNEP-UNESCO, 1989).

10. K. Echelmeyer, *et al.*, *Journal of Glaciology* **42**, 538 (1996).

11. J. Sapiano, W. Harrison, K. Echelmeyer, *Journal of Glaciology* **44**, 119 (1998).

12. G. Aðalgeirsdóttir, K. Echelmeyer, W. Harrison, *Journal of Glaciology* **44**, 570 (1998).

13. B. Rabus, K. Echelmeyer, *Journal of Glaciology* **44**, 333 (1998).

14. M. Dyurgerov, M. Meier, *Proceedings of the National Academy of Sciences of the United States of America* **97**, 1406 (2000).

15. W. Krabill, *et al.*, *Science* **289**, 428 (2000).

16. C. Cabanes, A. Cazenave, C. Le Provost, *Science* **294**, 840 (2001).

17. T. Jóhannesson, C. Raymond, E. Waddington, *Journal of Glaciology* **35**, 355 (1989).

18. W. Harrison, D. Elsberg, K. Echelmeyer, R. Krimmel, *Journal of Glaciology* **47**, 659 (2001).

19. S. M. Hodge, *et al.*, *Journal of Climate* **11**, 2161 (1998).

20. M. S. Pelto, M. M. Miller, *Northwest Science* **64** (1990).

21. M. M. Miller, M. S. Pelto, *Geografiska Annaler* **81A**, 671 (1999).

Table 2.1: Table of profiled glaciers, their characteristics and measured changes. "Symbol" associates the glacier name with the three-letter codes on Fig. 1. The regions are: 1 = Alaska Range; 2 = Brooks Range; 3 = Coast Range; 4 = Kenai Mountains; 5 = St. Elias Mountains (includes Eastern Chugach Range); 6 = Western Chugach Range; 7 = Wrangell Mountains. "Type" includes: TW = tidewater glacier; L = land terminating glacier; LK = lake terminating glacier; SGT = surge-type glacier; two listed types for a glacier indicate a change in type during the measurement period. Water equivalent rates of glacier volume change ($\dot{V}$) and ice equivalent rates of glacier-wide average thickness change ($\dot{z}$) are negative when the glacier is losing mass. ($\dot{L}$) is the average rate of terminus advance (positive) or retreat (negative). For tidewater glaciers we have included only volume changes above sea level, as these form the only contributions to the ocean volume.

Glacier Name	Symbol	Latitude (degrees)	Longitude (degrees)	Region	Type	Area (km^2)	$\dot{V}$ (10^6 m^3/yr; water eq.) Early	Recent
Aialik	AIA	59.95	-149.73	4	TW	118	0.7 ± 32.8	.
Arey	ARY	69.23	-143.80	2	L	5	-2.4 ± 1.5	.
Baird	BAI	57.18	-132.52	3	L	523	-151.4 ± 63.2	-418.1 ± 30.2
Bear	BEA	59.93	-149.53	4	TW/LK	229	-154.3 ± 61.3	.
Bear Lake	BLK	60.18	-149.25	4	L	7	-1.7 ± 0.7	-6 ± 0.4
Bench	BEN	61.03	-145.68	6	L	9	-12.5 ± 0.8	.
Bering	BER	60.30	-143.42	5	L(SGT)	2190	-1520.2 ± 376.4	-5974.6 ± 1082.3
Black Rapids	BLR	63.49	-146.42	1	L(SGT)	289	90.2 ± 37.7	-187.3 ± 11
Brady	BRA	58.58	-136.78	5	TW	605	-214.3 ± 51.8	-543.2 ± 24
Bravo	BRV	69.27	-143.80	2	L	2	-0.4 ± 0.4	.
Chernof	CHE	59.83	-150.35	4	L	95	-26.3 ± 12.2	.
Chikiminuk	CHI	60.12	-159.28	1	L	6	0.2 ± 0.9	1.4 ± 0.9
Columbia	COL	61.30	-146.88	6	TW	1090	-1397.4 ± 95.9	-7091.2 ± 30.5
Deserted	DES	61.00	-145.60	6	L	37	-27.2 ± 3	.
Dinglestadt	DIN	59.70	-150.42	4	L	79	-50.4 ± 10.1	.
Double	DOU	60.67	-152.67	1	L	232	-155.6 ± 31.5	4.9 ± 9.5
East Fork Susitna	SEF	63.42	-146.83	1	L	44	-12.8 ± 2.5	-25.3 ± 1.9
East Okpilak	OKE	69.17	-143.98	2	L	9	-3 ± 2.6	.
Esetuk	ESE	69.30	-144.32	2	L	7	-2.3 ± 1.3	.
Exit	EXI	60.20	-149.50	4	L	43	-2.4 ± 11.2	.
Gillam	GIL	63.70	-147.12	1	L	131	-28.3 ± 11.3	-82.2 ± 5.3
Glacier Fork Tlikakila	GFT	60.85	-153.48	1	L	119	-51.5 ± 12.6	.
Gooseneck	GOS	69.30	-143.70	2	L	1	-0.3 ± 0.2	.
Gulkana	GUL	63.24	-145.47	1	L	20	-7.8 ± 2.9	-13 ± 0.8
Hanging	HAN	59.85	-138.90	2	L	1	0 ± 0.2	.
Holgate	HOL	59.85	-149.87	4	TW	64	-14.5 ± 8.8	.
Hubbard	HUB	60.32	-139.37	5	TW	2460	244.4 ± 316.9	.
Kachemak	KAC	59.53	-150.50	4	L	55	-17.8 ± 9.7	.
Kahiltna	KAH	62.77	-151.30	1	L	507	-212.6 ± 42.7	.
Kaskawulsh	KAS	60.70	-139.25	5	L	854	-1203.6 ± 102.5	-388.9 ± 27.1
Lamplugh	LAM	58.83	-136.89	5	TW	142	46.9 ± 13.2	-25 ± 5.9
LeConte	LEC	56.83	-132.38	3	TW	454	-212 ± 52.4	-999 ± 28.2
Lemon Creek	LEM	58.36	-134.36	3	L	14	-9 ± 1.8	-18.2 ± 1.2
Little Dinglestadt	LDG	59.70	-150.38	4	TW/L	32	-5.6 ± 4.3	.
Little Jarvis	JAR	59.42	-136.42	5	L	3	0 ± 0.3	.

Table 2.1: Continued

Glacier Name	$\dot{z}$ (m/yr; ice eq.)		$\dot{L}$ (m/yr)		Map	Profile 1	Profile 2	Number Yrs.	
	Early	Recent	Early	Recent	Year	Date	Date	Early	Recent
Aialik	0.01 ± 0.3	.	12	.	1950	5/29/94	.	44	.
Arey	-0.58 ± 0.33	.	-28	.	1973	1/1/93	.	20	.
Baird	-0.32 ± 0.13	-0.86 ± 0.06	6	.	1948	6/14/96	6/1/99	48	3
Bear	-0.76 ± 0.29	.	-35	.	1950	5/28/94	.	44	.
Bear Lake	-0.28 ± 0.11	-0.95 ± 0.07	-10	.	1950	5/28/94	5/13/99	44	5
Bench	-1.68 ± 0.11	.	-16	.	1950	8/25/00	.	50	.
Bering	-0.77 ± 0.11	-3.1 ± 0.04	.	.	1972	6/10/95	8/26/00	23	5
Black Rapids	0.34 ± 0.14	-0.66 ± 0.04	-3	.	1954	5/18/95	1/1/00	41	5
Brady	-0.39 ± 0.09	-0.97 ± 0.04	11	.	1948	6/4/95	5/24/00	47	5
Bravo	-0.29 ± 0.2	.	-8	.	1956	1/1/95	.	39	.
Chernof	-0.3 ± 0.14	.	-16	.	1950	5/20/96	.	46	.
Chikiminuk	0.04 ± 0.17	0.28 ± 0.17	.	.	1957	5/12/96	5/13/01	39	5
Columbia	-1.44 ± 0.1	-7.42 ± 0.03	-142	-796	1950	5/31/94	5/10/99	44	5
Deserted	-0.82 ± 0.09	.	-3	.	1950	8/25/00	.	50	.
Dinglestadt	-0.72 ± 0.13	.	-50	.	1950	5/19/96	.	46	.
Double	-0.74 ± 0.15	0.02 ± 0.04	-24	.	1957	5/16/96	5/14/01	39	5
East Fork Susitna	-0.32 ± 0.06	-0.64 ± 0.05	-12	132	1950	5/19/95	6/1/00	45	5
East Okpilak	-0.37 ± 0.32	.	-51	.	1973	1/1/93	.	20	.
Esetuk	-0.35 ± 0.2	.	-22	.	1956	1/1/93	.	37	.
Exit	-0.06 ± 0.29	.	-11	.	1950	5/29/95	.	45	.
Gillam	-0.24 ± 0.1	-0.7 ± 0.04	-45	.	1951	4/25/96	4/28/00	45	4
Glacier Fork Tlikakila	-0.47 ± 0.12	.	-13	.	1957	5/14/01	.	44	.
Gooseneck	-0.33 ± 0.21	.	0	.	1956	1/1/95	.	39	.
Gulkana	-0.45 ± 0.16	-0.79 ± 0.04	-22	.	1954	5/17/95	6/9/00	41	5
Hanging	-0.01 ± 0.22	.	-7	.	1956	1/1/94	.	38	.
Holgate	-0.25 ± 0.15	.	-6	.	1950	5/23/95	.	45	.
Hubbard	0.11 ± 0.14	.	41	.	1959	5/2/00	.	41	.
Kachemak	-0.36 ± 0.19	.	-20	.	1952	5/19/96	.	44	.
Kahiltna	-0.46 ± 0.11	.	.	.	1951	7/31/94	.	43	.
Kaskawulsh	-1.58 ± 0.13	-0.51 ± 0.03	-107	.	1977	5/21/95	5/29/00	18	5
Lamplugh	0.36 ± 0.1	-0.19 ± 0.05	7	.	1948	6/4/95	5/24/00	47	5
LeConte	-0.52 ± 0.13	-2.37 ± 0.07	-27	-202	1948	6/15/96	5/31/99	48	3
Lemon Creek	-0.71 ± 0.14	-1.47 ± 0.09	-15	.	1948	5/31/95	6/4/99	47	4
Little Dinglestadt	-0.2 ± 0.15	.	-8	.	1952	5/19/96	.	44	.
Little Jarvis	0 ± 0.19	.	.	.	1956	6/1/94	.	38	.

Table 2.1: Continued

Glacier Name	Symbol	Latitude (degrees)	Longitude (degrees)	Region	Type	Area (km^2)	$\dot{V}$ (10^6 m^3/yr; water eq.) Early	Recent
Malaspina	MAL	59.71	-140.63	5	L(SGT)	3190	-2665.5 ± 634.5	-2787.7 ± 122
Mccall	MCC	69.33	-143.82	2	L	6	-1.6 ± 1.3	.
Mccarty	MCY	59.78	-150.22	4	TW	109	-13.7 ± 14.9	.
Mendenhall	MEN	58.50	-134.53	3	TW	114	-96.7 ± 10.8	-144.6 ± 5.2
Nabesna	NAB	61.93	-143.08	7	L	1040	-160.4 ± 64.2	.
Northeastern	NEA	60.00	-149.98	4	TW/L	15	-27.7 ± 1.7	.
Northwestern	NWN	59.85	-150.05	4	TW	66	-7.7 ± 12.2	.
North Fork Tlikakila	NFT	60.77	-153.48	1	L	41	-34.5 ± 2.7	.
North Hubley	NHU	69.28	-143.70	2	L	2	-1 ± 0.3	.
Polychrome	POL	63.46	-149.85	1	L	2	-0.4 ± 0.3	.
Reid	REI	58.79	-136.79	5	TW	60	21.8 ± 5.6	-10.9 ± 3.6
Scott	SCO	60.68	-145.18	6	L	168	-101.8 ± 15	.
Shamrock	SHA	61.05	-152.83	1	LK	135	-12 ± 20.9	24.8 ± 5.5
Sheridan	SHE	60.63	-145.15	6	L	104	-66.3 ± 10.4	.
Skilak	SKI	60.32	-150.03	4	L/LK	217	-11.3 ± 45.4	.
South Hubley	SHU	69.28	-147.70	2	L	1	-0.3 ± 0.2	.
Susitna	SUS	63.52	-147.02	1	L	202	.	-114.5 ± 8.3
Taku	TAK	58.62	-134.30	3	TW	816	513.7 ± 118.6	-213.5 ± 31.7
Tanaina	TAN	60.92	-152.83	1	LK	168	-116.3 ± 27.1	-0.2 ± 7
Tazlina	TAZ	61.74	-146.43	6	L/LK	433	-229.3 ± 36.9	-559.7 ± 19.8
Toklat	TOK	63.43	-149.67	1	L	9	-14.7 ± 0.7	.
Triumph	TRI	57.50	-132.10	3	L	46	-16.8 ± 3.8	-72.8 ± 2.8
Turquoise	TUR	60.78	-153.67	1	L	20	-16.2 ± 2.9	-16.5 ± 0.9
Tustumena	TUS	60.00	-150.40	4	L	297	-97.1 ± 51	.
Tuxedni	TUX	60.12	-153.12	1	L	91	-59.7 ± 7.1	14.3 ± 3.4
Valdez	VAL	61.28	-146.20	6	L	164	-182.9 ± 19	.
West Gulkana	WGU	63.26	-145.49	1	L	4	-2.4 ± 0.4	.
West Okpilak	OKW	69.17	-144.05	2	L	11	-5.7 ± 3.1	.
Wolverine	WOL	60.45	-148.75	4	L	19	-8.7 ± 3.7	-17.3 ± 1.1
Wolverine Crag	WLC	69.19	-143.70	2	L	2	-1.1 ± 0.4	.
Worthington	WOR	61.17	-145.71	6	L	9	1.8 ± 1.5	-7.9 ± 0.4
Wortmanns	WRT	61.00	-145.73	6	L	59	-27.5 ± 5.7	.

Table 2.1: Continued

Glacier Name	$\dot{z}$ (m/yr; ice eq.)		$\dot{L}$ (m/yr)		Map	Profile 1	Profile 2	Number Yrs.	
	Early	Recent	Early	Recent	Year	Date	Date	Early	Recent
Malaspina	-0.91 ± 0.22	-0.95 ± 0.04	.	.	1972	6/5/95	6/5/00	23	5
Mccall	-0.28 ± 0.19	.	.	.	1956	6/1/93	.	37	.
Mccarty	-0.14 ± 0.15	.	-15	.	1950	5/20/96	.	46	.
Mendenhall	-0.95 ± 0.11	-1.42 ± 0.05	-25	.	1948	6/3/95	6/4/99	47	4
Nabesna	-0.17 ± 0.07	.	.	.	1957	6/20/00	.	43	.
Northeastern	-2.09 ± 0.12	.	-29	.	1950	5/19/96	.	46	.
Northwestern	-0.14 ± 0.2	.	-90	.	1950	5/19/96	.	46	.
North Fork Tlikakila	-0.93 ± 0.07	.	-10	.	1957	5/14/01	.	44	.
North Hubley	-0.61 ± 0.19	.	-27	.	1956	1/1/94	.	38	.
Polychrome	-0.23 ± 0.17	.	.	.	1957	6/10/94	.	37	.
Reid	0.4 ± 0.1	-0.2 ± 0.06	0	.	1948	6/4/95	5/24/00	47	5
Scott	-0.67 ± 0.1	.	-10	.	1950	6/21/00	.	50	.
Shamrock	-0.1 ± 0.17	0.21 ± 0.04	-24	.	1957	5/15/96	5/14/01	39	5
Sheridan	-0.72 ± 0.11	.	-13	.	1950	6/21/00	.	50	.
Skilak	-0.06 ± 0.23	.	-70	.	1950	5/29/95	.	45	.
South Hubley	-0.29 ± 0.25	.	-23	.	1956	1/1/94	.	38	.
Susitna	.	-0.62 ± 0.04	.	.	1950	5/19/95	6/1/00	45	5
Taku	0.69 ± 0.16	-0.29 ± 0.04	38	.	1948	1/1/93	1/1/99	45	6
Tanaina	-0.78 ± 0.18	0 ± 0.05	-31	.	1957	5/15/96	5/14/01	39	5
Tazlina	-0.59 ± 0.09	-1.41 ± 0.05	-16	.	1950	5/30/94	5/12/99	44	5
Toklat	-1.82 ± 0.09	.	-13	.	1950	5/7/96	.	46	.
Triumph	-0.4 ± 0.09	-1.71 ± 0.07	-9	.	1948	6/14/96	6/1/99	48	3
Turquoise	-0.9 ± 0.16	-0.92 ± 0.05	-10	.	1957	5/17/96	5/14/01	39	5
Tustumena	-0.36 ± 0.19	.	-16	.	1950	5/29/94	.	44	.
Tuxedni	-0.72 ± 0.09	0.17 ± 0.04	7	.	1957	5/14/96	5/14/01	39	5
Valdez	-1.24 ± 0.13	.	-6	.	1950	8/25/00	.	50	.
West Gulkana	-0.68 ± 0.15	.	.	.	1957	6/1/92	.	35	.
West Okpilak	-0.56 ± 0.31	.	-21	.	1973	1/1/93	.	20	.
Wolverine	-0.52 ± 0.22	-1.03 ± 0.06	-6	.	1950	5/27/94	5/13/99	44	5
Wolverine Crag	-0.62 ± 0.25	.	-7	.	1956	1/1/95	.	39	.
Worthington	0.22 ± 0.18	-0.95 ± 0.05	-9	.	1950	5/31/94	5/12/99	44	5
Wortmanns	-0.52 ± 0.11	.	-4	.	1950	8/25/00	.	50	.

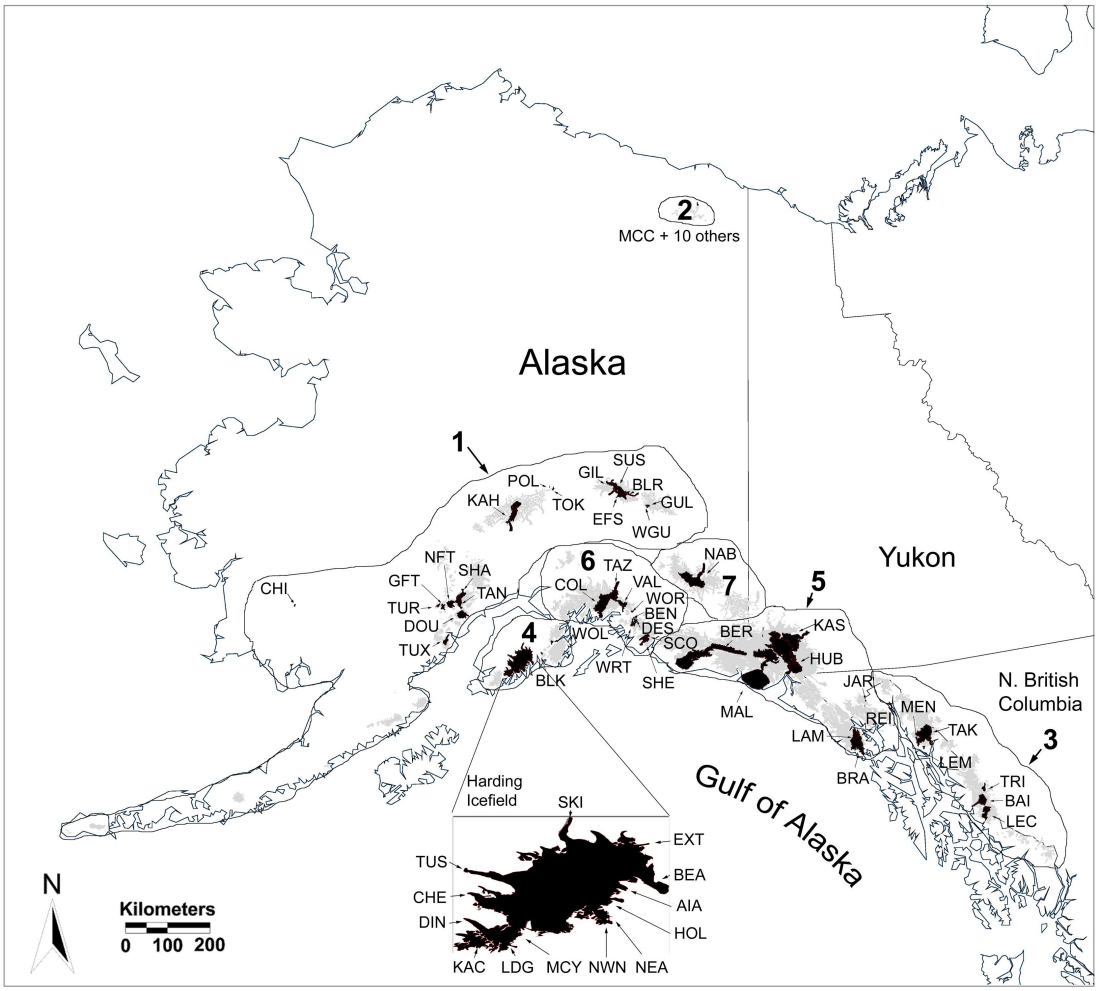

Figure 2.1: Location of 67 surveyed glaciers, shown in black, separated into seven geographic regions: 1 = Alaska Range; 2 = Brooks Range; 3 = Coast Range; 4 = Kenai Mountains; 5 = St. Elias Mountains (includes Eastern Chugach Range); 6 = Western Chugach Range; 7 = Wrangell Mountains. Glacier names associated with 3 letter codes are in Table 2.1. Forty-three glaciers are located entirely in Alaska, 11 span the border between Alaska, U.S.A. and Yukon Territory/northwest British Columbia, Canada, and one is entirely located in Yukon Territory. The total surface area of glaciers in our sample is about 19 000 km^2, shown in black; the total area of glacier ice in Alaska, Yukon, and Northwest British Columbia (north of 54^{o}N latitude) shown in gray, is 90 000 km^2. Glaciers outside the seven regions account for 0.2 percent of the total glacier area.

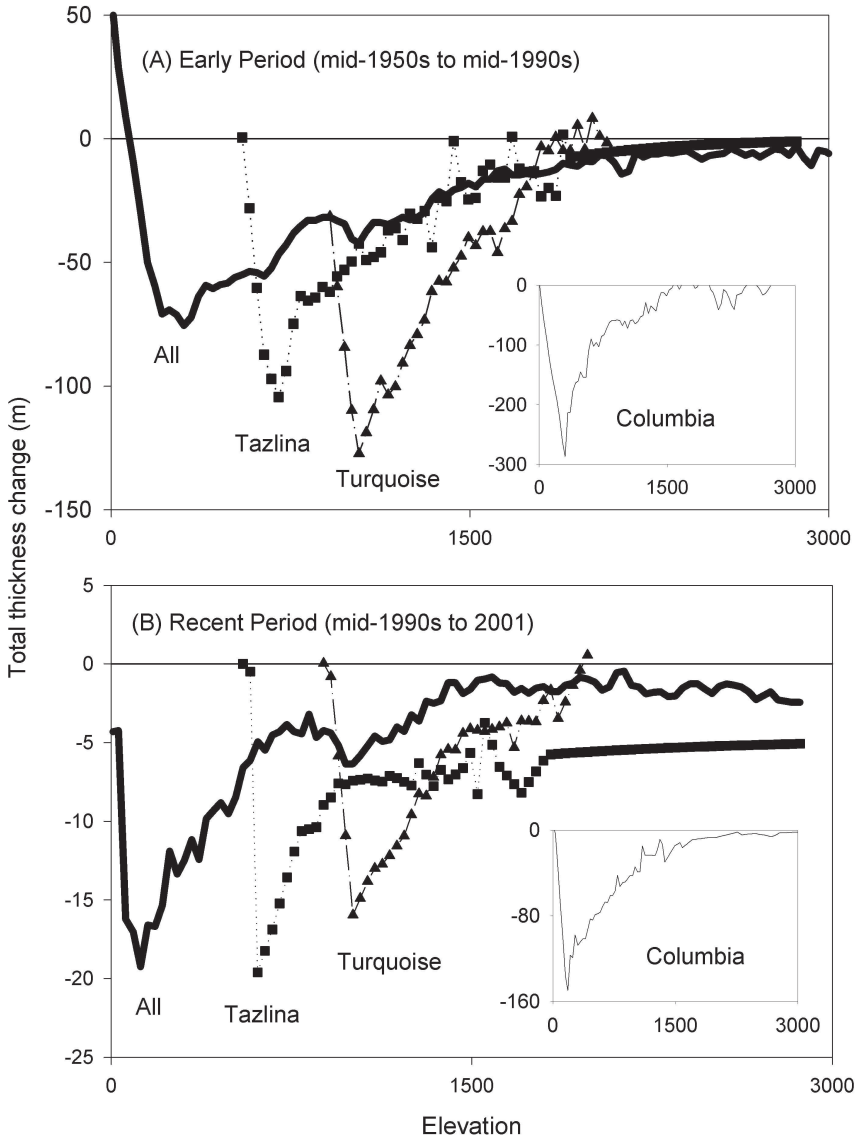

Figure 2.2: Elevation change versus map-date elevation during the early (A) and recent (B) periods: ALL = average of all glaciers (not including Columbia, Hubbard, LeConte and Taku tidewater Glaciers); Tazlina, a large valley glacier; Turquoise, a small valley glacier; and Columbia, a large, retreating tidewater glacier (plotted on separate axis due to exceptionally large rates of thinning). The profiles show substantial thinning at low elevations, with a nearly exponential decrease in thinning up to higher elevations, where the thinning approaches zero. The sharp reduction in thinning at low elevations occurs because the thin ice that existed at the terminus was removed completely as the terminus retreated, leaving unchanging bedrock that was later profiled.

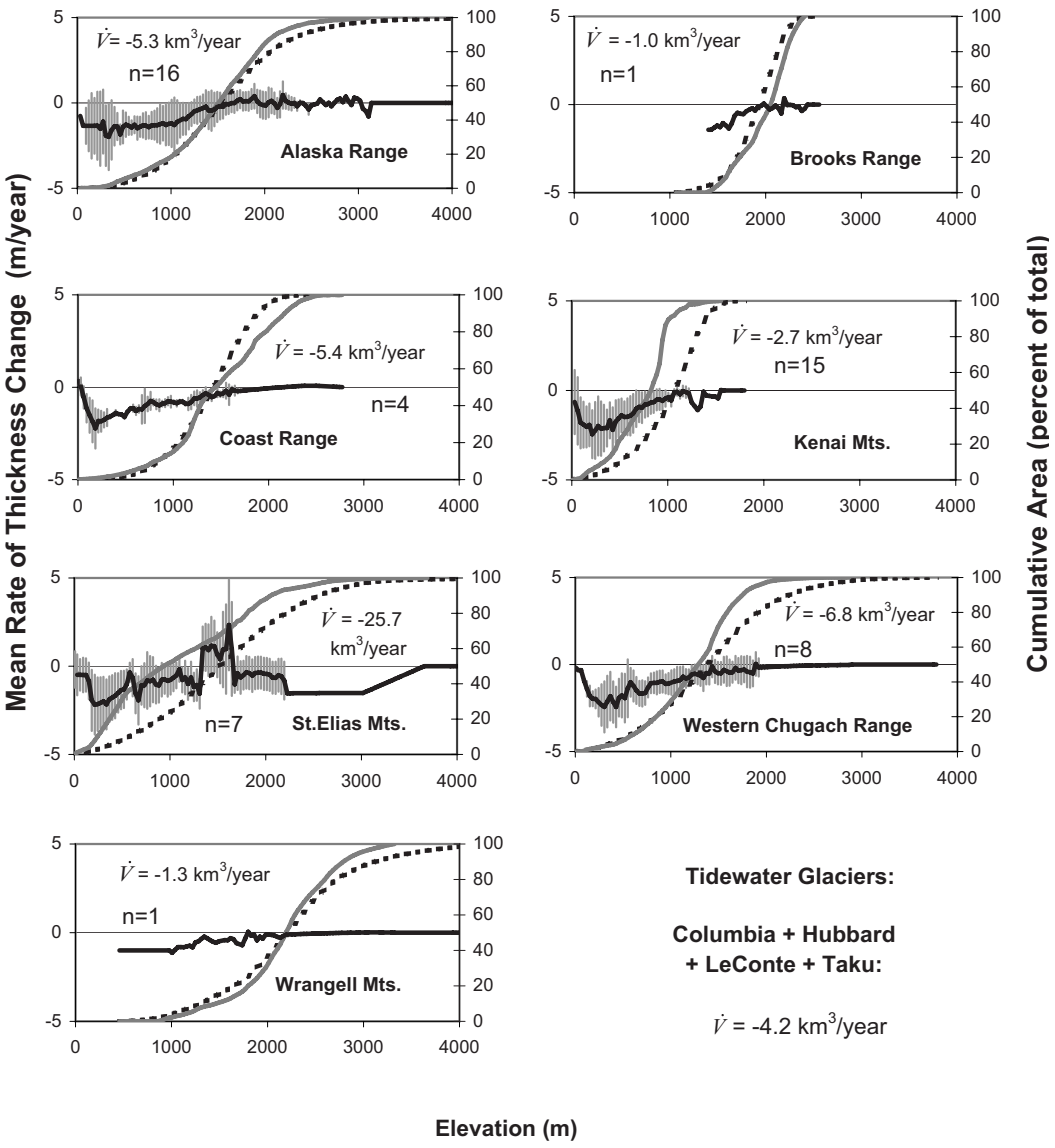

Figure 2.3: Rate of glacier-wide, area-weighted average thickness change versus elevation for the early measurement period (solid black line, left axis), with gray bars indicating measured variations of one standard deviation about the mean. The gray line (right axis) shows regional average curves of cumulative area distribution (%); the dotted black line (right axis) shows cumulative area distribution (%) of glaciers sampled in this study. Comparison of the gray and dotted black lines shows how well we sampled glacier area with elevation for each region. $\dot{V}$ is the total volume change rate for the region, and n is the number of glaciers sampled in the region. Four tidewater glaciers (Columbia, Hubbard, LeConte, and Taku) are treated as separate regions. Similar curves were developed for the recent period.

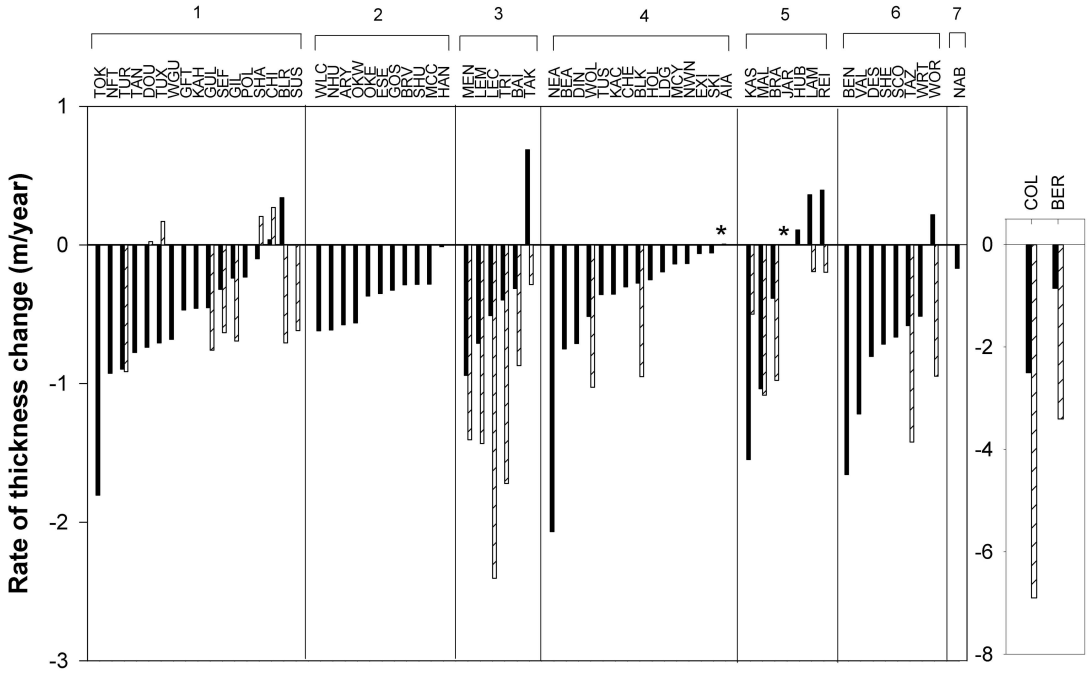

Figure 2.4: Rate of glacier-wide average thickness change of 67 glaciers in Alaska during the early period (ca. 1950 to 1990 - solid black bars) and 28 glaciers during the recent period (ca. 1995 to 2001 - hatched bars). Two large glaciers are plotted separately due to their exceptionally high rates of thinning. The (*) labels thickness changes not resolved by the scale of the plot.

Chapter 3
Updated Estimates of Glacier Volume Changes in the Western Chugach Mountains, Alaska, USA and a Comparison of Regional Extrapolation Methods [1]

3.1 Abstract

We used airborne altimetry measurements to determine the volume changes of 23 glaciers in the Western Chugach Mountains, Alaska, USA between 1950/57 to 2001/2004. Average net balance rates ranged between -3.1 to 0.16 m yr^{-1} for the tidewater and -1.5 to -0.02 m yr^{-1} for the non-tidewater glaciers. We tested several methods for extrapolating these measurements to the all glaciers of the Western Chugach Mountains, using cross-validation. Predictions of individual glacier changes appears to be difficult, probably due to the effects of glacier dynamics which, on long (multi-decadal) time scales, complicates regional changes due to climate. In contrast, estimates of regional contributions to rising sea level were similar for different methods, mainly because the large glaciers, whose changes dominated the regional total, were among those measured. For instance, the above sea level net balance rate of Columbia Glacier (-3.1$\pm$0.08 km^3 yr^{-1} water equivalent (w.e.) or an equivalent rise in sea level (SLE) of 0.0090$\pm$0.0002 mm yr^{-1}) was nearly half of the total regional net balance rate of the Western Chugach Mountain glaciers (-7.4$\pm$1.1 km^3 yr^{-1} w.e. or 0.020$\pm$0.003 mm yr^{-1} SLE between 1950/1957 to 2001/2004). Columbia Glacier is a rapidly retreating tidewater glacier that has lost mass through processes largely independent of climate. Tidewater glaciers should therefore be treated separately when performing regional extrapolations.

3.2 Introduction

Global sea level rise (GSLR) is an important societal and ecological problem, but there is considerable uncertainty in the magnitude of change and the attribution of its causes. GSLR results primarily from ocean thermal expansion (steric rise) and additions to the mass of the ocean (eustatic rise), but the estimated sum of these contributors during the twentieth century is less than that measured directly by tide gages [*Church*, 2001]. Mass

[1] In Press as A. Arendt, K. Echelmeyer, W. Harrison, C. Lingle, S. Zirnheld, V. Valentine, B. Ritchie, M. Druckenmiller. Updated Estimates of Glacier Volume Changes in the Western Chugach Mountains, Alaska, USA and a Comparison of Regional Extrapolation Methods. Journal of Geophysical Research.

loss from glaciers and ice sheets is probably the largest contributor to eustatic change [*Dyurgerov*, 2002; *Meier*, 2003], and improved mass balance measurements will help reduce the uncertainty in GSLR estimates.

Efforts are underway to measure the changes in elevation and extent of Earth's glaciers but many regions remain unmeasured. To arrive at global estimates of glacier changes it is therefore necessary to extrapolate from a small sample of measured glaciers to a particular glacier region, a process we will term "regionalization". Many regionalization methods extrapolate from area-weighted averages of glacier mass changes [*Meier*, 1984; *Dyurgerov and Meier*, 1997; *Cogley and Adams*, 1998; *Dyurgerov*, 2002], or averages of elevation change measurements [*Arendt et al.*, 2002; *Abdalati et al.*, 2004], within specific mountain ranges. Other methods predict changes in volume from changes in area via empirical scaling theories [*Bahr*, 1997; *Bahr et al.*, 1997] or use nearby weather station data to model mass balance [*Oerlemans and Fortuin*, 1992; *Zuo and Oerlemans*, 1997; *Hock*, 1999; *Tangborn*, 1999; *Braithwaite and Raper*, 2002].

The goal of this paper is to present new measurements for glaciers in the Western Chugach Mountains (WCM), Alaska, to use these data to test several regionalization methods, and to arrive at an updated estimate of glacier mass change for this area. In our previous work we sampled nine WCM glaciers using small aircraft altimetry that determined the elevation of each glacier along its central flowline [*Echelmeyer et al.*, 1996; *Arendt et al.*, 2002]. By differencing with elevations on US Geological Survey (USGS) maps from the 1950s, we calculated elevation-dependent thickness changes, and by multiplying these by the glacier area at specific elevations we obtained volume changes. Our regionalization method involved taking the mean of all elevation-dependent thickness changes to obtain a single thickness change function for a region. This function was multiplied by the area distribution function of unmeasured glaciers to obtain an estimate of total regional volume change. Using this approach we arrived at a value of -8.2 $km^3 yr^{-1}$ w.e. for the WCM between 1950 to 2001.

In 2004 we resurveyed seven and added 14 new glaciers to our sample for this region. Our current dataset of 23 WCM glaciers (including two glaciers surveyed in 2001) is well distributed and includes coastal and inland glaciers over wide ranges of sizes and types that helps minimize spatial and size biases common in conventional mass balance

datasets. In particular we now have information on glacier changes on the northwest side of the mountain range that were previously unsampled. We will use these data to re-evaluate our regionalization method that uses elevation-dependent thickness changes. There is potential for error in this method because thickness changes at specific elevations are a function of both climate (the glacier balance) and ice flow (the glacier dynamics). While we expect it may be possible to define regions of similar climate, glacier dynamics are largely determined by the geometry of each individual glacier. We will compare our approach with regionalization methods that use net glacier balances and area-volume scaling. We do not consider mass balance models driven by climate station data in this paper because their errors are largely determined by the availability of representative climate data, a serious problem in most remote areas.

3.3 Geographic Setting

Glaciers of the WCM Range include those west of Copper River, east of Turnagain Arm and north of Sargent Icefield (Figure 3.1). We include the glaciers of the Talkeetna Mountains in order to remain consistent with regions defined by *Arendt et al.* [2002]. The surface area of these glaciers at the time of mapping (1950 and 1957) by the US Geological Survey (USGS) was 9.3×10^9 m^2 [*Manley*, 2005]. About half of these glaciers drain into Prince William Sound to the south and several of these are tidewater glaciers.

3.4 Data and Methods

Components of the altimetry system and methods for calculating volume changes are detailed in previous publications [*Echelmeyer et al.*, 1996; *Aðalgeirsdóttir et al.*, 1998; *Rabus and Echelmeyer*, 1998; *Sapiano et al.*, 1998; *Arendt et al.*, 2002]. Here we summarize these methods and detail new approaches not described in our previous publications.

3.4.1 Thickness Changes

We measured centerline surface elevations of 23 glaciers of the WCM using airborne altimetry [*Echelmeyer et al.*, 1996]. Elevation profiles were collected from 4-8 September 2004, with the exception of two glaciers (Harvard and Yale) surveyed on 21 May 2001. The altimetry system consists of a nadir-pointing rangefinder, a gyro and a Global Positioning

System (GPS) receiver to determine glacier surface elevations along the main trunk and major tributaries of a glacier. A second GPS receiver is run simultaneously at a nearby ground base station and kinematic differential GPS processing is used to determine the position of the aircraft each second. Elevations measured from this system were subtracted from contour elevations on USGS 1:63,360 scale maps (made from 1950s aerial photographs) to obtain the thickness changes (Δh) along the profile. Δh divided by the time interval yields the time average rates of thickness change ($\Delta \dot{h}$, m yr^{-1}) at each contour elevation, which we use for intercomparison of measurements.

3.4.2 Area and Length Changes

The glacier area was digitized from USGS Digital Raster Graphs. In general we outlined all glacier ice within its hydrological basin, although in some cases we decided not to include a particular basin if it was not well represented by our altimetry data. For example we excluded steep high elevation areas where we had no measurements and where the thickness changes were probably much different from those of the measured areas. We updated glacier outlines using Landsat 7 Enhanced Thematic Mapper (ETM+) satellite images from 8 August 2002. These images have a nominal positional accuracy of $\pm$ 75 m and are a composite of bands 7, 4 and 2 [*Kalluri et al.*, 2000]. Several glaciers in our study had debris-covered termini and these areas were included in the glacier outline if they appeared to be underlain by active ice as determined by the presence of surface flow features. Debris-covered areas with substantial vegetative cover were not included as part of the glacier. To determine changes in glacier length (ΔL) we averaged the length of three to five lines drawn along the flow direction between the old and new terminus locations.

3.4.3 Volume Changes

We used a digital elevation model [*Gesch et al.*, 2002] to obtain the hypsometry of the glacier at the time of the map, which we classed into 30.48 m bins to correspond with 100 foot contours on the USGS maps. For each bin, volume changes were calculated by multiplying Δh by the glacier surface area at that bin. Δh measured along the central flow line was assumed representative of all areas at that elevation, and was averaged by elevation

whenever more than one altimetry profile was available for a given glacier, except in cases where Δh showed different patterns in different basins of the same glacier. For these cases we treated each basin as its own glacier. Note that for tidewater glaciers we report as volume changes only that portion of the glacier above sea level.

The net balance rate ($\dot{B}$, $km^3 yr^{-1}$) was determined by summing all volume changes, multiplying by 0.9 (the ratio of the density of ice to water, ρ_i/ρ_w), and dividing by the time interval. This assumes that the net change in mass was in the form of glacier ice, which is true if the density structure of the accumulation area did not change with time [*Bader*, 1954]. To compare mass changes of different sized glaciers we divided $\dot{B}$ by the average of the old and new glacier areas. This yields $\bar{\dot{b}}$ (m yr^{-1}), which we term the "average net balance rate" following the work of *Paterson* [1994]. Others refer to $\bar{\dot{b}}$ as the "mean specific balance rate" [*Kaser et al.*, 2003].

3.4.4 Unmeasured Glaciers

Outlines of glaciers not measured by altimetry were obtained from a map of glacier ice extent compiled by *Manley* [2005]. This was derived from 1:63,360 USGS digital maps and includes all ice areas in the WCM mountains, but does not discriminate between individual glacier basins. The area-altitude distribution of measured glaciers relative to the entire region is shown in Figure 3.2. Our inventory of measured glaciers covers 45% of the 9.3×10^9 m^2 of glacier ice in this region.

3.4.5 Error Analysis

An analysis of errors in volume change estimates is in Appendix B. The USGS maps are probably the largest source of random and systematic errors in our analysis, due to problems with improperly drawn contours, poorly defined map dates and poor geodetic controls. Random errors are independent and their relative magnitude decreases with the number of measurements. These errors are dominated by ablation and accumulation area map contour errors, followed by errors associated with the assumption that one or a few profiles represent changes on the entire area of a glacier (the profile-to-glacier errors). Random error estimates are listed in Table 3.1 and were summed in quadrature (square root

of the sum of squares) for each glacier. We did not calculate systematic errors for each glacier because we lack sufficient information to quantify their magnitude. Systematic errors can have potentially large effects on overall volume change estimates and we attempt to estimate these in the supplemental online material.

3.5 Results

3.5.1 Thickness Changes

$\Delta\dot{h}$ versus elevation for the 23 glaciers are shown in Figure 3.3. Most glaciers show patterns of thickness change typical of our measurements of other glaciers in Alaska: near zero changes at high elevations, decreasing to a maximum rate of thinning at the elevation of the new terminus location. This pattern of change is a well-documented observation for land-terminating glaciers experiencing a net loss in mass over time [*Nye*, 1960; *Jóhannesson et al.*, 1989; *Schwitter and Raymond*, 1993], and occurs because mass losses are propagated downstream and cumulate to large values towards the terminus, and also because extensive/compressive strain rates cause a reduction/increase in thickness changes occurring due to mass balance variations. COL and YLE are tidewater glaciers in the retreat phase of their cycles and show this trend as well but for different reasons. Retreating tidewater glaciers lose large amounts of mass due to dynamic instabilities at the terminus, which then result in a drawdown of ice over the length of the glacier [*Meier and Post*, 1987].

Not all glaciers in our sample showed these typical patterns of thinning. CLY, KNS, MAE, MAW, TON and WOD thickened at elevations above 1000 to 1650 m, comprising about 20% of their total areas. HAR thickened across its entire length because it is a tidewater glacier in the advancing stage of its cycle. A large landslide resulting from the Good Friday Earthquake in 1964 covers the terminus region of SHM glacier [*Shreve*, 1966]. Comparison of altimetry measurements in 2000 and 2004 for this glacier show that the debris-covered areas have not changed in thickness during the past 4 years, probably because the debris has insulated the surface from melting and has cut off that area from the flow of the rest of the glacier. BEN has thinned across its entire surface. This small glacier has little or no accumulation area and is rapidly disappearing under present climate conditions.

3.5.2 Net Mass Balance Rate and Area Changes

Rates of net balance and area change ($\dot{B}$ and $\Delta\dot{A}$) for each of the 23 glaciers are shown in Table 2. COL had the most negative of any $\dot{B}$ and $\Delta\dot{A}$ values (-3.1$\pm$0.08 km^3 yr^{-1} and -0.58 km^2 yr^{-1} respectively). HAR is the only glacier with positive $\dot{B}$ and $\Delta\dot{A}$ (0.052$\pm$0.03 km^3 yr^{-1} and 0.05 km^2 yr^{-1} respectively). All other glaciers had negative $\dot{B}$ values and negative or zero $\Delta\dot{A}$ values.

$\dot{B}$ divided by the average of the old and new areas is $\bar{\dot{b}}$, the average net balance rate. This value is directly comparable with average net balance rates measured by conventional programs and forms the basis of our following regional comparisons in the next section. Glaciers on the north side of the WCM (CLY, KNS, MAW, MAE and NEL) have some of the least negative $\bar{\dot{b}}$ values of -0.03 to -0.39 m yr^{-1} (Figure 3.4). Two of the three tidewater glaciers (COL and YLE) were in a stage of retreat during our measurement period and had large negative changes (-3.01 m and -0.96 yr^{-1} respectively) while HAR was in a stage of advance (0.16$\pm$0.09 m yr^{-1}). Glaciers in the southeastern portion of the WCM (SCO, SHE, SHM and ALN) had similar $\bar{\dot{b}}$ values (-0.64 to -0.89 m yr^{-1}).

3.6 Regionalization Methods

Having described our measurements of glaciers in the WCM, our goal is to extrapolate them to the unmeasured glaciers to determine the total regional contribution to rising sea level. Here we describe several regionalization methods and test each using our altimetry measurements.

3.6.1 Method A: Thickness Changes

This method uses measured $\Delta\dot{h}(z)$ along an elevation profile, determined for example from airborne altimetry. *Arendt et al.* [2002] estimated the net mass balance rate of unmeasured glaciers as:

$$\dot{B}' = \int_Z \Delta\dot{h}_r(z)a'(z)dz \tag{3.1}$$

where $\Delta\dot{h}_r$ is a thickness change with elevation function, regionally-averaged over bands of identical elevation, $a(z)$ is the area distribution function, and primes indicate variables

associated with the unmeasured glacier. This method assumes similarities in climate and flow dynamics of all glaciers within a specific region.

3.6.2 Method B: Normalized Thickness Changes

In general, glaciers that are losing mass overall thin more at the terminus than at higher elevations (see Figure 3.3). This creates a potential problem with Method A: large terminus changes strongly affect a regional average thickness change curve, but the elevation at which these changes occur, even for glaciers with similar dynamics and geometries, can be quite variable. To deal with this issue, *Schwitter and Raymond* [1993] normalized thickness change curves by the rate of thickness change at the terminus, and normalized their spatial variable (distance along the glacier) by the total glacier length. We follow a similar approach for thickness changes, dividing each $\Delta\dot{h}$ by the negative of the thickness change at the new terminus, $\Delta\dot{h}_t$. For our spatial variable (elevation), we normalize by the elevation range of the glacier, so that $z_{norm} = (z - z_t)/(z_h - z_t)$, where z_{norm} is the normalized elevation, z_h and z_t are the elevations of the glacier head and terminus, respectively. This normalization ensures the curves in Figure 3.3 all have termini that are at the same elevation, and scales all thickness changes to the minimum (terminus) value (Figure 3.5).

3.6.3 Method C: Mean Specific Balance Rates

If the average net balance rate $\bar{\dot{b}}$ is available for more than one glacier in a region, it can be averaged over a region to obtain $\bar{\dot{b}}_r$. Then $\dot{B}'$ of the unmeasured glacier is determined by scaling $\bar{\dot{b}}_r$ by the total area of the unmeasured glacier (A'):

$$\dot{B}' = \bar{\dot{b}}_r A' \tag{3.2}$$

Usually $\bar{\dot{b}}_r$ is calculated as an area-weighted average, due in part to the bias in many mass balance datasets towards small glaciers. Equation 3.2 would be exact if the balance curves and hypsometries were the same on measured and unmeasured glaciers [*Furbish and Andrews*, 1984]. An advantage to this approach is its simplicity and many studies have used Equation 3.2 to estimate the contribution of glaciers to rising sea level [*Dyurgerov and Meier*, 1997; *Cogley and Adams*, 1998].

3.6.4 Method D: Area/Volume Scaling

Bahr [1997] found there was a power-law relationship between total glacier volume and area (V_{total} and A_{total} respectively):

$$V_{total} = cA_{total}^{\gamma} \tag{3.3}$$

where γ is a dimensionless scaling coefficient based on both theoretical considerations of *Bahr* [1997] and measured area/volume data, and c is a constant in units of length raised to the power $(3-2\gamma)$. The time derivative of Equation 3.3, after converting to a water equivalent value, yields the net mass balance rate as a function of total area and the rate of area change:

$$\dot{B} = (\rho_i/\rho_w)\, c\gamma {A_{total}}^{(\gamma-1)} \Delta\dot{A} \tag{3.4}$$

This method has been used by *Chen and Ohmura* [1990], *Van de Wal and Wild* [2001] and *Shiyin et al.* [2003] to estimate glacier volume changes on the basis of area change. An obvious advantage to this method is that it does not require any *a priori* knowledge of the surface elevation changes of glaciers in the region of interest, provided the parameters are chosen correctly. Previous studies calculated a value of γ=1.36 (based on measured total area and volume of 144 glaciers around the world, *Meier and Bahr* [1996]) and 1.375 (based on theoretical considerations, *Bahr et al.* [1997]) for valley glaciers. The value of c can vary from glacier to glacier to account for differences in flow regime and climatic environment (for example, continental versus maritime). Assuming a fixed value of γ = 1.375, *Bahr* [1997] obtained a mean value of c = 0.19 $\pm$ 0.07 $m^{(3-2\gamma)}$, using the dataset of 144 measured glaciers, and *Van de Wal and Wild* [2001] calculated a slightly lower value, c = 0.12 $m^{(3-2\gamma)}$, based on global estimates of glacier volume and area. In the following we set γ = 1.375 and test the Method D with a value of c= 0.16 $m^{(3-2\gamma)}$, an average of these two published values.

3.6.5 Testing of Extrapolation Methods

In this section we use our airborne altimetry data to test the extrapolation methods described above. We use cross-validation to compare Methods A to C. For a dataset of size

n, cross-validation involves removing a single observation, labeling it as "unmeasured", and using the remaining $(n-1)$ observations to predict the "unmeasured" value [*Chernick*, 1999]. The entire procedure is run n times so that all observations in the dataset are removed once. The advantage to this approach is that it is relatively simple, and it makes efficient use of the data because $(n-1)$ observations are always used for fitting the model. We do not include tidewater glaciers (COL, HAR and YLE) in the following analysis because they have dynamics that are distinctly different from the other glaciers in our sample. In Section 3.6.6 we determine the best methods for extrapolating to tidewater glaciers.

There are two measures of model performance we wish to examine. The first will illustrate how well the models predict $\bar{\dot{b}}$ for a given glacier based on averages of measurements on other glaciers in that region. This is required in applications attempting to predict the mass balance of glaciers and their response to climate. The second test determines how well each model predicts the total regional volume change. This is of relevance to studies of rising global sea level. We assess model estimates of regional volume change by calculating the percent error (P_{err}) for each glacier as:

$$P_{err} = \left[\frac{\left(\dot{B}_m - \dot{B}_p\right)}{\sum \dot{B}} \text{x}100 \right] \tag{3.5}$$

where subscripts m and p indicate the measured and predicted net balance rate, and $\sum \dot{B}$ is the total net balance rate of all altimetry glaciers. P_{err} shows how different the regional volume change prediction would be from the actual value if that one glacier had not been measured.

Figure 3.6 shows there is considerable scatter in the model predictions of the average net balance rates ($\bar{\dot{b}}$) relative to the measured values. For example the very negative $\bar{\dot{b}}$ values measured at BEN and VAL were not well predicted by averages of the remaining glaciers (Methods A to C) or by area-volume scaling (Method D). The scatter in Figure 3.6 illustrates the difficulty in determining $\bar{\dot{b}}$ for unmeasured glaciers on the time scale of our altimetry measurements.

When we incorporate the surface area of the glaciers and calculate net balance rates ($\dot{B}$) a slightly different pattern emerges. Figure 3.7 shows that the very negative mass losses at VAL are still difficult to predict from averages of the remaining glaciers or from area-

volume scaling. This is because VAL is a large glacier and errors in predicting its total mass loss are large relative to the regional total. In contrast, BEN has very small errors relative to the regional total because it has a small area. Methods A-C were relatively consistent in over- or under-predicting mass loss at specific glaciers: each underestimated thinning at TAZ and VAL and overestimated mass loss at KNS, MAE and MAW. Area/volume scaling (panel D, Figure 3.7) systematically underestimated the thinning of all 20 glaciers using the literature values of γ and c.

We emphasize that the errors calculated in Equation 3.5 are for model intercomparison purposes only. Their sum does not describe the total error in regionalization to all unmeasured glaciers in the WCM. This would only be the case if we had measured all glaciers in the WCM by altimetry. Nevertheless, we require some method to compare total errors for each method and to estimate errors in our regionalization to unmeasured glaciers. We use two different ways to combine errors, one which determines the sum of the absolute values ($\sum |P_{err}|$) and the other the sum of actual values ($\sum P_{err}$). The former is appropriate for combining correlated errors that occur when performing cross-validation. The latter allows for under- or over-estimation of $\dot{B}$ values to cancel each other.

Table 3.3 shows that Method A had the smallest $\sum P_{err}$, followed by Method C. Area-volume scaling (Method D) resulted in total regional volume changes that were 64% too positive (an underprediction of glacier mass loss). Considering the absolute value of the errors, ($\sum |P_{err}|$) ranged between 15 to 19%, with Methods B and C having the lowest errors.

3.6.6 Treatment of Tidewater Glaciers

So far we have removed tidewater glaciers from our analysis of extrapolation methods because they have distinct dynamics, and their potentially large changes can dominate any regional averages. Cross-validation testing of Methods A and C including the three tidewater glaciers (COL, HAR and YLE, not plotted) shows that all methods predict glacier wide balances for COL that are about 75% too positive (underpredicting the rapid thinning). This illustrates the importance of treating tidewater glaciers separately in regionalization.

Area-volume scaling for the tidewater glaciers resulted in larger parameter values than for the non-tidewater glaciers. We solved Equation 3.4 to obtain γ=1.41 by least squares

fitting, with $c = 0.12^{(3-2\gamma)}$. The large value of γ is due to the extremely large change at COL that dominates the calculations. If we used the literature values of γ and c, thinning at COL would have been underestimated by 160% compared to the measured value.

The similarity between normalized thickness change curves of COL and YLE in Figure 3.5B warrants further investigation. A rapidly retreating tidewater glacier such as COL has thickness changes that are dominated by dynamic rather than mass balance effects. It is possible that these dynamic conditions, for instance fast basal motion resulting from instabilities at the terminus, cause similar thickness change profiles for tidewater glaciers. If this is true, it suggests extrapolation to tidewater glaciers from thickness change measured on other tidewater glaciers may be easier than for non-tidewater glaciers, where mass balance effects dominate.

3.6.7 Defining a Region of Extrapolation

We find little evidence for robust patterns in the spatial distribution of measured $\bar{\dot{b}}$ or glacier characteristics. We do find some spatial coherence in the data provided we select a sufficiently small region. For instance SCO, SHE, SHM, and ALN in the southeastern portion of the WCM have similar $\bar{\dot{b}}$ values (standard deviation=0.08 m yr^{-1}, Figure 3.4, Table 2). In particular, the two adjacent glaciers SCO and ALN have similar $\Delta\dot{h}$ versus z profiles, although differences in $a(z)$ account for slight variations in $\bar{\dot{b}}$. Even for such a small sub-region, we note that one anomalous glacier (SHM, due to the landslide covering the terminus) can throw off regional estimates. Another potential sub-region with similar $\bar{\dot{b}}$ values is the northwestern side of the range (CLY, KNS, KNN, MRB, MAE and MAW), with a standard deviation of 0.25 m yr^{-1}. Again we note that MRB, although located in the center of this sub-region, appears anomalous because it has thinning over most of its length, whereas several nearby glaciers are thickening at high elevations.

Our findings do not necessarily dispute previous work showing correlations between mass balance time series over relatively large spatial scales (up to 1200 km) [*Lliboutry*, 1974; *Reynaud*, 1980; *Cogley and Adams*, 1998; *Rasmussen*, 2004]. We expect that with a higher temporal resolution in our dataset we would observe correlations in the trends of $\bar{\dot{b}}$. *Letréguilly and Reynaud* [1989] observed such trends for glaciers in the Swiss Alps but found that the mean value over which these fluctuations occurred varied according to the physical char-

acteristics of each individual glacier. With only a single measurement of change, we are observing those differences occurring not only due to climatic variations but also dynamical adjustments.

3.7 Best Estimate of Regional Contribution to Rising Sea Level

The complexity of observed glacier changes in the WCM suggests no single extrapolation method is applicable to all glaciers in the region. Here we develop our best estimate of glacier changes in this area by combining a variety of methods. We begin by examining the region of unmeasured glaciers for any tidewater glaciers. Our measurements suggest tidewater glaciers can have potentially large changes over short time periods and may change in ways that are not linked to climate. Apart from the small outlet glaciers emptying into the west side of College Fjord, we find 7 unmeasured tidewater glaciers: Barry, Cascade, Coxe, Harriman, Meares, Shoup, and Surprise. We outlined these glaciers using the USGS maps and Landsat images to obtain 1950s and 2002 outlines. Six of these glaciers advanced during our measurement period, while only Shoup Glacier retreated. Together with the 3 measured tidewater glaciers, there are 10 tidewater glaciers in the WCM comprising 22% of its total glacerized area. We used $\bar{\dot{b}}$ from HAR and multiplied it by the unmeasured advancing tidewater glacier areas (regionalization Method C) to obtain $\dot{B}_r$ = 0.056$\pm$0.034 km^3 yr^{-1} for the 6 advancing glaciers. For Shoup Glacier we used the mean thickness change curves from COL and YLE (regionalization method A) to obtain $\dot{B}_r$ = -0.19$\pm$0.03 km^3 yr^{-1} (Table 3.4).

The remaining unmeasured glaciers cover about 30% of the glacerized area in the WCM and we must choose a regionalization method to predict the changes of these glaciers. Methods B and C (normalized thickness changes and net glacier balances) had the smallest percent error (Table 3.3). We will use Method C because it is simple and, unlike method B, does not require outlining of individual glaciers or an estimate of the terminus thickness change. The area-weighted $\bar{\dot{b}}$ from all non-tidewater measured glaciers (-0.55 m yr^{-1} w.e.) multiplied by the area of unmeasured non-tidewater glaciers (4560 km^2) yields $\dot{B}$ = -2.5$\pm$0.11 km^3 yr^{-1} w.e. The sum of all measured and estimated $\dot{B}_r$ values for the WCM is -7.4$\pm$1.1 km^3 yr^{-1} w.e. or 0.02$\pm$0.003 mm SLE.

We calculated the errors in $\dot{B}_r$ (reported above) for the measured glaciers by summing

individual glacier errors in quadrature. For the unmeasured glaciers we assumed the error determined using cross-validation (Section 3.6.5) applied to the unmeasured glaciers. This assumption would be correct if the characteristics of the unmeasured glaciers, such as size and hypsometry, were the same as the measured glaciers.

Our previous study predicted $\dot{B}$= -8.2 km^3 yr^{-1} for glaciers in the WCM [*Arendt et al.*, 2002], which is about 10% more negative than our current prediction but within our range of errors. There are several possible reasons for this discrepancy. Our updated outlines for all WCM glaciers is ∼1000 km^2 smaller than our previous outline. Assuming $\bar{\dot{b}}$ = -0.55 m yr^{-1} for the entire region, this accounts for a difference of 0.55 km^3 yr^{-1} or about 20% of the unmeasured non-tidewater glacier change. Also our previous measurements in this area did not include any of the high elevation glaciers on the northwest side of the range except for KNN. We have found many of these high elevation glaciers to have lower $\bar{\dot{b}}$ than others in the region. Finally, in this paper we have conducted a detailed analysis of unmeasured glaciers and found several advancing tidewater glaciers. Previously these areas of ice were assumed to be thinning, and removing them from the extrapolation has decreased the overall regional volume losses. It is interesting to note that our previous estimates for the Coast Range glaciers in Alaska underestimate the mass losses determined from recently acquired geodetic mass balance methods (C. Larsen, manuscript in preparation, 2005). In that region we undersampled the many rapidly retreating tidewater glaciers and used the same regionalization method for both tidewater and non-tidewater glaciers.

3.8 Sensitivity Analysis of Power Law Method

The power law method (Method D) has been used to scale mass balance models to glacier regions and predict glacier contribution to rising sea level [*Gregory and Oerlemans*, 1998; *Van de Wal and Wild*, 2001], but there have been few opportunities to test this method and confirm the best choice of parameter values. Here we use our dataset to estimate power law scaling parameters for the WCM. We follow the methods of *Bahr* [1997], who demonstrated that trends in the area/volume relationship for glaciers are described by a fixed power law exponent (γ), but that the value of c varies for each glacier to describe its particular flow and mass balance regime. We fixed $\gamma = 1.375$ and solved for c = 0.28 m$^{(3-2\gamma)}$ by the method of least squares. This is larger than Bahr's $c = 0.19 \pm 0.07$ m$^{(3-2\gamma)}$.

The data in this paper indicate that area/volume scaling, used without careful consideration of appropriate parameter values, causes large errors. The large values of c suggested by our data could indicate that glaciers in the WCM have much higher rates of sliding or mass turnover than others measured in the global inventory. It could also result from biases in the global inventory of glacier volume measurements towards small mountain glaciers. Also, there may be limitations in the area/volume scaling theory that assumes perfect plasticity such that the glacier area responds instantaneously to a change in glacier volume. Interestingly, such limitations should result in an overestimation, rather than underestimation of volume loss. In any case, it may be that rapid changes in the WCM cannot be described fully by this theory, or that many glaciers have a large lag time between volume and area changes [*Harrison et al.*, 2001, 2003]. Although we do not intend to redefine the value of c and γ for future studies, we caution against using the power law method without some calibration against glacier measurements within a region.

3.9 Alternate Methods of Regionalization

As shown above, the net balance rate $\dot{B}$ is estimated as the integral of the rate of thickness change ($\Delta\dot{h}(z)$) multiplied by the glacier hypsometry. We can also arrive at $\dot{B}$ by substituting $\dot{b}(z)$, the glacier balance at a specific point, for $\Delta\dot{h}(z)$. This is because the dynamic effects incorporated into measurements of $\Delta\dot{h}(z)$ sum to zero over the entire glacier surface due to mass continuity. The function $\dot{b}(z)$ is called the balance curve and is what is measured in many conventional mass balance programs.

Most regionalization studies define climatically homogenous glacier regions over which to perform extrapolations from measured to unmeasured glaciers. If climate conditions are homogenous on some spatial scale, this should result in similar balance curves for glaciers in a region. When balance curves are known for several glaciers in a region, they can be averaged to represent other unmeasured glaciers (eg: *Hagen et al.* [2003]). We would expect this to be the ideal method for regionalization because dynamic effects, which depend on local flow conditions, would be removed.

In Alaska there are only a few glaciers where $\dot{b}(z)$ is measured on a regular basis. The closest one to the WCM is Wolverine Glacier, a small 17.2 km^2 land terminating glacier located at 60.4°N, 148.9°W, approximately 150 km from the center of our study area, with

an elevation range of 430 to 1680 m [*Mayo et al.*, 2004]. We used the balance measurements at Wolverine Glacier to predict changes of the 20 non-tidewater glaciers measured by altimetry in the WCM, assuming a linear balance curve. The resulting $\dot{B}$ values were far too positive than those measured by altimetry. Because Wolverine Glacier is at a lower elevation than many glaciers in our sample it did not adequately represent changes on many high elevation glaciers. This method could be improved by obtaining additional mass balance data from higher elevations, but doing so is logistically difficult.

It is likely that the dynamics of individual glaciers makes regionalization difficult over multi-decadal time scales. We investigated whether simple parameters such as mean glacier slope, elevation or length accounted for spatial variations in average net balances, but found no coherent patterns. We conclude that we lack enough information to account fully for the effects of glacier dynamics on long-term net balances. Future studies using measurements of surface velocities and ice thickness, perhaps using remote sensing, could provide significant insights into this problem.

3.10 Conclusions and Recommendations

We have observed patterns in glacier thickness changes and net balances that are difficult to generalize on a regional scale. This should not be surprising given the complex interactions between glacier dynamics and climate, the strong variability of climate with elevation in mountain regions, and regional differences in glacier geometry and size. *Jóhannesson et al.* [1989] and *Harrison et al.* [2003] describe a volume time scale that is the time for each glacier to adjust from one steady-state condition to another after some change in climate. It is likely that most glaciers in our study have time scales less than the $\sim$54 year measurement period. However we know that no steady-state has occurred and each glacier will have been in a different stage of response to a varying climate at the beginning and end our measurement period. We also note that the climate changes driving the glacier mass balance probably vary in magnitude with elevation. In addition, calving occurring on both lake and tidewater glaciers is a component of mass loss that is largely independent of climate. Large rates of calving can result in drawdown of ice and increased negative rates of $\bar{\dot{b}}$ relative to that which would occur due to climate alone.

Our tests show that regionalization methods based on averages of glacier measure-

ments (Methods A to C) produce similar estimates of total regional volume changes, but that it is important to examine the data carefully and possibly remove outliers. Of particular importance are tidewater glaciers, some of which have potentially catastrophic mass losses while others are in a state of quiescence or advance. The tidewater glacier cycle is not linked to climate in any simple way, it is not spatially homogenous, and it requires that tidewater glaciers be treated independently, or at least separated into categories of advance and retreat, in any regionalization study. Fortunately large tidewater glacier retreats are easy to identify from maps and satellite images, and we recommend using these tools to improve regional mass balance estimates. We found that, because dynamic effects dominate the changes measured on rapidly retreating tidewater glaciers, the shape of the thickness change with elevation curve might be similar for these glaciers. Therefore measurements at one retreating tidewater glacier might represent others in a region, provided the thickness changes are scaled by the thinning rate at the terminus.

The area/volume scaling method is complicated by the fact that some glaciers have small changes in area but large changes in surface elevation. The method is attractive because it does not require averages of measured glaciers, but we suggest that a combination of area/volume scaling methods with some glacier measurements would allow for a more accurate estimate of scaling parameters. This could help improve estimates of the mountain glacier contribution to rising sea level used in mass balance sensitivity models [*Gregory and Oerlemans*, 1998; *Van de Wal and Wild*, 2001]. Close attention should be paid to the correct choice of parameters used for tidewater glaciers.

It is important to obtain accurate outlines of glacier surface area when estimating glacier contribution to rising sea level. Our findings show that errors in regionalization methods are about the same as the error in using an older, inaccurate map of glacier surface area.

It is unfortunate that many conventional mass balance programs are poorly supported, because the time series they provide would greatly improve our ability to perform accurate regional extrapolations. It is well established that there are correlations in annual mass balance time series for glaciers in specific regions, but the correspondence between glaciers becomes less clear with longer time between measurements, due to dynamical effects and the unique geometry of each individual glacier. Mass balance data generally provide good spatial but poor temporal coverage, while the opposite is true for altimetry data. Therefore

a combination of both types of data is necessary to refine methods for performing regional extrapolations and increase our understanding of the links between glaciers and climate.

Bibliography

Abdalati, W., et al. (2004), Elevation changes of ice caps in the Canadian Arctic Archipelago, *J. Geophys. Res.*, *109*, 4007–+, doi:10.1029/2003JF000045.

Aðalgeirsdóttir, G., K. Echelmeyer, and W. Harrison (1998), Elevation and Volume Changes on the Harding Icefield, Alaska, *J. Glaciol.*, *44*(148), 570–582.

Arendt, A. A., K. A. Echelmeyer, W. D. Harrison, C. S. Lingle, and V. B. Valentine (2002), Rapid wastage of Alaska glaciers and their contribution to rising sea level, *Science*, *297*, 382–386.

Bader, H. (1954), Sorge's law of densification of snow on high polar glaciers, *J. Glaciol.*, *2*(15), 319–322.

Bahr, D., M. Meier, and S. Peckham (1997), The physical basis of glacier volume area scaling, *J. Geophys. Res.*, *102*, 20,355–20,362.

Bahr, D. B. (1997), Width and length scaling of glaciers, *J. Glaciol.*, *43*(145), 557–562.

Bahr, D. B. (1997), Global distributions of glacier properties: A stochastic scaling paradigm, *Water Resour. Res.*, *33*, 1669–1680, doi:10.1029/97WR00824.

Braithwaite, R. J., and S. C. Raper (2002), Glaciers and their contribution to sea level change, *Physics and Chemistry of the Earth*, *27*, 1445–1454.

Chen, J., and A. Ohmura (1990), Estimation of alpine glacier water resources and their change since 1870s, *IAHS*, *193*, 127–135.

Chernick, M. R. (1999), *Bootstrap methods: a practitioner's guide*, 260 pp., John Wiley and Sons, Inc.

Church, J. (2001), How fast are sea levels rising?, *Science*, *294*, 802–803.

Cogley, G., and W. Adams (1998), Mass balance of glaciers other than the ice sheets, *J. Glaciol.*, *44*(147), 315–325.

Dyurgerov, M. (2002), Glacier mass balance and regime: data of measurements and analysis, *Occasional Paper 55*, Institute of Arctic and Alpine Research, University of Colorado.

Dyurgerov, M., and M. Meier (1997), Year-to-year fluctuations of global mass balance of small glaciers and their contribution to sea-level changes, *Arctic and Alpine Research*, *29*(4), 392–402.

Echelmeyer, K., W. Harrison, C. Larsen, J. Sapiano, J. Mitchell, J. DeMallie, B. Rabus, G. Aðalgeirsdóttir, and L. Sombardier (1996), Airborne Surface Profiling of Glaciers: A Case-Study in Alaska, *J. Glaciol.*, *42*(142), 538–547.

Furbish, D., and J. Andrews (1984), The use of hypsometry to indicate long-term stability and response of valley glaciers to changes in mass transfer, *J. Glaciol.*, *30*(105), 199–211.

Gesch, D., M. Oimoen, S. Greenlee, C. Nelson, M. Steuck, and D. Tyler (2002), The national elevation dataset, *Journal of the American Society for Photogrammetry and Remote Sensing*, *68*(1).

Gregory, J., and J. Oerlemans (1998), Simulated future sea-level rise due to glacier melt based on regionally and seasonally resolved temperature changes, *Nature*, *391*, 474–476.

Hagen, J. O., K. Melvold, F. Pinglot, and J. D. Dowdeswell (2003), On the net mass balance of the glaciers and ice caps in Svalbard, Norwegian Arctic, *Arctic, Antarctic and Alpine Research*, *35*(2), 264–270.

Harrison, W., D. Elsberg, K. Echelmeyer, and R. Krimmel (2001), On the characterization of glacier response by a single time scale, *J. Glaciol.*, *47*(159), 659–664.

Harrison, W. D., C. F. Raymond, K. A. Echelmeyer, and R. M. Krimmel (2003), A macroscopic approach to glacier dynamics, *J. Glaciol.*, *49*(164), 13–21.

Hock, R. (1999), A distributed temperature-index ice- and snowmelt model including potential direct solar radiation, *J. Glaciol.*, *45*(149), 101–111.

Jóhannesson, T., C. Raymond, and E. Waddington (1989), Time-scale for adjustment of glaciers to changes in mass balance, *J. Glaciol.*, *35*(121), 355–369.

Kalluri, S., D. Grant, C. Tucker, F. Policelli, J. Dykstra, and P. Bearden (2000), NASA creates global archive of ortho-rectified Landsat data, *Trans. Am. Geophys. Union (EOS)*, *81*(50), 609, 617–618.

Kaser, G., A. Fountain, and P. Jansson (2003), A manual for monitoring the mass balance of mountain glaciers, *Technical Documents in Hydrology 59*, International Hydrological Programme.

Letréguilly, A., and L. Reynaud (1989), Spatial patterns of mass-balance fluctuations of North American glaciers, *J. Glaciol.*, *35*(120), 163–168.

Lliboutry, L. (1974), Relation between the mass balance of western Canadian mountain glaciers and meteorological data, *Jounral of Glaciology*, *34*(116), 11–18.

Manley, W. (2005), *Glaciers of Alaska*, Geospatial inventory and analysis of glaciers: A case study for the eastern Alaska Range, USGS Professional Paper 1386-K.

Mayo, L., D. Trabant, and R. March (2004), A 30-year record of surface mass balance (1966-95), and motion and surface altitude (1975-95) at Wolverine Glacier, Alaska, *U.S. Geological Survey open-file report*, *2004-1069*, 105.

Meier, M. (1984), Contribution of small glaciers to global sea level, *Science*, *226*(4681), 1418–1421.

Meier, M. (2003), Glaciers and sea level: new approaches to an old problem, *Milestones in Physical Glaciology - from the pioneers to a modern science*, pp. 39–52.

Meier, M., and D. Bahr (1996), Counting glaciers: use of scaling methods to estimate the number and size distribution of the glaciers of the world, *Special Report 69-27*, CRREL.

Meier, M., and A. Post (1987), Fast tidewater glaciers, *J. Geophys. Res.*, *92*(B9), 9051–9058.

Nye, J. (1960), The response of glaciers and ice-sheets to seasonal and climatic changes, *Royal Society of London Proceedings. Series A.*, *256*, 559–584.

Oerlemans, J., and J. Fortuin (1992), Sensitivity of glaciers and small ice caps to greenhouse warming, *Science*, *258*(5079), 115–117.

Paterson, W. (1994), *The Physics of Glaciers*, 3rd ed., Elsevier Science Ltd., Oxford, England.

Rabus, B., and K. Echelmeyer (1998), The mass balance of McCall Glacier, Brooks Range, Alaska, U.S.A.; its regional revelance and implications for climate change in the Arctic, *J. Glaciol.*, *44*(147), 333–351.

Rasmussen, L. (2004), Altitude variation of glacier mass balance in Scandinavia, *Geophys. Res. Lett.*, *31*, 1–3.

Reynaud, L. (1980), *Can the linear balance model be extended to the whole Alps?*, *Workshop at Riederalp 1978 - World Glacier Inventory*, vol. 126, pp. 273–284.

Sapiano, J., W. Harrison, and K. Echelmeyer (1998), Elevation, Volume and Terminus Changes of Nine Glaciers in North America, *J. Glaciol.*, *44*(146), 119–135.

Schwitter, M., and C. Raymond (1993), Changes in the longitudinal profiles of glaciers during advance and retreat, *J. Glaciol.*, *39*(133), 582–590.

Shiyin, L., S. Wenxin, S. Yongping, and L. Gang (2003), Glacier changes since the Little Ice Age maximum in the western Qilian Shan, northwest China, and consequences of glacier runoff for water supply, *J. Glaciol.*, *49*(164), 117–124.

Shreve, R. L. (1966), Sherman Landslide, Alaska, *Science*, *154*, 1639–1643.

Tangborn, W. (1999), A mass balance model that uses low-altitude meteorological observations and the area-altitude distribution of a glacier, *Geografiska Annaler*, *81 A*(4), 753–765.

Van de Wal, R., and M. Wild (2001), Modelling the response of glaciers to climate change by applying volume-area scaling in combination with a high resolution GCM, *Clim. Dynam.*, *18*, 359–366.

Zuo, Z., and J. Oerlemans (1997), Contribution of glacier melt to sea-level rise since AD 1865: a regionally differentiated calculation, *Clim. Dynam.*, *13*, 835–845.

Table 3.1: Summary of random (independent) errors affecting the calculation of glacier thickness changes from the comparison of airborne altimetry profiles with USGS topographic maps. Systematic errors are estimated in the supplemental online material.

Error Component	Magnitude
Ablation area contour error	$\pm$15 m
Accumulation area contour error	$\pm$45 m
Profile-to-Glacier error, clean ice	$\pm$2.4 m
Profile-to-Glacier error, dirty ice	$\pm$8.2 m
Altimetry system error	$\pm$0.3 m
Map date errors	$\pm$2.5 m

Table 3.2: Summary of glacier changes measured by comparison of airborne altimetry and USGS map elevations. $\dot{B}$ is the net balance rate (km^3 yr^{-1} w.e.); $\bar{\dot{b}}$ is the average net balance rate (m yr^{-1} w.e.); "Symbol" is a 3-letter code identifying each glacier; "Type" describes whether the glacier is land terminating (L), lake terminating (LK) or tidewater (TW) and two listed types for a glacier indicate a change in type between the earlier/later time. Note that $\dot{B}$ of tidewater glaciers (COL, HAR and YLE) include only that portion of the glacier above sea level.

Name	Symbol	Lat (°N)	Long (°W)	Type	Area (km^2)	$\dot{B}$ (km^3 yr^{-1}w.e.)	$\bar{\dot{b}}$ (m yr^{-1} w.e.)	$\Delta\dot{A}$ (km^{2}yr^{-1})	Map Year	Profile Date	Number Years
Allen	ALN	60.8	144.8	L/LK	214	-0.17±0.02	-0.88±0.08	-0.27	1950	9/4/2004	54
Bench	BEN	61	145.7	L	8	-0.012±0.001	-1.51±0.1	-0.02	1950	9/5/2004	54
Colony	CLY	61.2	148.3	LK	96	-0.021±0.01	-0.22±0.11	-0.03	1954	9/8/2004	50
Columbia	COL	61.3	146.9	TW	1054	-3.1±0.08	-3.01±0.08	-0.58	1957	9/6/2004	47
Deserted	DES	61	145.6	L	36	-0.027±0.003	-0.75±0.08	-0.02	1950	9/4/2004	54
Harvard	HAR	61.4	147.4	TW	324	0.052±0.03	0.16±0.09	0.05	1957	5/21/2001	44
Knik North	KNN	61.4	148.2	L	207	-0.10±0.02	-0.50±0.08	-0.06	1954	9/8/2004	50
Knik South	KNS	61.4	148.2	L	241	-0.057±0.02	-0.24±0.09	-0.05	1954	9/8/2004	50
Marcus Baker	MRB	61.5	148	L	168	-0.11±0.01	-0.65±0.07	-0.06	1954	9/6/2004	50
Matanuska East	MAE	61.7	147.6	L	102	-0.015±0.01	-0.15±0.07	0.00	1957	9/6/2004	47
Matanuska West	MAW	61.7	147.6	L	170	-0.004±0.01	-0.02±0.05	-0.03	1957	9/6/2004	47
Nelchina	NEL	61.6	146.9	L	245	-0.088±0.02	-0.36±0.07	-0.29	1950	9/5/2004	54
Scott	SCO	60.7	145.2	L	167	-0.12±0.01	-0.72±0.08	-0.03	1950	9/4/2004	54
Sheridan	SHE	60.6	145.2	L	100	-0.088±0.01	-0.89±0.09	-0.12	1950	9/4/2004	54
Sherman	SHM	60.6	145.1	L/LK	58	-0.037±0.01	-0.64±0.09	0.00	1950	9/4/2004	54
South Fork Tsina	STS	61.2	145.8	L	19	-0.008±0.002	-0.41±0.10	-0.01	1950	9/4/2004	54
Tazlina	TAZ	61.7	146.4	L/LK	415	-0.28±0.03	-0.69±0.07	-0.55	1950	9/5/2004	54
Tonsina	TON	61.3	145.8	L	48	-0.027±0.01	-0.58±0.10	-0.05	1950	9/5/2004	54

Table 3.2: Continued

Name	Symbol	Lat (°N)	Long (°W)	Type	Area (km^2)	$\dot{B}$ (km^3 yr^{-1}w.e.)	$\bar{\dot{b}}$ (m yr^{-1} w.e.)	$\Delta\dot{A}$ (km^2yr^{-1})	Map Year	Profile Date	Number Years
Tsina	TSI	61.3	145.9	L	36	-0.035±0.004	-0.98±0.10	-0.06	1950	9/5/2004	54
Valdez	VAL	61.3	146.2	L/LK	156	-0.21±0.02	-1.37±0.11	-0.22	1950	9/5/2004	54
Woodworth	WOD	60.9	145.5	L	133	-0.061±0.01	-0.47±0.07	-0.10	1950	9/4/2004	54
Wortmanns	WRT	61	145.7	L	58	-0.033±0.01	-0.58±0.09	-0.05	1950	9/4/2004	54
Yale	YLE	61.3	147.5	TW	167	-0.16±0.02	-0.96±0.10	-0.37	1957	5/21/2001	44

Table 3.3: Comparison of regional volume change extrapolation methods. $\sum P_{err}$ and $\sum |P_{err}|$ are the sums of the actual and absolute values of the percent error between measured and predicted volume changes. Method D uses $\gamma = 1.375$ and $c = 0.16$ m$^{(3-2\gamma)}$.

Extrapolation Method	$\sum P_{err}$	$\sum \lvert P_{err} \rvert$
Method A: Thickness Changes	0.04%	16%
Method B: Normalized Thickness Changes	9.3%	15%
Method C: Average Net Balances	-1.7%	15%
Method D: Area/Volume Scaling	+64%	19%

Table 3.4: Best estimates of the regional net balance rate ($\dot{B}_r$) of glaciers in the Western Chugach Mountains. "TW" refers to tidewater glaciers.

Type	**Area** (km^2)	$\dot{B}_r$ ($km^3\ yr^{-1}$)
	Measured	
Advancing TW	324	0.05±32
Retreating TW	1220	-3.3±100
Non-TW	2680	-1.5±0.06
	Unmeasured	
Advancing TW	363	0.056±0.034
Retreating TW	154	-0.19±0.03
Non-TW	4560	-2.5±1.1
	Total	
Advancing TW	687	0.11±0.05
Retreating TW	1370	-3.5±0.1
Non-TW	7240	-4.0±1.1
All Glaciers	9300	-7.4±1.1

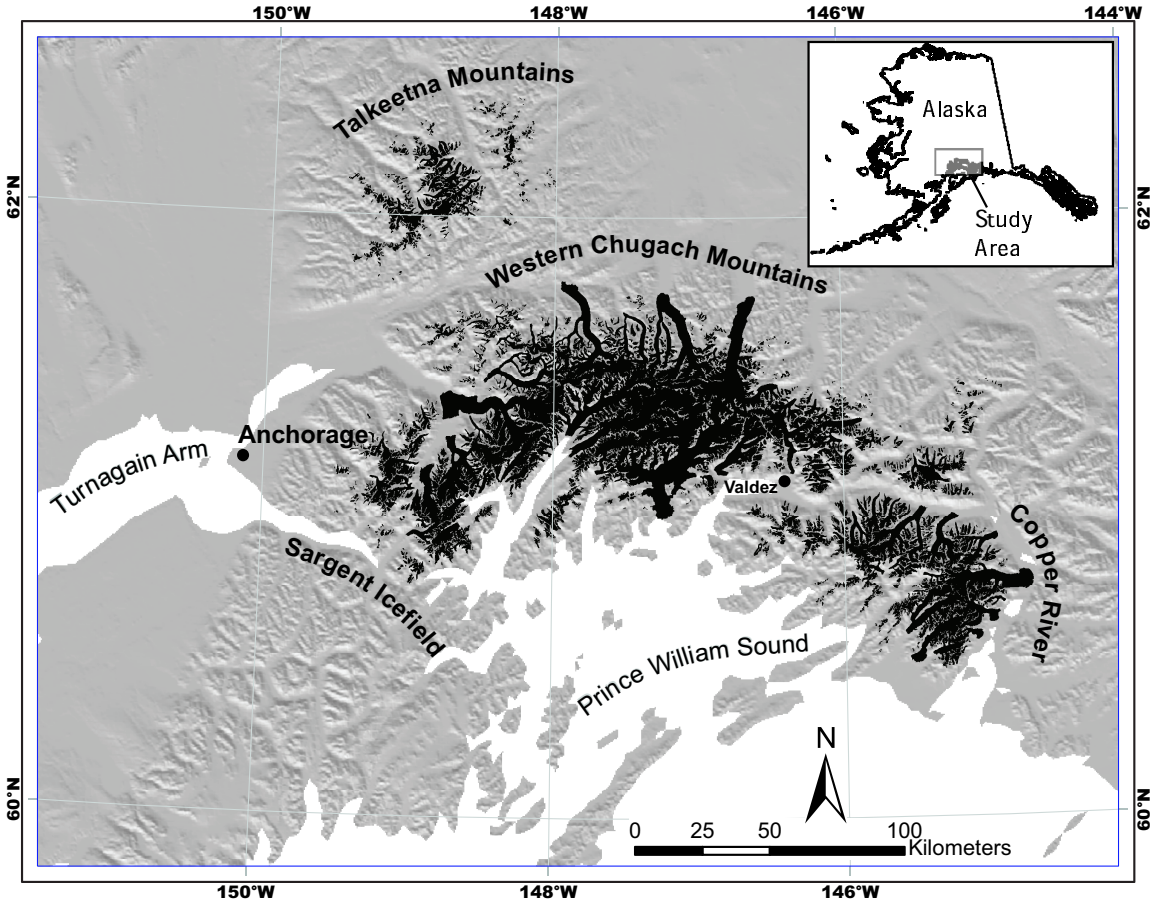

Figure 3.1: Location of the Western Chugach and Talkeetna Mountains, Alaska USA. Glaciers in this region (shown in black) cover an area of 9.3×10^9 m^2.

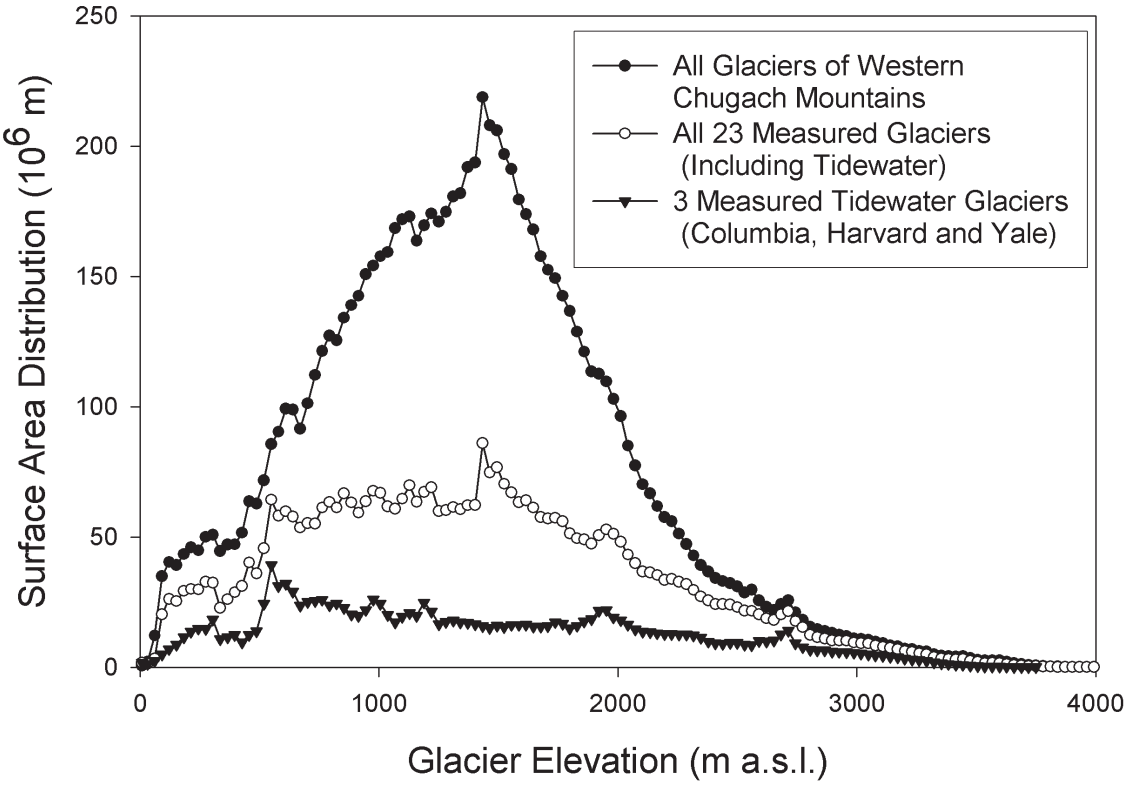

Figure 3.2: Distribution of glacier surface area (10^6 m) with elevation (m asl), determined from 1950/57 USGS contour maps, of three tidewater glaciers: Columbia, Harvard and Yale (triangles); all 23 glaciers measured by airborne altimetry, including the tidewater glaciers (open circles); and all glaciers in the Western Chugach Mountains (filled circles), including all measured glaciers.

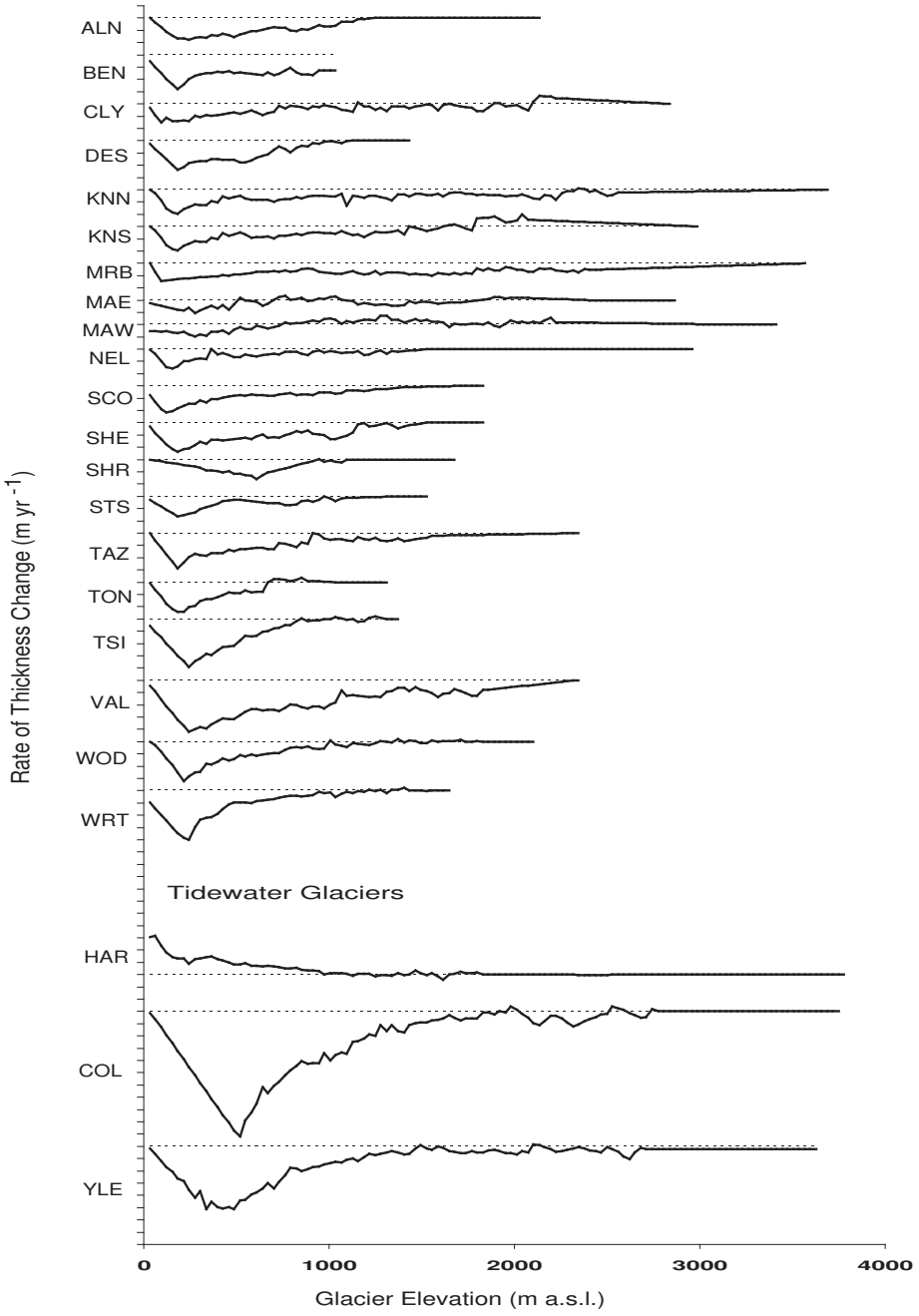

Figure 3.3: Time average rate of glacier thickness change $\Delta\dot{h}$ (m yr^{-1}) as a function of elevation on the glacier at the time of mapping, determined from total thickness changes between 1950/57 to 2001/04. Dotted line represents 0 change and values below this line indicate a reduction in surface elevation relative to the map. Each tick mark on the vertical scale is 1 m yr^{-1} of thickness change. Three letter glacier codes are listed in Table 3.2.

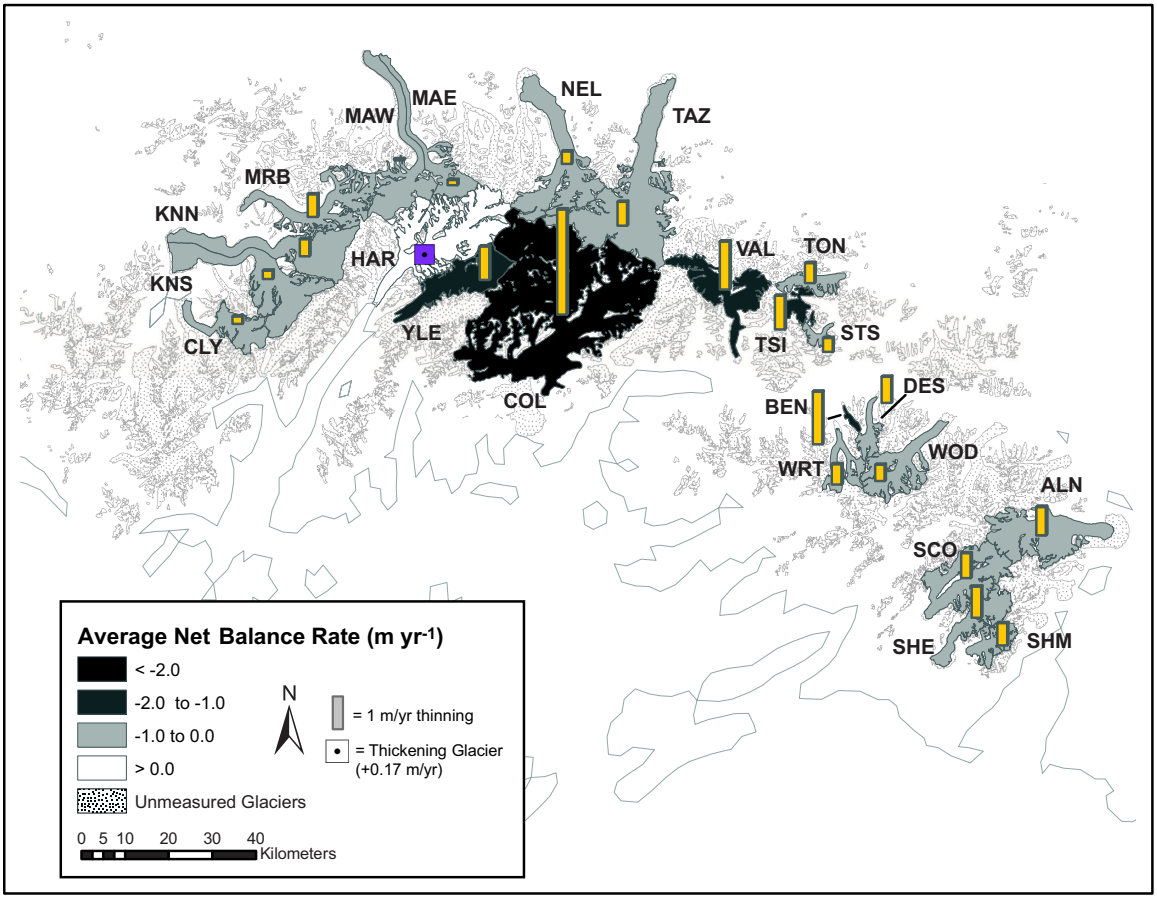

Figure 3.4: Average net balance rate (m w.e. yr^{-1}) between 1950/57 to 2001/04, represented by gray scale shading and bar length. Dotted fill represents glaciers of the Western Chugach Mountains at the time of mapping by the USGS (1950 or 1957). Glacier outlines for altimetry glaciers represent 2002 surface area. A key of the three letter glacier codes is given in Table 3.2.

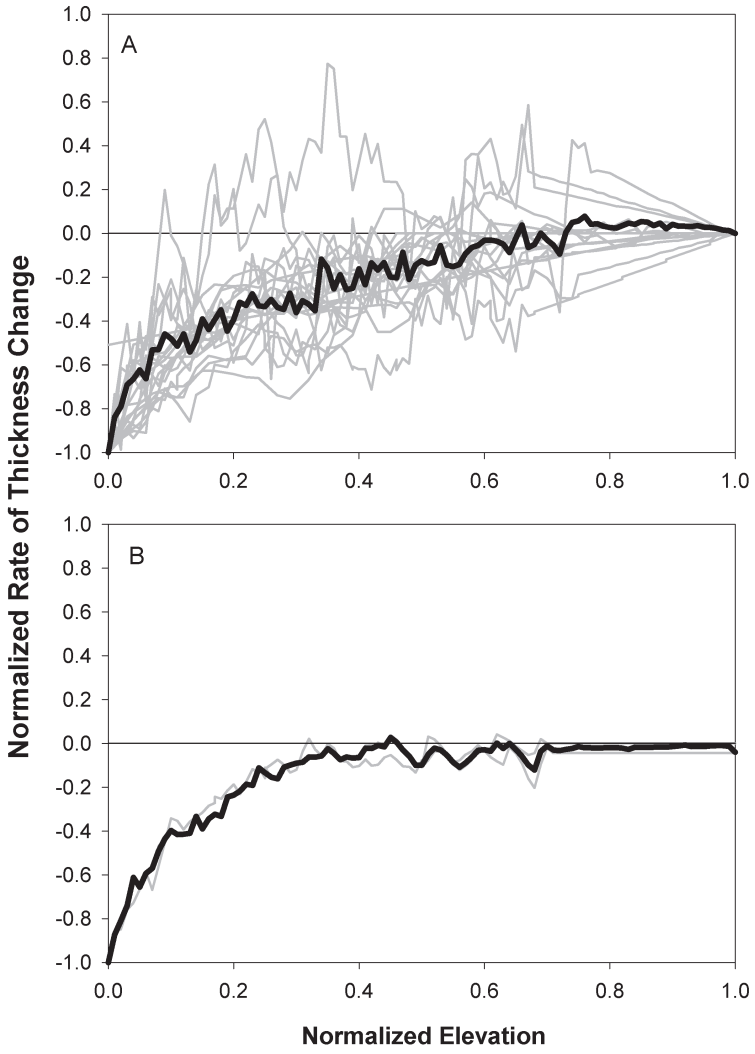

Figure 3.5: Normalized rate of thickness change ($\Delta\dot{h}/-\Delta h_t$) versus normalized elevation ($(z-z_t)/(z_h-z_t)$) for glaciers of the Western Chugach Mountains, Alaska. Group A is comprised of all glaciers except tidewater glaciers and an obvious outlier, BEN. Group B is comprised of two retreating tidewater glaciers COL and YLE. Gray curves show normalized thickness changes of all glaciers and black curves are area-weighted averages of the gray curves.

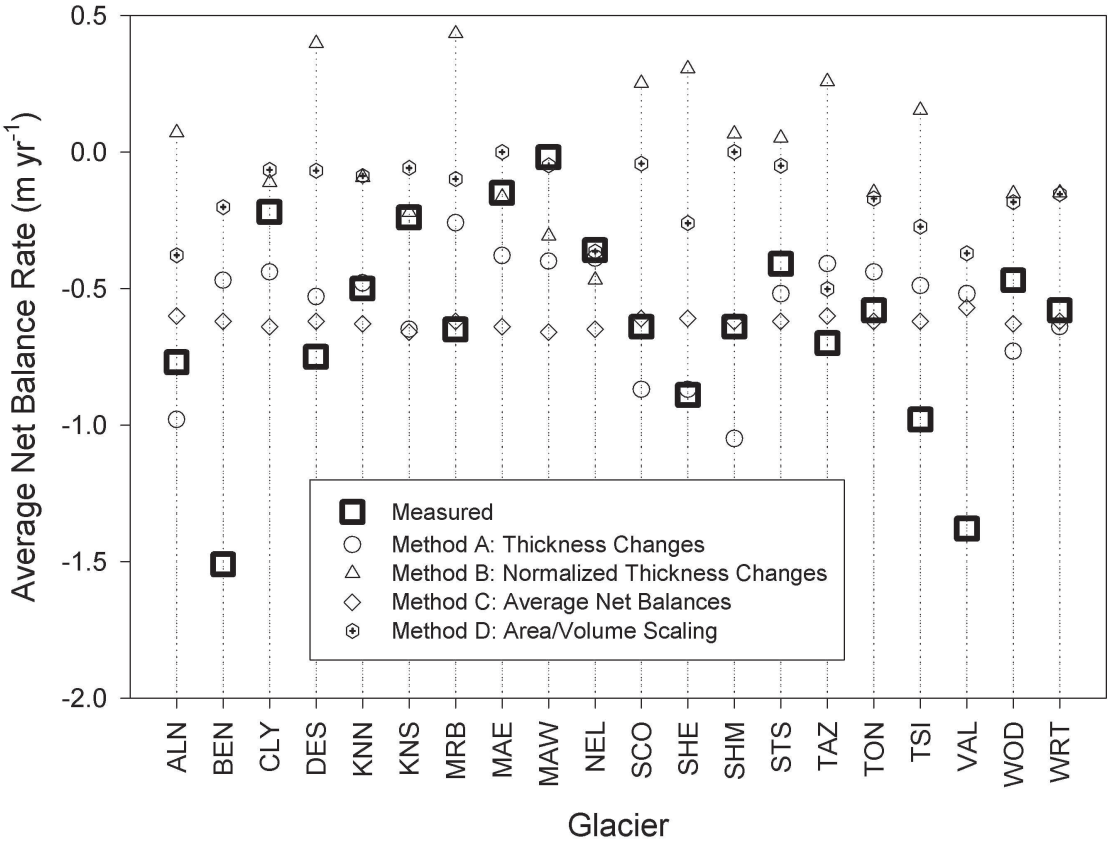

Figure 3.6: Comparison of four regionalization methods to determine average net balance rates (m yr^{-1}) of 20 non-tidewater glaciers in the Western Chugach Mountains. Measured changes are shown as squares.

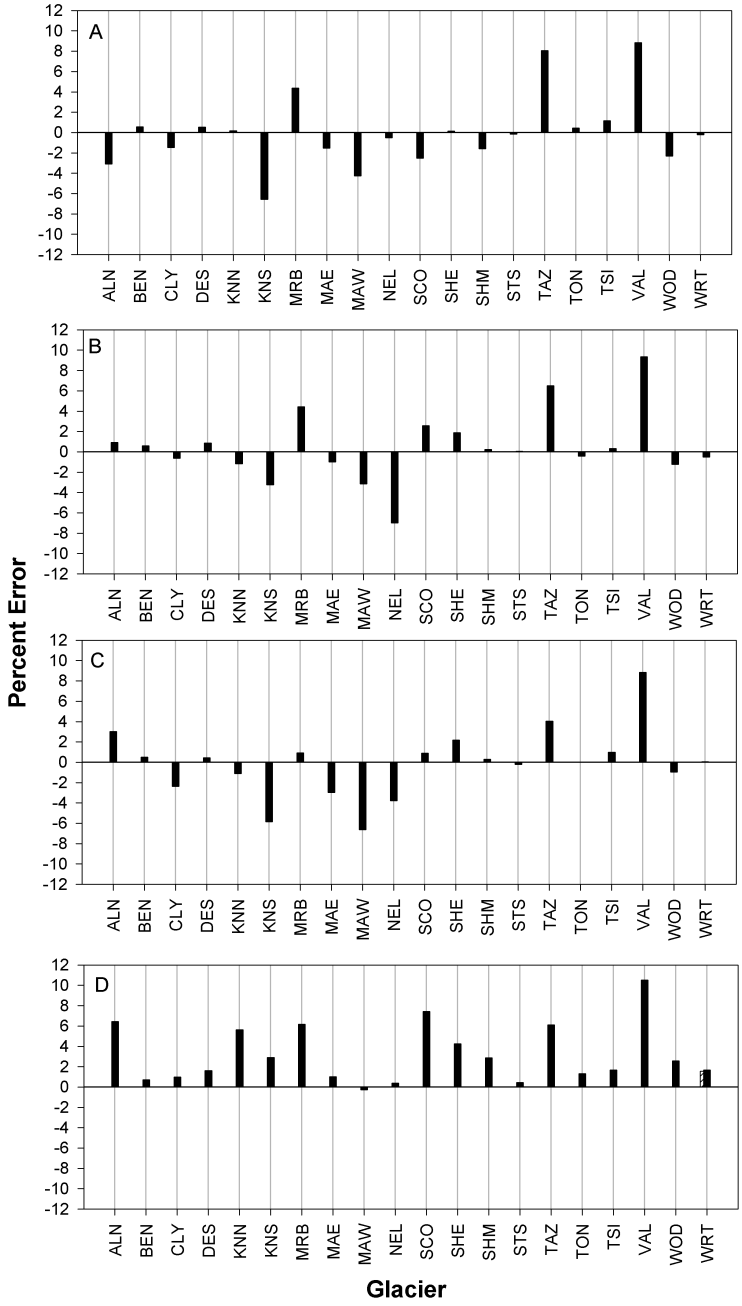

Figure 3.7: Error (measured - predicted) in predicting individual net balance rates ($\dot{B}$), expressed as a percentage of the total measured regional net balance rate ($\sum \dot{b}$) of all non-tidewater glaciers measured by altimetry. Method A: extrapolation from mean $\Delta\dot{h}$ as a function of elevation; Method B: extrapolation from normalized mean $\Delta\dot{h}$; Method C: extrapolation from average net balance rates $\bar{\dot{b}}$; Method D: extrapolation using area-volume scaling with $\gamma = 1.375$, $c = 0.16\ \mathrm{m}^{(3-2\gamma)}$. Methods A, B and C are tested using cross-validation.

Chapter 4
Changes of Glaciers and Climate during the Last 50 Years in Northwestern North America [1]

4.1 Abstract

About 75% of 47 glaciers measured using repeat airborne altimetry in northwestern North America have been losing mass at an increasing rate during 1995-2004, relative to an earlier period beginning in the 1950s (and in a few cases, the 1970s). The remaining glaciers have been either gaining volume during the past decade, or continue to lose volume but at a decreasing rate. We separated glaciers into seven regions and compared their changes with 1950-2002 trends in low elevation climate station air temperature, precipitation and melt season length (MSL), and NCEP/NCAR upper air freezing level heights (FLH). Nearly all significant trends in winter and summer air temperatures and MSL at 77 low elevation climate stations were positive (0.4 ± 0.2, 0.2 ± 0.1°C (decade)$^{-1}$ and 4 ± 2 days, respectively), and all seasonally averaged values of FLH in the glacier regions increased. There were no clear spatial trends and few significant changes in precipitation, although large and significant increases occurred at Yakutat (230 mm (decade)$^{-1}$). Average regional glacier changes, modelled using mass balance sensitivities and climate station temperature and precipitation trends, agreed within the limits of reported errors. In the Alaska and Kenai regions, more mass loss was predicted than measured, probably due to large seasonal variations in accumulation which complicated the glacier/climate comparison. In the Coast, St. Elias and Western Chugach regions, the predicted mass loss was less than that which was measured. No climate data were available for the Wrangell Region. FLH variations superimposed on regional glacier hypsometries show that all of the maritime glacier systems (Coast, Kenai, St. Elias and Western Chugach) are more sensitive to variations in the mean position of the winter FLH than interior regions. Therefore strong winter warming has probably affected these regions in addition to the summer changes. Our measurements augment the increasingly strong evidence of late 20th century climate change in northwestern North America.

[1] Prepared for submission in The Journal of Applied Meteorology as Arendt, A. , Walsh, J. , Harrison, W. , Echelmeyer, K. and Lingle, C. Changes of Glaciers and Climate during the Last 50 Years in Northwestern North America.

4.2 Introduction

Airborne altimetry measurements have been used to determine glacier volume changes in Alaska and northwestern Canada (hereafter NW N. A.) [*Echelmeyer et al.*, 1996; *Aðalgeirsdóttir et al.*, 1998; *Sapiano et al.*, 1998; *Rabus and Echelmeyer*, 1998; *Arendt et al.*, 2002, in press]. The majority of measured glaciers have been losing mass during the past 50 years, and on average, the rate of mass loss has increased during the past decade. These measurements are indicators for climatic changes in the mountainous regions of NW N. A. [*ACIA*, 2004], but the exact magnitude and type of change (eg: increases in summer temperatures versus decreases in winter precipitation) has not yet been quantified. Our goal here is to investigate glacier changes on a regional basis and determine to what extent they can be explained by climatalogical variations.

Previous work has shown that annual average air temperatures at 20 low elevation stations in Alaska increased by 1.8°C during 1949 to 2003 [*Alaska Climate Center*, 2005]. This increase is qualitatively consistent with the glacier changes, but it occurred primarily during the winter season and might therefore have had only a small effect on glacier mass balance. *Rasmussen and Conway* [2003] found a significant increase in summer temperatures at a maritime location in Alaska and suggested this increase has been the primary driver of the observed glacier changes. These authors also used upper-air vapor fluxes to infer an increase in snowfall, but suggested these were probably offset by increases in winter temperatures. At the same time, ice core data show increasing rates of twentieth-century accumulation at an elevation of about 5300 m on Mt. Logan, Yukon [*Moore et al.*, 2002]. Accumulation patterns below this, where most glaciers in NW N. A. exist (regional mean elevations of 900 to 2200 m), are not well known due to a lack of measurements.

While the above studies provide insights into regional climate variations, they do not quantify the link between glacier and climate changes that help improve model projections of glacier contribution to rising sea level [*IPCC*, 2001]. In this paper we will provide an updated climatology of NW N. A. , and then use these climate parameters to explain regional variations in glacier volume change. We choose four climatic parameters, three of which will be determined from low elevation climate stations: (1) winter and summer average air temperatures; (2) annual total precipitation (rain and snow); and (3) melt season length (MSL), describing the number of days with above 0°C temperatures at the elevation of the

climate station. A fourth parameter, freezing level height (FLH) describes the altitude at which the air temperature is 0°C, and will be determined from the National Centers for Environmental Prediction/National Center for Atmospheric Research (hereafter "NCEP") upper air reanalysis. These parameters, or some variation thereof, are common in the climatological literature [*Keyser*, 2000; *Frich et al.*, 2002]. We select these particular ones because of their relevance to glacier mass balance [*Diaz et al.*, 2003; *Paterson*, 1994; *Barry*, 1990].

Detailed mass balance models are commonly used to link glacier and climate changes [*Oerlemans and Fortuin*, 1992; *Braithwaite and Raper*, 2002]. These models are best suited to glaciers where annual mass balance, and ideally, local meteorological conditions, are measured. There are only a few such "benchmark" glaciers in Alaska, and several studies have examined the correlation of their mass balances with North Pacific sea surface temperatures [*Hodge et al.*, 1998; *Bitz and Battisti*, 1999] or upper air temperature and moisture fields [*Rasmussen and Conway*, 2003]. Our altimetry measurements describe glacier changes during two different time periods, therefore lacking sufficient temporal resolution necessary to calibrate mass balance simulation models [*Oerlemans*, 2001]. When direct modeling of glacier mass balance is not feasible, mass balance sensitivities can be used to link changes in climate to changes in glacier balances [*de Woul and Hock*, in press; *Raper and Braithwaite*, 2006]. Here we use mass balance sensitivities determined for Gulkana and Wolverine glaciers and assume they represent glaciers in continental and maritime regions, respectively, of NW N. A. .

We will complete our analysis by examining the observed changes in the context of broad climatic variations. Synoptic scale teleconnections occur between sea level pressure and surface air temperatures [*Chao*, 2000], and these appear to have natural modes of variability. There is recent evidence of abrupt changes in these modes during our period of glacier measurements [*Thompson and Wallace*, 1998]. Therefore we will examine the timing of these shifts relative to our measurements in an effort to explain recent trends in glacier change.

4.3 Data

4.3.1 Climate

We assembled 48 first order National Oceanic and Atmospheric Administration (NOAA) climate station and 29 Environment Canada (EC) climate station records (daily maximum and minimum temperature, total daily precipitation) in NW N. A. (Figure 4.1; Table 4.2). We chose these stations from a list of several hundred based on the criteria that they included at least 30 years of record, had less than 20% missing observations and had records through at least 2000. We selected all possible years between 1950 to 2002. Missing observations were reconstructed by running cross-correlations between all stations and choosing pairs of stations with highest coefficients of correlation to use for reconstruction (personal communication from Wendell Tangborn, 2004). Then the mean difference (for temperature) or ratio (for precipitation) between all available measurements of the paired stations was used to adjust observations at the station with data to the one without. We supplement the precipitation data with snowdepth data from the US Department of Agriculture, Alaska Natural Resources Conservation Service (NRCS) Snow Program (www.ak.nrcs.usda.gov/Snow). These data are available in some mountainous areas and are determined by manual snowcourse or automated snow pillow measurements, but are not of sufficient length to provide information on long-term trends.

The NCEP reanalysis model output is available on a regular 2.5°x2.5° lat/long grid [*Kalnay et al.*, 1996]. We extracted mean daily air temperature and geopotential height fields between 50 to 75°N latitude and 130 to 170°W longitude at 1000, 925, 850, 700 and 600 mb levels for the years 1950 to 2002. Temperature and geopotential height fields are classed as variables strongly influenced by observations and are in the most reliable class of all NCEP variables.

Errors in climate parameters are difficult to quantify and are rarely reported by data collection agencies. We assume a random (uncorrelated) error in temperature measurements of $\pm$ 0.2 °C, based on unpublished temperature sensor calibration studies on Gulkana Glacier. In some areas temperature measurements may be skewed towards higher values due to the proximity of many climate stations to human infrastructure which can alter the thermal regime of the surrounding landscape.

4.3.2 Altimetry

Glaciers measured by airborne altimetry and analyzed in this study are shown in Figure 4.2. In this paper we report on 46 glaciers covering 14,000 km^2, about 15% of the total glacier ice in NW N. A. Glacier surface elevations were measured along one or several main tributaries of glaciers in NW N. A. , using a small aircraft outfitted with a rangefinder, gyro and global positioning system (GPS) [*Echelmeyer et al.*, 1996; *Arendt et al.*, 2002]. These elevations were compared with contours on US Geological Survey (USGS) maps from the 1950s, or Energy, Mines and Resources Canada (EMRC) maps from the 1970s, or with a previous altimetry profile, to determine changes in surface elevation. Volume changes are determined by integrating the elevation change over the surface area distribution of the glacier determined from USGS digital elevation models. The net balance rate ($\dot{B}$, km^3 yr^{-1}) is the total change in volume of the glacier divided by the time interval between measurements. The average net balance rate ($\bar{\dot{b}}$, m yr^{-1}) in water equivalent units is $\dot{B}$ divided by the average of the area at the earlier and later times, and corrected for the differences in density between ice and water. We assume that the density profile from the surface to the bed does not change in time, and hence that all mass loss occurs as glacier ice.

We compare glacier changes over two measurement periods: an "early" period from the USGS or EMRC maps (1950s or 1970s) to a first set of altimetry measurements (1993-1996, except the Western Chugach Mountains, measured in 2000); and a "recent" period documenting change, determined from repeat measurements, taken three to seven years after the first set of measurements. The change in the average net balance rate $\bar{\dot{b}}$ (recent minus early period changes) is $\Delta\bar{\dot{b}}$.

A detailed discussion of methods and error estimates is in previous publications [*Echelmeyer et al.*, 1996; *Sapiano et al.*, 1998; *Arendt et al.*, 2002, in press]. In Appendix C we provide a new method for estimating recent period measurement errors, taking into consideration errors due to seasonal differences in snowfall. These errors can be large over short time periods, especially in regions where precipitation variability is large, such as the southern coastal regions of Alaska.

4.3.3 Benchmark Glaciers

Gulkana (63.24°N, 145.5°W) and Wolverine (60.45°N, 148.8°W) glaciers have been monitored from 1966 to present [*March*, 2003; *Mayo et al.*, 2004]. Mass balance measurements are recorded during spring and fall campaigns at three index sites (1370, 1683 and 1835 m above sea level (a.s.l.) on Gulkana and 595, 1070 and 1295 m a.s.l. on Wolverine) and extrapolated over the surface to obtain net balances. The mass balances were independently confirmed using photogrammetric methods [*Cox and March*, 2004]. Gulkana Glacier is located in a continental climate regime with low rates of snowfall and relatively high summer temperatures, while Wolverine Glacier is located in a maritime location with high rates of snowfall and has less extreme variations in temperature [*Hodge et al.*, 1998; *de Woul and Hock*, in press]. The average net balances determined at these glaciers compare well with those estimated by airborne altimetry; therefore we will use Gulkana Glacier to represent continental glaciers and Wolverine Glacier to represent maritime glaciers.

4.3.4 Regional Topography

A digital elevation model for NW N. A. (available from http://agdc.usgs.gov/data/usgs/erosafo/300m/300m.html) was used to determine the area-altitude distribution of each glacier region. Glacier outlines representing the surface at the time of mapping were obtained from http://glims.colorado.edu, and divided into seven regions based on mountain ranges, as defined by *Field* [1975]. The quality of these outlines is poor and can introduce errors in regional volume change estimates of up to 10% relative to results using accurate outlines [*Arendt et al.*, in press]. However, we have obtained improved versions of map date (1950 or 1957) outlines for the Western Chugach Mountains [*Manley*, 2005].

4.4 Methods

4.4.1 Calculation of Climate Parameters

Trends in the four climate parameters described below were quantified by the slope of a least-squares linear regression line and are reported as a change per decade. Trends were considered significant at the 95% confidence level ($p < 0.05$). In other words, the trend was significant if there was less than 5% chance that it could result from random noise.

4.4.2 Average Temperature and Total Precipitation

Daily average air temperatures were calculated as the mean of the maximum and minimum daily temperatures, and grouped into annual, winter (October to April) and summer (May to September) categories. Total precipitation measurements include the sum of all liquid and solid precipitation.

4.4.3 Melt Season Length (MSL)

A 30-day running mean was calculated for each surface air temperature time series, and a count was made of all days in a year with positive temperatures which we defined as the melt season length. One MSL value was calculated for each station and each year of record. Using a running mean ensures that temperatures only cross the freezing threshold twice in a year. This removes uncertainty in deciding the start and end dates of a melt season due to unusually warm or cold days during the spring and fall months, respectively. However, in doing this we sacrifice some precision in our delineation of MSL because of smoothing.

4.4.4 Freezing Level Height (FLH)

We linearly interpolated between geopotential heights of atmospheric layers bracketing 0°C to determine the geopotential height at 0°C, assumed to be the height of the freezing level above sea level (FLH). Variations in the mean position of the summer FLH have been found to correlate with variations in equilibrium line altitudes (ELAs), the elevation on a glacier where the net annual balance is zero [*Bradley*, 1975; *Diaz et al.*, 2003]. This is because temperature is a good proxy for melt energy availability, and the freezing level roughly describes the threshold at which melting will begin. The FLH also determines the relative proportions of precipitation reaching the surface as rain or snow during the melt season. FLH values were averaged annually and by season for each station.

4.4.5 Glacier/Climate Interactions

Because the climate parameters described above come from low elevation climate stations, their absolute magnitudes do not represent climate conditions of glaciers, except perhaps near Gulf of Alaska coastal areas where many glaciers descend to sea level. Therefore

we relate changes in glacier balances to changes in climate parameters, on the assumption that factors controlling climate variability are regionally consistent. There is good evidence from previous work that this is true. For example, balances measured at Wolverine and South Cascade glaciers, 2000 km apart, were correlated due to teleconnections with atmospheric and oceanic conditions in the North Pacific [*Hodge et al.*, 1998]. Next we discuss mass balance sensitivity parameters which we use to link glacier and climate variability.

4.4.6 Mass Balance Sensitivities

Mass balance sensitivities describe the change in glacier balance resulting from a change in temperature or precipitation [*Oerlmans et al.*, 1998; *Braithwaite and Zhang*, 1999b; *Braithwaite and Raper*, 2002]. Here we use a degree-day mass balance model which relates positive air temperature and solid precipitation to the summer and winter balances at Gulkana and Wolverine glaciers [*de Woul and Hock*, in press]. Net summer and winter balances were linearly correlated with nearby weather stations data, adjusted to conditions at the equilibrium line altitude using an air temperature lapse rate. The lapse rate was tuned to obtain the best fit between the positive air temperatures and the summer balances. Sensitivities were calculated by re-running the model and perturbing the temperature and precipitation records by some fixed amount, and comparing the modeled and measured values. We use Gulkana Glacier sensitivities ($S_t = -0.65$ m yr^{-1} $^{\circ}$C^{-1}; $S_p = 0.04$ m yr^{-1} 10%$^{-1}$) for glaciers in a continental climate (Alaska Range), Wolverine Glacier sensitivities ($S_t = -0.84$ m yr^{-1} $^{\circ}$C^{-1}; $S_p = 0.23$ m yr^{-1} 10%$^{-1}$) for maritime glaciers (Coast, Kenai, St.Elias, Western Chugach and Wrangell), and McCall Glacier ($S_t = -0.10$ m yr^{-1} $^{\circ}$C^{-1}; $S_p = 0.05$ m yr^{-1} 10%$^{-1}$) for high Arctic Glaciers (Brooks Range; Table 4.1). We assume an error in mass balance sensitivities of 0.1 m yr^{-1} $^{\circ}$C^{-1} [*Braithwaite and Zhang*, 1999a].

In the literature, the sensitivities used here are known as "static", indicating they represent the changes that would occur if the glacier surface geometry did not change with time. In reality, most modeling studies use mass balances that have been affected by the changing surface geometry, so that the resulting sensitivities are not necessarily static. We lack sufficient information to account for the role of dynamic glacier adjustments to climate but discuss their potential effects on our calculations in a later section.

4.5 Climate Changes in Northwestern North America

We begin the presentation of our results by providing a broad overview of climatic variability in NW N. A. . Our goal is to obtain an idea of large scale regional patterns in climate which will form the basis of synoptic interpretations in a later section. This justifies our inclusion of many climate stations which may be some distance from the glacierized regions. Also, we use the same subset of years (1950 to 2002) for these large scale analyses, even though the glaciers may have been measured in different years. For the surface climate data we show time series of temperature, precipitation and MSL for Juneau, Fairbanks and Barrow (stations 33, 22 and 5) to illustrate typical climate trends through time (Figures 4.3, 4.4, 4.5 and 4.6).

4.5.1 Air Temperature

About 50% of stations had significant increases in summer temperature, and 80% of stations had significant increases in winter temperature (0.20 ± 0.08 and 0.38 ± 0.15°C (decade)$^{-1}$ respectively (Table 4.3; Figure 4.7)). Temperature increases were largest at interior stations during the winter, with maximum values occurring at Mayo, station 43 (0.61°C (decade)$^{-1}$). Significant temperature decreases occurred at only two stations in winter (Paxson and Seward, stations 54 and 59) and one station in summer (Kasilof 3 NW, station 34).

4.5.2 Total Precipitation

Only 17% of stations had significant changes in total annual precipitation (Table 4.3; Figure 4.8). Large increases occurred at Seward and Yakutat, stations 59 and 77 (83 and 230 mm (decade)$^{-1}$ respectively) and large decreases occurred at Annette Island and Ketchikan, stations 3 and 36 (-201 and -143 mm (decade)$^{-1}$ respectively). Time series for individual stations illustrate the variability in long-term precipitation trends between stations (Figure 4.5).

4.5.3 Melt Season Length

23% of stations had significant changes in MSL (Table 4.3; Figure 4.9). Large and significant increases occurred at southern coastal stations including Seward and Yakutat (stations 59 and 77). Barrow, Nicholson and Tuktoyaktuk (stations 5, 49 and 71) on the northern Arctic coast had increases between 1.9 to 4.2 days (decade)$^{-1}$. Increases in the interior were generally of smaller magnitude than in maritime areas. Only 9% of stations had a decrease in MSL.

4.5.4 Freezing Level Height

Annual FLH increased everywhere in NW N. A. during 1950 to 2002 with the largest increases (30 to 40 m (decade)$^{-1}$) in northern Yukon Territory (Table 4.3; Figure 4.10). Summer FLH increased in western Alaska (20 to 30 m (decade)$^{-1}$) and decreased in southeastern Alaska and Yukon (-10 to 0 m (decade)$^{-1}$, Figure 4.11), while winter (October to April) FLH increased in all but the western fringe of Alaska, with the largest changes (40 to 50 m (decade)$^{-1}$) in interior Yukon Territory (Figure 4.12).

4.5.5 Discussion of Large Scale Climate Patterns

In general, the climate of NW N. A. is showing a strong and significant signal of increasing temperatures but a weak signal of increasing precipitation. Winter warming is more pronounced than summer and is largest at interior locations. MSL increases are larger at maritime regions than at interior locations, and FLH is increasing nearly everywhere in NW N. A. .

Our findings are broadly consistent with other climatic summaries. *Stafford et al.* [2000] analyzed 25 stations in Alaska from 1949 to 1998 and found winter, spring and summer temperature increases, and a mix of small increases and decreases in autumn. They found temperature increases of 2.2°C in interior Alaska in the winter (December to February), which compares well with our value of 2.4°C. The discrepancy is due to different choices of years and the fact that we include more months in our designation of the winter season. In general, our results show smaller differences between summer and winter temperature changes than other studies because we defined two rather than four seasons.

4.6 Glacier/Climate Comparisons

In this section we narrow our analysis of the climatic datasets to those closest to the glacerized regions. We report glacier and climate changes for each region of NW N. A. and model their changes using the sensitivity parmeters described above. We choose time intervals in the climate data so that they span the entire time period sampled by both the early and recent period glacier measurements. We determine regional changes in average net balance, the difference between the later and earlier period denoted $\Delta\bar{b}$, by taking the arithmetic rather than area-weighted mean of values. Also, the following analysis does not formally account for adjustments of glacier geometry during the period of altimetry measurements. In reality, as climate changes, a glacier responds by redistributing mass, changing its length and surface elevation to achieve a more stable geometry. We lack information to account for these dynamic adjustments, and we discuss the implications of ignoring them in a later section. Tidewater, lake calving and surge-type glaciers introduce additional dynamical complications and are not linked in any simple way to climate. We therefore consider glaciers in two separate categories, those that are only land terminating, and all others including tidewater and lake terminating glaciers.

4.6.1 Alaska Range

Nine glaciers in the Alaska range were measured during the spring of 1995/96 and spring or summer of 2000/2001 (Table 4.4). Nearly half of the measured glaciers in this region had a positive change in average net balance (DOU, SHA, TAN and TUX), and these glaciers were located in the southern and western (denoted "SW") maritime portions of the Alaska Range. The remaining five glaciers were distributed across the northern and eastern (denoted "NE") interior portion of the range. The resulting regional average change in balance for the entire region was slightly positive ($\Delta\bar{b}$=0.09$\pm$0.5 m yr$-$1; Table 4.5).

We used nine climate stations to represent summer temperature changes in the Alaska Range (Big Delta, Iliamna Airport, Intricate Bay, King Salmon Airport, McKinley Park, Paxson, Paxson River, Puntilla, and Talkeetna). We did not observe either decreases in temperature or increases in precipitation to account for the thickening of the four glaciers in the SW portion of the range. As a result, calculated changes in glacier balance determined using mass balance sensitivities predicted significantly more negative changes

($\Delta\bar{\dot{b}}$=-0.45±0.25 m yr−1) than the average of measured values (Figure 4.13).

Errors due to seasonal differences in snowfall (see Appendix C) are large in this region because our measurements happened to occur during unusually low and high snowfall years. Glaciers in the SW Alaska Range were measured in the spring of 1996 and 2001. NRCS snow course data show that 1996 had the lowest amount of snow during the 18 year record, and 2001 had nearly the highest amount of snow (Figure 4.14). Wolverine Glacier mass balances show similar results, with a net winter balance in 2001 that was 1.7 m w.e. greater than in 1996. Nevertheless, after accounting for seasonal variability in snowfall, the change in balance rate for these four glaciers was positive and exceeded the measurement errors. Therefore, the positive change in average net balance has not been explained by the climate datasets.

Glaciers in the NE Alaska Range were measured during the spring of 1995 and 2000 (with the exception of GIL, first measured in 1996) and also suffer from errors due to snowfall amounts, but to a lesser extent. 1995/2000 were relatively low/high snowfall years, but the range of variability was smaller than in the SW Alaska Range, with a 2000 net winter balance that was 0.52 m w.e. greater than in 1995. The fact that NE Alaska Range glaciers had increases in mass loss while experiencing an increase in precipitation suggests that summer temperatures during 1995 to 2000 were sufficient to overcome the mass gains during the winter season. This is supported by data from Gulkana Glacier which shows increases in winter balance from 1995 to 2000 were offset by strongly negative summer balances, resulting in overall glacier mass loss during the 5 year period.

4.6.2 Brooks Range

We only have repeat measurements on McCall Glacier ($\Delta\dot{b}$=-0.13±0.30 m yr^{-1}, *Nolan et al.* [in press]) which we use to represent the entire Brooks Range. We used temperature data from Inuvik to represent the Brooks Range because previous work has shown that it correlated best with annual mass balances on McCall Glacier [*Rabus and Echelmeyer*, 1998]. Inuvik had a temperature increase of 0.25°C (decade)$^{-1}$. The modeled change in balance was -0.16±0.40 m yr^{-1}, which is slightly more negative than the measured value $\Delta\bar{\dot{b}}$=-0.09±0.03 m yr−1.

4.6.3 Coast Range

The Coast Range glaciers were first measured in summer 1993, 1995 or 1996 and all repeat measurements were made in summer 1999. All six glaciers measured in the Coast Range had an increase in the rate of mass loss from the early to recent period (Table 4.4). The rate of mass loss at LEC was four times larger during the recent period than the early period, but these changes were due to dynamic tidewater glacier instabilities [*O'Neel et al.*, 2001]. TAK was a tidewater glacier in recent times but is presently land terminating [*Motyka and Beget*, 1996], and switched from a regime of positive to negative elevation changes during the early/recent periods.

Eleven climate stations were used to model the changes of glaciers in the Coast Range (Annete Island, Atlin, Beaver Falls, Juneau, Ketchikan, Little Port Walter, Mill Bay, Premier, Sitka Japonski Airport, Sitka Magnetic Obsy. and Stewart). Summer temperature trends ranged between 0.0 to 0.3 °C (decade)$^{-1}$. Precipitation increased at eight stations, up to 80 mm (decade)$^{-1}$, and decreased at the remaining three (-3 to -201 mm (decade)$^{-1}$). The average change in precipitation was not significantly different from zero. Modeled $\Delta\bar{\dot{b}}$ for the Coast Range was -0.69$\pm$0.35 m yr^{-1} (Figure 4.13). This was less negative than the average $\Delta\bar{\dot{b}}$ determined from altimetry measurements of land terminating glaciers (-0.87$\pm$0.40 m yr^{-1}).

4.6.4 Kenai Range

Most of the glaciers in the Kenai Range flow from the Harding Icefield, a large (1800 km^2) icefield with at least 38 glaciers [*Aðalgeirsdóttir et al.*, 1998]. We measured 10 glaciers on the Harding Icefield and two other nearby glaciers beginning in 1994 and 1996, and ending in 1999 and 2001. Measured glacier changes in this region are complex, owing to the dynamic nature of the icefield and the change of many glaciers between tidewater, land or lake terminating, which may explain the poor relationship between glacier and climate changes described below (Table 4.4). The average change in net balance rate was 0.070 $\pm$ 0.30 m yr^{-1} for the land terminating glaciers and 0.060 $\pm$0.40 m yr^{-1} for all glaciers, showing that there was no significant difference between the two groups. Error bars on the measured changes are large due to large differences in snowfall amounts during the two

measurement periods. Like the SW Alaska Range, the Kenai Range had extremely low and high amounts of precipitation during 1996 and 2001 respectively (Figure 4.14), and the four glaciers measured at those times (CHE, DIN, KAC, MCY) had positive changes in average net balance.

Six stations (Cooper Lake Project, Kasilof, Kenai, Homer and Moose Pass, Seward) were used to represent this region. Summer temperatures increased by 0.1 to 0.3 °C $(\text{decade})^{-1}$, except at Kasilof, where the summer temperatures changed by -0.2 °C $(\text{decade})^{-1}$. Precipitation changes ranged between -6.0 to 83 mm $(\text{decade})^{-1}$. The predicted change in average balance was -0.33 $\pm$ 0.35 m yr^{-1} which is more negative than the measured change of 0.080 $\pm$ 0.42 m yr^{-1} but still within the range of reported errors.

4.6.5 St. Elias Mountains

The St. Elias Mountains have more glacerized areas (about 40,000 km^2) than any other region in this study and include the two largest glaciers in North America, the Bering (BER) and Malaspina (MAL) glaciers. The change in average balance on Bering Glacier was large ($\Delta\bar{\dot{b}}$= -2.3$\pm$0.10 m yr^{-1}) from the early to recent period. In 1995 the glacier surged [*Muskett et al.*, 2003], resulting in a large drawdown of mass that could melt more rapidly at low elevations, and a fracturing of the surface increasing the surface area exposed to solar radiation. Malaspina Glacier had small changes ($\Delta\bar{\dot{b}}$= -0.040$\pm$0.20 m yr^{-1}) but the uncertainty of these measurements is large due to complex dynamics of the piedmont lobe, part of which surged during our measurement period, and the relatively small area of the glacier actually sampled by the altimetry surveys.

Overall there was only a small difference between average balance changes for land terminating and all glaciers measured in this region (-0.74 and -0.78$\pm$0.40 m yr^{-1} respectively). The glaciers were measured first in 1995 or 1996 and later in 2000, and the difference in snowdepths between these two years was relatively small (Figure 4.14).

Climate stations in this region are sparse and we rely only on measurements at Cordova, Haines Junction and Yakutat. Temperatures increased by 0.1 to 0.2 °C $(\text{decade})^{-1}$. Precipitation increased by only 20 to 30 mm $(\text{decade})^{-1}$ at Cordova and Haines Junction, but very a large increase occurred at Yakutat (230 mm $(\text{decade})^{-1}$). We will assume this large increase in precipitation represented increases in snowfall at higher elevations;

however we note that snowfall records at Yakutat (located at sea level) indicate snowfall amounts actually decreased during this time. The modeled change in glacier balance was -0.55±0.30 m yr^{-1}. This is less negative than the observed value for land terminating glaciers ($\Delta\dot{\bar{b}}$=-0.74±0.4 m yr−1), but within the range of reported errors.

4.6.6 Wrangell Mountains

We have no repeat measurements of glaciers in the Wrangell Mountains.

4.6.7 Western Chugach Mountains

We have repeat altimetry measurements on eight glaciers in the Western Chugach Mountains. All glaciers were measured first on 8 August 2000 (except for Scott Glacier, measured on 21 June 2000) and later on 4 or 5 September 2004. Because data were collected in the fall when the glacier had a minimum snowcover, it was not necessary to account for differences in snow depth. Therefore repeat measurement errors are smaller here than in the other regions.

On average, glaciers in the Western Chugach Mountains had the most negative change in glacier balance of any region. For land terminating glaciers, $\Delta\dot{\bar{b}}$ = -1.0 ± 0.20 m yr^{-1}, while for all glaciers, including tidewater and lake terminating, $\Delta\dot{\bar{b}}$ = -1.9±0.20 m yr^{-1}. The change in balance rate nearly doubled when we included tidewater glaciers because of the large increase in mass loss recorded at Columbia Glacier ($\Delta\dot{\bar{b}}$= -6.0±0.10 m yr^{-1}). This change is the largest in our sample and occurred due to the unstable retreat of this tidewater glacier [*O'Neel et al.*, 2005].

We used climate data from stations Cordova M K Smith AP, Matanuska AES and Valdez WSO with measured increases in summer temperature of 0.1 to 0.2°C $(decade)^{-1}$. Precipitation changes ranged between -4.1 to 53 mm $(decade)^{-1}$. The modeled $\Delta\dot{\bar{b}}$ was -0.69±0.35 m yr^{-1}. This is less negative than the average of altimetry measurements for land terminating glaciers but within the reported range of errors.

Mass balance measurements at Gulkana and Wolverine, and independent measurements on Black Rapids Glacier, show that extremely high temperatures during summer 2004 resulted in the most negative summer and net balances on record [*Truffer et al.*, in

press]. Our altimetry measurements in the Chugach Mountains record the effects of this extreme summer and are the most likely reason for the large increase in rates of mass loss relative to the other regions.

4.6.8 Summary and Discussion of Glacier/Climate Comparisons

In all regions, trends in low elevation climate station measurements of temperature and precipitation predict glacier changes measured by airborne altimetry measurements within reported error limits. The largest differences between predicted and measured values occurred in the Alaska and Kenai Ranges which may indicate a different climate regime has occurred at high elevations that was not represented by the low elevation climate station. Interpreting measurements in these two regions is complicated by large seasonal differences in snowcover and hence the density of ice and snow near the surface. This is a common problem in many altimetry studies, especially those carried out over relatively short timescales [*McConnell et al.*, 2000; *Thomas et al.*, 2001; *Rignot et al.*, 2003]. The complex tidewater dynamics of the Harding Icefield, from which most of the measurements in the Kenai Range were obtained, also obscures the glacier/climate interpretation. Tidewater glacier retreat may be initiated by climatic change, but once started, can progress unstably and independently of climate [*Meier and Post*, 1987]. In the Coast, St. Elias and Western Chugach Regions, the predicted values underestimated the observed mass losses. This may be explained by the fact that we did not consider dynamic glacier adjustments, as discussed below. In addition, different glaciers have different geometries, described by the area-altitude distribution. This means that each glacier will sample the climate differently and have a show different patterns of response, even if the climate signal in a region is the same for all glaciers.

In general, changes in summer temperature appear to be driving the increased rates of mass loss of glaciers in NW N. A. , in agreement with the findings of *Rasmussen and Conway* [2003]. However the role of large increases in winter temperatures is not obvious and should not be ignored [*Tangborn*, 2003]. At high polar latitudes or in continental regions, glaciers rarely experience above freezing temperatures during winter months, and winter temperature shifts probably have little effect on the glacier mass balance. The exception to this is polar glaciers which respond to increases in near-surface ice temperatures via

a reduction in superimposed ice formation, having a negative effect on glacier mass balance. However, increased temperatures can provide additional energy to the atmosphere causing increased rates of evaporation and precipitation. For example, Wolverine Glacier experienced warming temperatures during 1976 to 1988, but also had increases in precipitation which resulted in overall neutral or slightly positive mass balances [*Mayo and March*, 1990].

To assess the role of winter temperature changes, we plotted the mean position of winter FLH relative to the distribution of glacier area in each region. The FLH in polar (Brooks) and continental (Alaska and Wrangell) regions was near or below the lowest elevation glaciers (Figure 4.15). In these regions winter warming, which would cause an increase in the winter FLH, would have little or no effect on the glacier mass balance. In contrast, the four maritime regions (Coast, Kenai, St.Elias and Western Chugach) have mean winter FLH values above 6 to 27% of the glacier ablation areas. It is therefore likely that maritime glaciers, at least those which have area at low elevations, melt not only during the summer season as defined in this study. Changes in winter temperatures, which result in an increase in the FLH, expose more of the glacier area to above freezing temperatures. This would have two effects: there would be an increase in available thermal energy causing surface melting, and any precipitation which falls at those elevations would occur as rain rather than snow [*Diaz et al.*, 2003]. Both effects cause more negative mass balances at the glacier surface. The magnitude of this effect would depend on the magnitude of the shift in FLH, but also on the distribution of glacier area with elevation. For example, glaciers with large amounts of surface area near the location of the FLH (see Figure 4.15) would be more sensitive to changes in the FLH than those glaciers with small amounts of surface area near the FLH.

4.7 Accounting for Glacier Dynamics

The response of the volume of a glacier to climate is complicated because the changing surface configuration acts as a feedback which affects the response. Without feedback, glacier volume would decrease indefinitely in a constantly unfavorable climate, that is, one with increasing temperatures or decreasing precipitation. In practice, glaciers usually attain a new equilibrium volume through terminus retreat, reducing the amount of area at

low elevations where balances are most negative. An opposite, destabilizing effect occurs as the glacier surface elevation decreases, however this effect is usually secondary to those occurring due to terminus changes. The evolving surface configuration, and therefore the feedback process, can be approximately described by theories of glacier dynamics.

Consider a glacier which responds very slowly to climate, in the sense that the time scales for response are long compared to the intervals over which we measure volume changes. In this case all the balances, and the volume changes (the cumulative balances), would be "static", in the sense that they would not be influenced by the changing glacier surface. In other words, feedback would be unimportant because the time is too short for the surface to change significantly. In the terminology of *Elsberg et al*. [2001], the cumulative balances would be the same as the "reference surface" balances, the balances that would occur on a fixed surface. By considering the difference between the conventional and reference surface balances, one can get an idea of how large the feedback effects can be, and therefore the order of magnitude of the errors associated with an incomplete or missing theory of glacier dynamics. Reference surface balances have been calculated for Gulkana and Wolverine Glaciers [*Harrison et al.*, 2005]. Over a 30 year period, the cumulative reference surface balances for these glaciers were more negative than the conventional ones by about 22% and 2% respectively. This shows that at Gulkana Glacier, dynamic effects are significant over a 30 year period and could be slightly larger over the longer period of our measurements.

Our method for calculating mass balance sensitivities (Section 4.4.6) used conventional balances at Gulkana and Wolverine glaciers to calibrate the mass balance model. Therefore, the resulting sensitivities do include dynamic feedback effects. There is no reason to assume these dynamic effects should apply to other glaciers, but the above analysis shows the magnitude of errors we might expect when feedback is not given proper treatment. However, we expect that the errors due to dynamic feedback effects are probably on the same order of magnitude as the glacier measurement errors, and thus in retrospect it seems reasonable to have neglected them. Over longer intervals the dynamical effects would be more important. It may be possible to model these effects, but it would require knowledge of glacier ice thickness and flow properties which is rarely available.

The above considers feedback effects occurring as the glacier geometry adjusts during

the period of altimetry measurements. Additional complications arise when considering the fact that glaciers, because they have a delayed response to climate, may be changing due to climatic events which occurred prior to the measurement period [*Jóhannesson et al.*, 1989; *Harrison et al.*, 2001, 2003]. It is possible that, during a period when the climate is trending toward more favorable conditions for glaciers, the glacier could be losing volume. This could occur, for example, when the glacier is over-extended and has large amounts of area at low elevations. This delayed response to climate could account for some of the positive glacier volume changes measured in the Alaska and Kenai Mountains. The glaciers may have been gaining mass even though the present climate conditions were unfavorable or neutral. We suspect that this is not the case because we would expect such a signal to be more widespread in our dataset. It is more likely that the positive changes were due to seasonal variability in surface accumulation which complicated the near surface density profiles, as discussed in Section 4.6.8.

4.8 Synoptic Climate Conditions

In this section we summarize large-scale climatic conditions in NW N. A. during the past half century and discuss their implications for our measurements. Temperature patterns in NW N. A. depend on a combination of synoptic scale climate signals such as the Pacific Decadal Oscillation (PDO), the positioning of the polar jet stream, the phase of the El Niño Southern Oscillation (ENSO), and other regional scale local effects such as radiative cooling and winds [*Papineau*, 2001]. The PDO consists of low frequency (20-30 year) oscillations in North Pacific sea level pressure and the strength of low pressure systems frequenting the southwestern regions of Alaska (the "Aleutian Low") which drives broad patterns in northwestern North American surface air temperatures [*Mantua et al.*, 1997]. Superimposed on these trends are 1-5 year duration ENSO events, or oscillations in the tropical Pacific ocean circulation which drive global climate patterns [*Ropelewski and Halpert*, 1986]. Alaska climate also depends on the positioning of the polar jet stream, the dividing line between cold polar and warm North Pacific airmasses. Jet stream position is coupled to the strength of the polar vortex whose variations are described by the Arctic Oscillation (AO), an index of sea-level pressure anomalies [*Thompson and Wallace*, 1998]. Local effects can play an important role, especially during the winter season when strong temperature

inversions occur due to radiative cooling at the surface.

In general, a positive phase PDO is associated with high air temperatures and high/low precipitation at maritime/continental regions of Alaska, and a positive phase AO indicates a strong polar vortex so that cold polar air cannot reach lower latitudes. The PDO shifted from a negative mode, which predominated from 1950, to a positive mode during winter 1976-1977. Since 1977 the PDO has generally remained in a positive phase, with some short returns to the negative phase in the late 1980s and early 2000s. The AO fluctuated between phases more frequently than the PDO, but had a large negative to positive shift during in 1989. Time series of environmental parameters provide independent empirical evidence for both 1977 and 1989 North Pacific climate changes, commonly referred to as "regime shifts" [*Hare and Mantua*, 2000].

Regime shifts appear in most Alaska climate records during the past half century and have been expressed in the Gulkana and Wolverine mass balance time series. At Gulkana Glacier, the rate of mass loss increased after 1977, and again more rapidly after 1989, while Wolverine Glacier gained mass after 1977 but lost mass rapidly after 1989 [*Trabant et al.*, 2003]. All of these changes are consistent with the general climatic expressions of the PDO and AO. The mass gains at Wolverine occurred because PDO-induced maritime precipitation increases had a greater effect on the mass balance than temperature increases. In the past decade, both glaciers have shown coherent, rapid losses in mass that are less tied to large scale oscillation patterns [*March*, 2003].

Our altimetry measurements lack the temporal resolution necessary to make definite inferences about the role of regime shifts. Considering the simplest case, suppose the regime shifts can be expressed as a step change from one constant state of climate to another. In the theoretical response of glaciers to changing climate, this step change would result in a rapid initial glacier volume change, followed by continued volume adjustments that decrease exponentially with time [*Oerlemans*, 1986; *Harrison et al.*, 2003]. If the 1977 and 1989 regime shifts were the primary climate signals driving the glacier change, we would have observed a smaller rate of volume loss in the recent period. The glaciers would still be losing volume to adjust to the shifted climate, but the rate would always be decreasing with time, because glaciers have a fading "memory" to past climate conditions. The overall increased rate of mass loss during the recent period would therefore suggest a recent

climatic forcing that has not been expressed in the climatic indicies. For example, the AO has been generally neutral since 1999 during a period of rapid glacier melting.

The temporal spacing of our altimetry measurements complicates this simple picture. In the early period, any random fluctuations will tend to be damped because of the relatively long period over which the measurements were averaged. In the recent period, just one year with particularly high summer temperatures can result in a volume loss that is greater than that which occurred in the early period.

4.9 Conclusions

Low elevation climate station data in NW N. A. show that, during the past half century, winter and summer temperatures have increased by about 0.4 ± 0.2 and 0.2 ± 0.1°C (decade)$^{-1}$ respectively. Precipitation trends are more difficult to quantify, but the data suggest an overall increase. Temperature increases were largest at interior locations. The length of the summer melt season increased at nearly all stations, with the greatest increases occurring at the coastal station. Freezing level heights increasing nearly everywhere in NW N. A. .

We have analyzed glacier changes over a long, early period (1950/70s to 1990s/2000s) and a short, recent period, each of which require special treatment when considering their links to climatic changes. The early measurements cover several decades which may be comparable to the response times for glaciers to changing climate [*Jóhannesson et al.*, 1989; *Harrison et al.*, 2001]. This means that the dynamic adjustment of the glacier geometry to climate should be considered. The recent, short timescale measurements, while more accurate than the early period measurements due to repeat altimetry along the same flight lines, are subject to errors due to annual variability in accumulation and ablation. Further complications arise because many glaciers in NW N. A. , such as tidewater or surge-type glaciers, have changes which are dominated by dynamic cycles, with low order effects occurring due to climate.

Despite these complications, we have measured enough glaciers in NW N. A. to observe a coherent signal in glacier mass loss. These losses are indicators of a changing climate in NW N. A. and provide a method for assessing regional climate patterns in areas where measurements are sparse. We find that glaciers in over half of the regions studied

have lost mass at a rate consistent with that modeled by data from low elevation climate stations. In the remaining regions, the mismatch between predicted and measured changes might indicate that low elevation stations are not representative of mountain conditions. However, we suspect that the lack of representative precipitation data is a key factor in these areas.

Increasing summer temperatures appear to account for the recent glacier changes, but more work is required to understand the role of even larger increases in winter temperatures, especially in maritime regions. We find that maritime glaciers are sensitive to changes in the winter freezing level heights which fluctuates around the elevation of the ablation zone of these glaciers and might be causing increased melting and reduced snow accumulation during the winter. Substantiation of this will require measurements of climatic conditions in mountain regions. In particular, the Wrangell Mountains, containing a large amount of glacier ice in Alaska, is very remote and has no representative climate data or available repeat altimetry profiles. Annual and seasonal mass balance measurements are crucial to provide corrections to short-timescale altimetry measurements and to calculate mass balance sensitivity parameters used to relate glacier and climate changes.

Future work should examine new climate reanalysis grids [*Uppala et al.*, 2005] which are available at a resolution several times better than the NCEP reanalysis used here. These grids might provide the resolution necessary to resolve climate variability within glacier regions, such as differences in temperature and precipitation regimes on different sides of a mountain range. Gridded climate data would be more representative of regional changes than point measurements, and might provide information necessary to divide mountain ranges into smaller, climatologically similar subregions.

Bibliography

ACIA (2004), Impacts of a warming Arctic, *Tech. rep.*, Arctic Climate Impact Assessment Report, Arctic Council.

Alaska Climate Center (2005), Temperature changes in Alaska. URL: http://climate.gi.alaska.edu/ClimTrends/Change.

Aðalgeirsdóttir, G., K. Echelmeyer, and W. Harrison (1998), Elevation and volume changes on the Harding Icefield, Alaska, *Journal of Glaciology*, *44*(148), 570–582.

Arendt, A., K. Echelmeyer, W. Harrison, C. Lingle, S. Zirnheld, V. Valentine, B. Ritchie, and M. Druckenmiller (in press), Updated estimates of glacier volume changes in the Western Chugach Mountains, Alaska, USA and a comparison of regional extrapolation methods, *Journal of Geophysical Research*.

Arendt, A. A., K. A. Echelmeyer, W. D. Harrison, C. S. Lingle, and V. B. Valentine (2002), Rapid wastage of Alaska glaciers and their contribution to rising sea level, *Science*, *297*, 382–386.

Barry, R. G. (1990), Changes in mountain climate and glacio-hydrological responses, *Mountain research and development*, *10*, 161–170.

Bitz, C., and D. Battisti (1999), Interannual to decadal variability in climate and the glacier mass balance in Washington, Western Canada, and Alaska, *Journal of Climate*, *12*, 3181–3196.

Bradley, R. (1975), Equilibrium-line altitudes, mass balance, and July freezing-level heights in the Canadian high Arctic, *Journal of Glaciology*, *14*(71), 267–273.

Braithwaite, R. J., and S. C. Raper (2002), Glaciers and their contribution to sea level change, *Physics and Chemistry of the Earth*, *27*, 1445–1454.

Braithwaite, R. J., and Y. Zhang (1999a), Relationships between interannual variability of glacier mass balance and climate, *Journal of Glaciology*, *45*(151), 456–462.

Braithwaite, R. J., and Y. Zhang (1999b), Modelling changes in glacier mass balance that may occur as a result of climate changes, *Geografiska Annaler*, *81A*(4), 489–496.

Chao, Y. (2000), Pacific interdecadal variability in this century's sea surface temperatures, *Geophysical Research Letters*, *27*(15), 2261–2264.

Cox, L. H., and R. S. March (2004), Comparison of geodetic and glaciological mass balance, Gulkana Glacier, Alaska, USA, *Journal of Glaciology*, *50*(170), 363–370.

de Woul, M., and R. Hock (in press), Static mass balance sensitivity of Arctic glaciers and ice caps using a degree-day approach, *Annals of Glaciology*, *42*.

Diaz, H. F., J. K. Eischeid, C. Duncan, and R. S. Bradley (2003), Variability of freezing levels, melting season indicators, and snow cover for selected high-elevation and continental regions in the last 50 years, *Climatic Change*, *59*(1 - 2), 33–52.

Echelmeyer, K., W. Harrison, C. Larsen, J. Sapiano, J. Mitchell, J. DeMallie, B. Rabus, G. Aðalgeirsdóttir, and L. Sombardier (1996), Airborne surface profiling of glaciers: A case-study in Alaska, *Journal of Glaciology*, *42*(142), 538–547.

Elsberg, D. H., W. D. Harrison, K. A. Echelmeyer, and R. M. Krimmel (2001), Quantifying the effects of climate and surface change on glacier mass balance, *Journal of Glaciology*, *47*(159), 649–658.

Field, W. O. (1975), *Mountain Glaciers of the Northern Hemisphere*, vol. 2, chap. 3, pp. 299–492, U.S. Army Cold Regions Research and Engineering Laboratory, Technical Information Analysis Center, Hanover, NH. U.S. Army Cold Regions Research and Engineering Laboratory, Technical Information Analysis Center.

Frich, P., L. Alexander, P. Della-Marta, B. Gleason, M. Haylock, A. Klein Tank, and T. Peterson (2002), Observed coherent changes in climatic extremes during the second half of the twentieth century, *Clmate Research*, *19*, 193–212.

Hare, S. R., and N. J. Mantua (2000), Empirical evidence for North Pacific regime shifts in 1977 and 1989, *Progress in Oceanography*, *47*, 103–145.

Harrison, W., D. Elsberg, K. Echelmeyer, and R. Krimmel (2001), On the characterization of glacier response by a single time scale, *Journal of Glaciology*, *47*(159), 659–664.

Harrison, W., D. Elsberg, and L. Cox (2005), Different mass balances for climatic and hydrologic applications, *Journal of Glaciology*, *accepted*.

Harrison, W. D., C. F. Raymond, K. A. Echelmeyer, and R. M. Krimmel (2003), A macroscopic approach to glacier dynamics, *Journal of Glaciology*, *49*(164), 13–21.

Hodge, S. M., D. C. Trabant, R. M. Krimmel, T. A. Heinrichs, R. S. March, and E. G. Josberger (1998), Climate variations and changes in mass of three glaciers in Western North America, *Journal of Climate*, *11*, 2161–2179.

IPCC (2001), Climate Change 2001: The Scientific Basis Contribution of Working Group I to the Third Assessment Report., *Tech. rep.*, Cambridge.

Jóhannesson, T., C. Raymond, and E. Waddington (1989), Time-scale for adjustment of glaciers to changes in mass balance, *Journal of Glaciology*, *35*(121), 355–369.

Kalnay, E., M. Kanamitsu, R. Kistler, W. Collins, D. Deaven, L. Gandin, and M. Iredell (1996), The NCEP/NCAR 40-year reanalysis project, *Bulletin of the American Meteorological Society*, *77*(3), 437–471.

Keyser, A. R. (2000), Simulating the effects of climate change on the carbon balance of North American high-latitude forests, *Global Change Biology*, *6*(s1), 185–195.

Manley, W. (2005), *Glaciers of Alaska*, chap. Geospatial inventory and analysis of glaciers: A case study for the eastern Alaska Range, USGS Professional Paper 1386-K.

Mantua, N. J., S. R. Hare, Y. Zhang, J. M. Wallace, and R. C. Francis (1997), A Pacific interdecadal climate oscillation with impacts on salmon production, *Bulletin of the American Meteorological Society*, *78*(6), 1069–1079.

March, R. (2003), Mass balance, meteorology, area altitude distribution, glacier-surface altitude, ice motion, terminus position, and runoff at Gulkana Glacier, Alaska, 1996 balance year, *Tech. rep.*, USGS.

Mayo, L., and R. March (1990), Air temperature and precipitation at wolverine glacier, alaska; glacier growth in a warmer, wetter climate, *Annals of Glaciology*, *14*, 191–194.

Mayo, L., D. Trabant, and R. March (2004), A 30-year record of surface mass balance (1966-95), and motion and surface altitude (1975-95) at Wolverine Glacier, Alaska, *U.S. Geological Survey open-file report*, *2004-1069*, 105.

McConnell, J. R., E. Mosley-Thompson, D. H. Bromwich, R. C. Bales, and J. D. Kyne (2000), Interannual variations of snow accumulation on the Greenland ice sheet (1985-1996): New observations versus model predictions, *Journal of Geophysical Research*, *105*, 4039–4046, doi:10.1029/1999JD901049.

Meier, M., and A. Post (1987), Fast tidewater glaciers, *Journal of Geophysical Research*, *92*(B9), 9051–9058.

Moore, G., G. Holdsworth, and K. Alverson (2002), Climate change in the North Pacific region over the past three centuries, *Nature*, *420*, 401–403.

Motyka, R. J., and J. E. Beget (1996), Taku Glacier, southeast Alaska, U.S.A.: Late holocene history of a tidewater glacier, *Arctic and Alpine Research*, *28*(1), 42–51.

Muskett, R., C. S. Lingle, W. V. Tangborn, and B. T. Rabus (2003), Multi-decadal elevation changes on Bagley Ice Valley and Malaspina Glacier, Alaska, *Geophysical Research Letters*, *30*(16), 1857–1860.

Nolan, M., A. Arendt, B. Rabus, and L. Hinzman (in press), Volume change of McCall Glacier, Arctic Alaska, from 1956 to 2003, *Annals of Glaciology*.

Oerlemans, J. (1986), Glaciers as indicators of a carbon dioxide warming, *Nature*, *320*(17), 607–609.

Oerlemans, J. (2001), *Glaciers and Climate Change*, A.A. Balkema, Brookfield, Vt.

Oerlemans, J., and J. Fortuin (1992), Sensitivity of glaciers and small ice caps to greenhouse warming, *Science*, *258*(5079), 115–117.

Oerlmans, J., B. Anderson, A. Hubbard, P. Huybrechts, et al. (1998), Modelling the response of glaciers to climate warming, *Climate Dynamics*, *14*, 267–274.

O'Neel, S., K. Echelmeyer, and R. Motyka (2001), LeConte Glacier, Alaska, U.S.A., *Journal of Glaciology*, *47*(159), 567–578.

O'Neel, S., W. Pfeffer, R. Krimmel, and M. Meier (2005), Evolving force balance at Columbia Glacier, during its rapid retreat, *Journal of Geophysical Research*, *110*(F3), 3012+–, doi:10.1029/2005JF000292.

Papineau, J. (2001), Wintertime temperature anomalies in Alaska correlated with ENSO and PDO, *International Journal of Climatology*, *21*(13), 1577–1592.

Paterson, W. (1994), *The Physics of Glaciers*, 3rd ed., Elsevier Science Ltd., Oxford, England.

Rabus, B., and K. Echelmeyer (1998), The mass balance of McCall Glacier, Brooks Range, Alaska, U.S.A.; its regional revelance and implications for climate change in the Arctic, *Journal of Glaciology*, *44*(147), 333–351.

Raper, S., and R. Braithwaite (2006), Low sea level rise projections from mountain glaciers and icecaps under global warming, *Nature*, *439*, 311–313.

Rasmussen, L., and H. Conway (2003), Climate and glacier variability in western north america, *Journal of Climate*, *17*, 1804–1815.

Rignot, E., A. Rivera, and G. Casassa (2003), Contribution of the Patagonia Icefields of South America to sea level rise, *Science*, *302*, 434–437.

Ropelewski, C., and M. Halpert (1986), North American precipitation and temperature patterns associated with the El Niño/Southern Oscillation (ENSO), *Monthly Weather Review*, *114*(12), 2352 – 2362.

Sapiano, J., W. Harrison, and K. Echelmeyer (1998), Elevation, volume and terminus changes of nine glaciers in North America, *Journal of Glaciology*, *44*(146), 119–135.

Stafford, J., G. Wendler, and J. Curtis (2000), Temperature and precipitation of Alaska: 50 year trend analysis, *Theoretical and Applied Climatology*, *67*, 33–44.

Tangborn, W. (2003), Winter warming indicated by recent temperature and precipitation anomalies, *Polar Geography*, *27*(4), 320–338.

Thomas, R., B. Csatho, C. Davis, C. Kim, W. Krabill, S. Manizade, J. McConnell, and J. Sonntag (2001), Mass balance of higher-elevation parts of the Greenland ice sheet, *Journal of Geophysical Research*, *106*, 33,707–33,716, doi:10.1029/2001JD900033.

Thompson, D. W., and J. M. Wallace (1998), The Arctic Oscillation signature in the wintertime geopotential height and temperature fields, *Geophysical Research Letters*, *25*(9), 1297–1300.

Trabant, D., R. March, L. Cox, W. Harrison, and E. Josberger (2003), Measured climate induced volume changes of three glaciers and current glacier-climate response prediction, SEARCH Open Science Meeting, Arctic Research Consortium of the United States (ARCUS).

Truffer, M., W. Harrison, and R. March (in press), Record negative glacier balances and low velocities during the 2004 heat wave in Alaska: Implications for the interpretation by Zwally and others in Greenland, *Journal of Glaciology*.

Uppala, S., et al. (2005), The era-40 re-analysis, *Quart. J. Roy. Meteor. Soc.*, *131*, 2961–3012.

Table 4.1: Mass balance sensitivities (S) to changes in temperature (T+1 K) and precipitation (P+10%) for Gulkana and Wolverine glaciers [*de Woul and Hock*, in press].

Glacier	S_t (m yr^{-1} $^{\circ}$C^{-1})	S_p (m yr^{-1} 10%$^{-1}$)
Gulkana	-0.65	0.04
McCall	-0.10	0.05
Wolverine	-0.84	0.23

Table 4.2: Location and names of NOAA and Environment Canada climate stations in northwestern North America used in this study. "Label" numbers the glaciers in alphabetical order and is used to identify station names on Figure 4.1. The start year 1950 was chosen as the earliest year, even for stations operating prior to that time.

Station	Label	Lat (°N)	Long (°W)	Elevation (m a.s.l.)	Start Year	End Year
Aklavik	1	68.22	-135	1.8	1950	2001
Anchorage Ted Stevens Intl Ap	2	61.19	-150	12.5	1952	2002
Annette Island Ap	3	55.05	-131.57	10.1	1950	2002
Atlin	4	60.75	-137.58	205.4	1950	2000
Barrow W Post-W Rogers Arpt	5	71.28	-156.77	2.7	1950	2002
Barter Is Wso Ap	6	70.13	-143.63	3.7	1950	1988
Beaver Falls	7	55.38	-131.47	3.4	1950	2002
Bethel Airport	8	60.78	-161.83	9.4	1950	2002
Bettles Airport	9	66.92	-151.51	59.7	1951	2002
Big Delta Allen AAF	10	64	-145.72	118	1950	2002
Carcross	11	60.18	-134.7	201.2	1950	2000
Carmacks	12	62.1	-136.3	160	1963	2000
Cassiar	13	59.28	-129.83	328.6	1954	1996
Cold Bay Arpt	14	55.22	-162.73	7.3	1950	2002
College Observatory	15	64.87	-147.83	57.6	1950	2002
Cooper Lake Project	16	60.4	-149.67	46.9	1958	2002
Cordova M K Smith Ap	17	60.5	-145.33	2.7	1950	2002
Dawson	18	59.57	-133.7	97.5	1950	1979
Dease Lake	19	58.42	-130	246	1950	2000
Eagle	20	64.78	-141.2	78.9	1950	2002
Eielson Field	21	64.67	-147.1	50.9	1950	2002
Fairbanks Intl Arpt	22	64.82	-147.85	40.5	1950	2002
Fort Good Hope	23	66.23	-128.65	25	1950	2001
Fort Good Hope2	24	66.25	-128.63	12.8	1950	1966
Ft Mcpherson	25	67.43	-134.88	9.4	1950	1977
Gulkana Airport	26	62.16	-145.46	146	1950	2002
Haines Jct	27	60.48	-133.3	182.6	1950	2000
Homer Arpt	28	59.65	-151.48	6.1	1950	2002
Iliamna Airport	29	59.75	-154.91	17.1	1950	2002
Intricate Bay	30	59.55	-154.5	11.3	1959	2002

Table 4.2: Continued

Station	Label	Lat (°N)	Long (°W)	Elevation (m a.s.l.)	Start Year	End Year
Inuvik	31	68.3	-133.48	20.7	1957	2001
Johnson'S Crossing	32	64.45	-138.22	210.3	1963	1995
Juneau Int'L Arpt	33	58.35	-134.58	1.2	1950	2002
Kasilof 3 NW	34	60.37	-151.38	6.4	1950	1997
Kenai Municipal AP	35	60.58	-151.23	8.5	1950	2002
Ketchikan Intl AP	36	55.35	-131.72	7	1950	2002
King Salmon Arpt	37	58.68	-156.65	4.3	1955	2002
Klondike	38	69.58	-140.18	292.6	1966	2000
Komakuk	39	63.62	-135.87	2.1	1958	1993
Kotzebue Ralph Wein Memorial	40	66.88	-162.6	0.9	1950	2002
Little Port Walter	41	56.38	-134.65	1.2	1950	2002
Matanuska AES	42	61.57	-149.25	15.8	1950	2002
Mayo	43	67.57	-139.83	153.6	1950	2000
McCarthy 1 NE	44	61.43	-142.92	116.1	1968	1983
Mcgrath ARPT	45	62.95	-155.6	30.8	1950	2002
Mckinley Park	46	63.72	-148.97	192.3	1950	2002
Mill Bay	47	55	-129.75	0.9	1950	1959
Moose Pass 3 NW	48	60.5	-149.43	43	1952	2002
Nicholson	49	69.93	-128.97	27.1	1957	1993
Nome Municipal Arpt	50	64.52	-165.45	1.2	1950	2002
Northway Airport	51	62.97	-141.93	159.1	1950	2002
Old Crow	52	68.95	-137.22	76.5	1951	2000
Palmer Job Corps	53	61.6	-149.1	21	1950	1998
Paxson	54	63.05	-145.45	250.9	1960	2002
Paxson River	55	62.95	-145.5	255.7	1968	1979
Pelly Ranch	56	60	-131.18	138.4	1950	2000
Premier	57	56.05	-130.02	125	1950	1996
Puntilla	58	62.08	-152.73	170.1	1950	2002
Seward	59	60.12	-149.45	11.6	1950	2002
Shingle Pt	60	60.17	-132.75	14.9	1957	1993
Sitka Japonski Airport	61	57.03	-135.36	1.5	1950	2002
Sitka Magnetic Obsy	62	57.05	-135.33	6.1	1950	1989
St Paul Island Arpt	63	57.16	-170.22	3.4	1950	2002
Stewart	64	55.95	-129.98	1.5	1950	1967

Table 4.2: Continued

Station	Label	Lat (°N)	Long (°W)	Elevation (m a.s.l.)	Start Year	End Year
Swift River	65	60.93	-129.22	271.6	1966	2000
Talkeetna Ap	66	62.32	-150.09	32.6	1950	2002
Tanana Calhoun Mem Ap	67	65.16	-152.1	21	1950	2002
Teslin	68	60.17	-132.75	214.9	1950	2000
Tonsina	69	61.65	-145.17	146.3	1963	2002
Tuchitua	70	60.93	-129.22	220.7	1967	2000
Tuktoyaktuk	71	69.45	-133	5.5	1957	1993
Unalakleet Field	72	63.88	-160.8	1.5	1950	1998
University Exp Sta	73	64.85	-147.87	44.2	1950	2002
Valdez Wso	74	61.13	-146.35	2.1	1964	2002
Whitehorse	75	60.72	-135.07	215.2	1950	2000
Whitehorse Rdale	76	60.72	-135.02	196	1959	2000
Yakutat State Arpt	77	59.52	-139.63	2.7	1950	2002

Table 4.3: Changes in melt season length (MSL), positive degree days (PDD), annual, winter and summer temperatures (T) and annual precipitation (P) at NOAA and Environment Canada climate stations, in rates per decade. Values in italics are significant at $p < 0.05$.

Label	ΔMSL (days decade^{-1})	ΔPDD (K days decade^{-1})	ΔT$_{annual}$	ΔT$_{winter}$	ΔT$_{summer}$ (K decade^{-1})	ΔPrcp (mm decade^{-1})
Aklavik	1.2	*28.7*	*0.4*	0.3	*0.2*	*11.9*
Anchorage Ted Stevens Intl Ap	0.2	*33.7*	*0.4*	*0.5*	*0.2*	5.7
Annette Island Ap	3.1	43.8	*0.2*	*0.2*	0.1	*-142.5*
Atlin	1.2	23.6	*0.4*	*0.4*	*0.2*	0.5
Barrow W Post-W Rogers Arpt	*4.2*	*23.8*	*0.3*	0.3	*0.3*	-6.8
Barter Is Wso Ap	*2.3*	*34.6*	*0.3*	0.2	*0.2*	-10.0
Beaver Falls	3.1	37.0	*0.2*	*0.2*	0.1	80.4
Bethel Airport	1.0	19.9	*0.4*	*0.4*	0.1	-3.4
Bettles Airport	1.4	*34.7*	*0.5*	*0.5*	*0.2*	11.4
Big Delta Allen AAF	1.3	23.4	*0.4*	*0.5*	0.1	4.4
Carcross	1.1	9.6	*0.3*	0.3	0.1	11.2
Carmacks	1.6	*25.0*	*0.4*	*0.5*	*0.2*	*21.5*
Cassiar	*3.0*	*16.3*	*0.4*	*0.5*	*0.2*	19.4
Cold Bay Arpt	3.7	*37.5*	*0.2*	0.2	*0.2*	*60.2*
College Observatory	0.9	*28.6*	*0.3*	*0.4*	0.1	2.2
Cooper Lake Project	3.6	7.3	*0.2*	*0.3*	0.1	27.3
Cordova M K Smith Ap	*7.1*	*52.1*	*0.3*	*0.4*	*0.2*	29.2
Dawson	*1.9*	*43.4*	*0.5*	*0.5*	*0.2*	6.7
Dease Lake	0.6	10.0	*0.3*	*0.3*	0.0	7.8
Eagle	0.8	12.6	*0.3*	*0.4*	0.1	3.3
Eielson Field	*1.9*	*39.8*	*0.5*	*0.6*	*0.2*	*-17.2*
Fairbanks Intl Arpt	1.4	*37.7*	*0.4*	*0.5*	*0.2*	0.1
Fort Good Hope	0.7	22.0	*0.4*	*0.3*	*0.2*	10.7
Fort Good Hope2	0.5	*24.0*	*0.4*	*0.3*	*0.2*	10.7
Ft Mcpherson	1.0	*34.2*	*0.4*	0.3	*0.2*	11.2
Gulkana Airport	0.7	13.5	*0.3*	*0.4*	0.1	3.8
Haines Jct	1.3	20.7	*0.4*	*0.5*	0.1	*20.0*
Homer Arpt	*5.6*	*70.7*	*0.4*	*0.4*	*0.3*	17.1
Iliamna Airport	2.5	*50.6*	*0.5*	*0.6*	*0.2*	-10.6
Intricate Bay	4.2	*71.8*	*0.5*	*0.6*	*0.3*	24.7
Inuvik	1.7	*35.4*	*0.4*	*0.4*	*0.2*	7.3

Table 4.3: Continued

Label	ΔMSL (days decade^{-1})	ΔPDD (K days decade^{-1})	ΔT_{annual}	ΔT_{winter}	ΔT_{summer}	ΔPrcp (mm decade $^{-1}$)
			(K decade^{-1})			
Johnson'S Crossing	1.5	12.8	*0.3*	*0.4*	0.1	0.9
Juneau Int'L Arpt	*7.3*	*65.4*	*0.4*	*0.4*	*0.2*	*64.6*
Kasilof 3 NW	-1.2	*-30.6*	0.2	*0.4*	*-0.2*	8.3
Kenai Municipal AP	-0.4	*31.3*	*0.4*	*0.4*	*0.2*	-6.1
Ketchikan Intl AP	-0.7	-27.4	0.0	0.0	-0.1	*-201.2*
King Salmon Arpt	*3.9*	*59.2*	*0.4*	*0.5*	*0.2*	-1.8
Klondike	0.8	6.4	*0.2*	0.3	0.1	5.4
Komakuk	*1.9*	*38.2*	*0.4*	0.3	*0.3*	*14.2*
Kotzebue Ralph Wein Memorial	0.2	19.0	*0.3*	0.3	0.1	*12.0*
Little Port Walter	3.5	*62.4*	*0.3*	*0.2*	*0.2*	79.0
Matanuska AES	-0.4	19.8	*0.3*	*0.3*	0.1	-4.1
Mayo	2.1	*43.1*	*0.5*	*0.6*	*0.2*	2.0
McCarthy 1 NE	0.0	7.0	*0.2*	*0.2*	0.0	-4.1
Mcgrath ARPT	1.3	*37.6*	*0.4*	*0.5*	*0.2*	10.0
Mckinley Park	0.8	10.9	*0.3*	0.3	0.1	6.2
Mill Bay	2.0	22.8	*0.2*	*0.2*	0.1	46.7
Moose Pass 3 NW	3.1	*51.5*	*0.4*	*0.5*	*0.2*	9.9
Nicholson	*1.9*	23.4	*0.3*	0.3	0.2	2.0
Nome Municipal Arpt	-0.1	23.2	*0.3*	0.3	0.1	5.8
Northway Airport	1.3	20.6	*0.4*	*0.5*	0.1	6.2
Old Crow	1.4	*34.1*	*0.4*	*0.4*	*0.2*	11.1
Palmer Job Corps	0.2	*30.0*	*0.3*	*0.4*	*0.1*	2.0
Paxson	0.8	-0.1	0.0	*-0.1*	0.1	-0.6
Paxson River	-0.8	4.6	0.1	0.0	0.1	5.7
Pelly Ranch	*1.9*	*27.3*	*0.5*	*0.6*	0.1	8.2
Premier	2.5	22.7	*0.2*	*0.3*	0.1	16.9
Puntilla	1.5	*28.6*	*0.2*	0.2	*0.2*	20.0
Seward	*7.0*	25.7	*0.2*	*0.3*	0.1	*82.8*
Shingle Pt	*2.3*	*36.8*	*0.4*	*0.4*	*0.3*	*24.8*
Sitka Japonski Airport	2.9	*42.6*	*0.2*	*0.2*	0.1	7.5
Sitka Magnetic Obsy	3.7	*50.4*	*0.2*	*0.3*	0.1	13.1
St Paul Island Arpt	0.6	*43.2*	*0.2*	0.1	*0.2*	0.7
Stewart	1.7	29.0	*0.2*	*0.3*	0.1	-3.0

Table 4.3: Continued

Label	ΔMSL (days decade^{-1})	ΔPDD (K days decade^{-1})	ΔT$_{annual}$	ΔT$_{winter}$	ΔT$_{summer}$	ΔPrcp (mm decade $^{-1}$)
			(K decade^{-1})			
Swift River	1.4	14.4	*0.3*	*0.3*	0.1	4.2
Talkeetna Ap	1.1	*43.6*	*0.5*	*0.5*	*0.2*	3.2
Tanana Calhoun Mem Ap	1.9	*43.3*	*0.5*	*0.6*	*0.2*	-4.9
Teslin	1.6	19.3	*0.3*	*0.4*	0.1	2.5
Tonsina	-0.6	-8.9	-0.1	*-0.2*	0.0	-3.8
Tuchitua	*2.1*	17.6	*0.3*	*0.4*	0.1	-8.6
Tuktoyaktuk	*2.3*	*36.4*	*0.4*	*0.3*	*0.3*	6.1
Unalakleet Field	0.1	19.9	*0.4*	*0.4*	0.1	8.6
University Exp Sta	0.7	19.8	*0.3*	*0.3*	0.1	-1.9
Valdez Wso	*3.7*	*44.3*	*0.4*	*0.6*	*0.2*	52.7
Whitehorse	0.3	-1.1	*0.3*	*0.4*	0.0	1.1
Whitehorse Rdale	0.6	13.5	*0.3*	*0.4*	0.1	1.8
Yakutat State Arpt	*6.8*	*42.1*	*0.3*	*0.3*	*0.1*	*230.1*

Table 4.4: Summary of glacier changes, by region, measured by comparison of airborne altimetry and USGS map elevations. "Symbol" is a 3-letter code identifying each glacier"Type" escribes whether the glacier is land terminating (L), lake terminating (LK), tidewater (TW) or surge-type (SGT), and two listed types for a glacier indicate a change in type between the earlier/later time; "Area" is the glacier surface area at the time of the USGS map; $\dot{B}$ is the net balance rate; $\bar{\dot{b}}$ is the average net balance rate; $\Delta\dot{A}$ is the rate of area change. Subscripts "early" and "recent" indicate map-to-profile and profile-to-profile measurements, respectively. Note that $\dot{B}$ of tidewater glaciers include only that portion of the glacier above sea level.

Name	Symbol	Type	Area	$\dot{B}_{early}$	$\dot{B}_{recent}$	$\bar{\dot{b}}_{early}$	$\bar{\dot{b}}_{recent}$	$\Delta\dot{A}$	Map	Profile 1	Profile 2
			(km^2)	($km^3 yr^{-1}$ w.e.)		($m\ yr^{-1}$ w.e.)		($km^2 yr^{-1}$)	Year	Date	Date
Region 1, Alaska											
Black Rapids	BLR	SGT	289.0	0.098±0.041	-0.204±0.013	0.34±0.14	-0.66±0.04	-0.02	1954	5/18/1995	1/1/2000
Double	DOU	L	232.0	-0.170±0.034	0.005±0.010	-0.74±0.15	0.02±0.04	-0.10	1957	5/16/1996	5/14/2001
East Fork Susitna	SEF	L	44.1	-0.014±0.003	-0.028±0.002	-0.32±0.06	-0.64±0.05	-0.01	1950	5/19/1995	6/1/2000
Gillam	GIL	L	131.0	-0.031±0.012	-0.090±0.006	-0.24±0.09	-0.70±0.04	-0.07	1951	4/25/1996	4/28/2000
Gulkana	GUL	L	19.7	-0.008±0.003	-0.014±0.001	-0.45±0.16	-0.79±0.05	-0.04	1954	5/17/1995	6/9/2000
Shamrock	SHA	LK	135.0	-0.013±0.023	0.027±0.006	-0.10±0.17	0.21±0.04	-0.13	1957	5/15/1996	5/14/2001
Tanaina	TAN	LK	168.0	-0.13±0.03	-0.000±0.008	-0.78±0.17	-0.00±0.05	-0.18	1957	5/15/1996	5/14/2001
Turquoise	TUR	L	19.9	-0.018±0.003	-0.018±0.001	-0.90±0.16	-0.92±0.05	-0.01	1957	5/17/1996	5/14/2001
Tuxedni	TUX	L	90.9	-0.065±0.008	0.016±0.004	-0.72±0.08	0.17±0.04	0.04	1957	5/14/1996	5/14/2001
Region 2, Brooks											
McCall	MCC	L	6.4	0.0020±0.0005	0.0030±0.0002	0.35±0.07	0.48±0.03	0.17	1956	7/27/1993	5/1/2003
Region 3, Coast											
Baird	BAI	L	523.0	-0.17±0.07	-0.455±0.033	-0.32±0.13	-0.86±0.06	0.00	1948	6/14/1996	6/1/1999
Leconte	LEC	TW	454.0	-0.23±0.06	-1.088±0.031	-0.52±0.12	-2.37±0.07	-0.04	1948	6/15/1996	5/31/1999
Lemon Creek	LEM	L	14.4	-0.010±0.002	-0.020±0.001	-0.71±0.14	-1.47±0.09	-0.02	1948	5/31/1995	6/4/1999
Mendenhall	MEN	LK	114.0	-0.11±0.01	-0.158±0.006	-0.95±0.11	-1.42±0.05	-0.06	1948	6/3/1995	6/4/1999
Taku	TAK	TW/L	802.0	0.560±0.13	-0.23±0.035	0.69±0.16	-0.28±0.04	0.33	1948	1/1/1993	1/1/1999
Triumph	TRI	L	46.3	-0.018±0.005	-0.08±0.003	-0.40±0.11	-1.71±0.06	-0.01	1948	6/14/1996	6/1/1999

Table 4.4: Continued

Name	Symbol	Type	Area (km^2)	$\dot{B}_{early}$ ($km^3 yr^{-1}$ w.e.)	$\dot{B}_{recent}$ ($km^3 yr^{-1}$ w.e.)	$\bar{\dot{b}}_{early}$ (m yr^{-1} w.e.)	$\bar{\dot{b}}_{recent}$ (m yr^{-1} w.e.)	$\Delta\dot{A}$ ($km^2 yr^{-1}$)	Map Year	Profile 1 Date	Profile 2 Date
Region 4, Kenai											
Aialik	AIA	TW	87.3	0.002±0.03	-0.010±0.006	0.02±0.35	-0.11±0.07	-0.01	1950	5/29/1994	5/18/2001
Bear	BEA	TW/LK	229.0	-0.18±0.04	-0.205±0.009	-0.85±0.19	-1.02±0.04	-0.66	1950	5/28/1994	5/18/2001
Bear Lake	BLK	L	7.1	-0.002±0.001	-0.007±0.000	-0.28±0.11	-0.95±0.07	-0.00	1950	5/28/1994	5/13/1999
Chernof	CHE	L	64.4	-0.043±0.007	-0.016±0.003	-0.75±0.11	-0.34±0.05	-0.34	1950	5/20/1996	5/18/2001
Dinglestadt	DIN	L	73.1	-0.056±0.007	-0.011±0.003	-0.82±0.10	-0.18±0.04	-0.23	1950	5/19/1996	5/18/2001
Exit	EXI	L	41.0	-0.008±0.011	-0.007±0.002	-0.21±0.27	-0.18±0.06	-0.05	1950	5/28/1994	5/28/2001
Holgate	HOL	TW	68.7	-0.021±0.011	-0.007±0.002	-0.31±0.16	-0.10±0.04	-0.04	1950	5/29/1994	5/18/2001
Kachemak	KAC	L	24.4	-0.008±0.003	0.002±0.001	-0.36±0.14	0.07±0.06	-0.06	1951	5/19/1996	5/18/2001
Mccarty	MCY	TW	126.0	0.007±0.020	0.034±0.006	0.06±0.16	0.29±0.05	-0.15	1950	5/19/1996	5/18/2001
Skilak	SKI	L/LK	203.0	-0.066±0.048	-0.050±0.009	-0.33±0.24	-0.26±0.04	-0.27	1950	5/29/1994	5/18/2001
Tustumena	TUS	L	302.0	-0.22±0.06	-0.156±0.012	-0.73±0.18	-0.54±0.04	-0.34	1950	5/29/1994	5/18/2001
Wolverine	WOL	L	18.6	-0.009±0.004	-0.019±0.001	-0.52±0.22	-1.03±0.06	-0.01	1950	5/27/1994	5/13/1999
Region 5, St.Elias											
Bering	BER	SGT	2190.0	-1.656±0.237	-6.508±0.085	-0.77±0.11	-3.10±0.04	0.00	1972	6/10/1995	8/26/2000
Brady	BRA	TW	604.6	-0.233±0.056	-0.592±0.026	-0.39±0.09	-0.97±0.04	0.01	1948	6/4/1995	5/24/2000
Hidden	HID	L	49.5	-0.077 ±0.005	-0.104 ±0.004	-1.63 ±0.09	-2.35 ±0.07	-0.10	1948	6/4/1996	6/23/2000
Kaskawulsh	KAS	L	854.0	-0.474±0.124	-0.440±0.033	-0.57±0.15	-0.52±0.04	-0.60	1977	5/21/1995	5/29/2000
Lamplugh	LAM	TW	141.6	0.051±0.014	-0.027±0.007	0.36±0.10	-0.19±0.05	0.00	1948	6/4/1995	5/24/2000
Malaspina	MAL	SGT	3190.0	-2.904±0.688	-3.037±0.133	-0.91±0.22	-0.95±0.04	0.00	1972	6/5/1995	6/5/2000
Novatak	NOV	L	154.0	-0.136 ±0.012	-0.259 ±0.009	-0.92 ±0.08	-1.88 ±0.06	-0.29	1948	6/4/1996	6/23/2000
Reid	REI	TW	60.2	0.024±0.006	-0.012±0.004	0.40±0.10	-0.20±0.07	-0.00	1948	6/4/1995	5/24/2000
West nunatak	WES	L	115.0	-0.216 ±0.013	-0.274 ±0.008	-1.93 ±0.11	-2.52 ±0.07	-0.10	1948	6/4/1996	6/23/2000
Yakutat East	YKE	L	276.0	-0.772 ±0.038	-1.125 ±0.021	-2.84 ±0.14	-4.25 ±0.08	-0.17	1948	6/4/1996	6/23/2000
Yakutat West	YKW	L	193.0	-0.435 ±0.016	-0.552 ±0.011	-2.35 ±0.08	-3.15 ±0.06	-0.31	1948	6/4/1996	6/23/2000

Table 4.4: Continued

Name	Symbol	Type	Area	$\dot{B}_{early}$	$\dot{B}_{recent}$	$\bar{\dot{b}}_{early}$	$\bar{\dot{b}}_{recent}$	$\Delta\dot{A}$	Map	Profile 1	Profile 2
			(km^2)	($km^3 yr^{-1}$ w.e.)		(m yr^{-1} w.e.)		($km^2 yr^{-1}$)	Year	Date	Date
Region 6, Chugach											
Allen	ALN	L/LK	221.9	-0.187±0.017	-0.240±0.017	-0.88±0.08	-1.16±0.08	-0.27	1950	8/25/2000	9/4/2004
Bench	BEN	L	8.7	-0.013±0.001	-0.021±0.001	-1.65±0.10	-2.67±0.10	-0.02	1950	8/25/2000	9/5/2004
Columbia	COL	TW	1067.7	-1.4±0.1	-7.217±0.000	-1.44±0.1	-7.42±0.00	-0.58	1957	5/31/1994	5/9/1999
Scott	SCO	L	167.6	-0.129±0.015	-0.359±0.015	-0.78±0.09	-2.16±0.09	-0.03	1950	6/21/2000	9/4/2004
Sheridan	SHE	L/LK	103.5	-0.096±0.010	-0.356±0.010	-0.97±0.10	-3.67±0.10	-0.12	1950	6/21/2000	9/4/2004
South Fork Tsina	STS	L	19.4	-0.008±0.002	-0.033±0.001	-0.44±0.11	-1.75±0.06	-0.01	1950	8/25/2000	9/4/2004
Valdez	VAL	L/LK	162.0	-0.230±0.019	-0.542±0.019	-1.50±0.12	-3.61±0.12	-0.22	1950	8/25/2000	9/4/2004

Table 4.5: Changes in regional average net balance rates $\Delta\bar{\dot{b}}$ for land terminating ("land") and all measured glaciers ("all"). The symbol n indicates the number of glaciers in each group.

Region	$\Delta\bar{\dot{b}}_{Land}$ (m yr^{-1})	$\Delta\bar{\dot{b}}_{All}$ (m yr^{-1})	n_{Land}	n_{All}
Alaska	0.09±0.5	0.07 ±0.6	7	10
Brooks	-0.09±0.03	-0.09 ±0.03	1	1
Coast	-0.98±0.3	-0.87 ±0.2	3	6
Kenai	0.06±0.4	0.07 ±0.3	7	12
St.Elias	-0.74±0.4	-0.78 ±0.4	6	12
Western Chugach	-1.0±0.3	-1.9 ±0.2	4	8

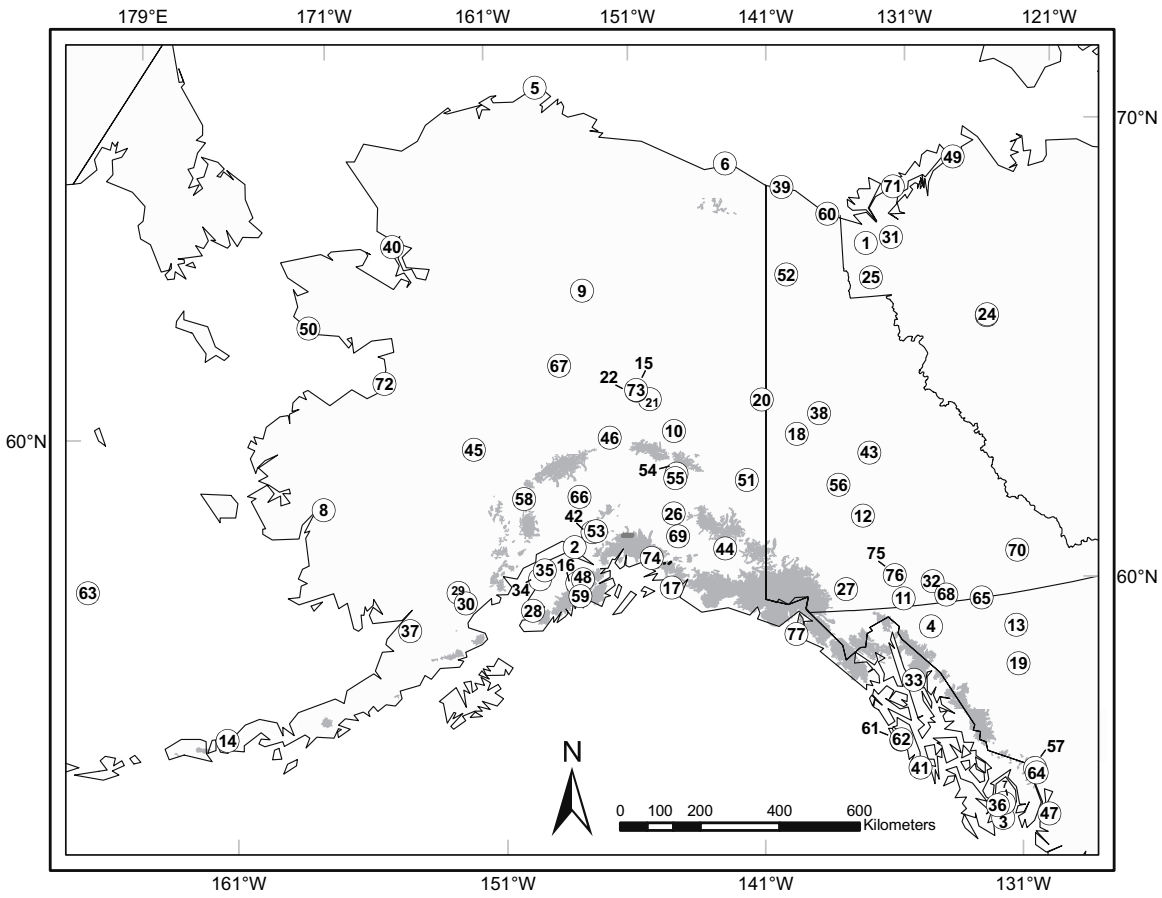

Figure 4.1: Location of NOAA and Environment Canada weather stations. Names associated with number labels are in Table 4.2. Gray shading shows all glaciers in northwestern North America.

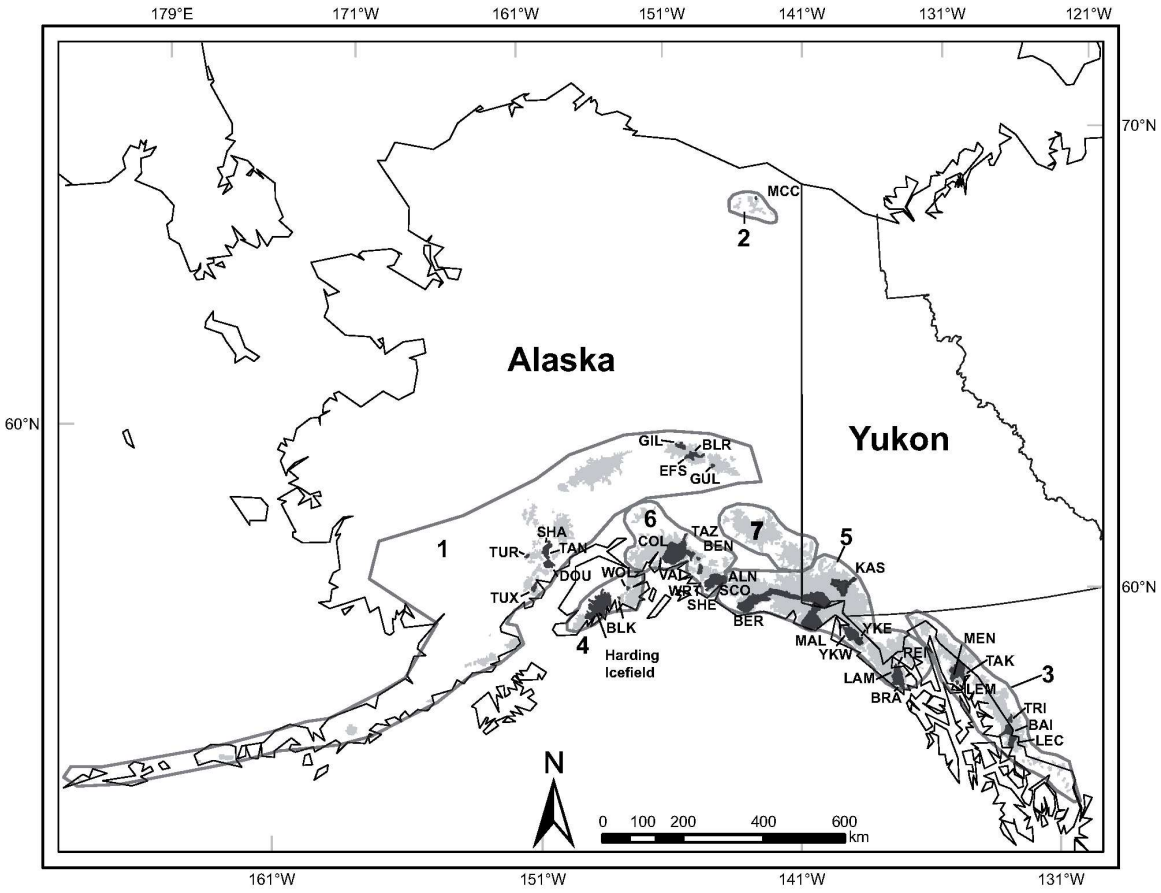

Figure 4.2: Location of 47 surveyed glaciers, shown in black, separated into seven geographic regions: 1, Alaska Range; 2, Brooks Range; 3, Coast Range; 4, Kenai Mountains; 5, St. Elias Mountains (including Eastern Chugach Range); 6, Western Chugach Range; and 7, Wrangell Mountains. Glacier names associated with three-letter glacier codes are in Table 4.4. Gray shading shows location of all glacier ice in northwestern North America.

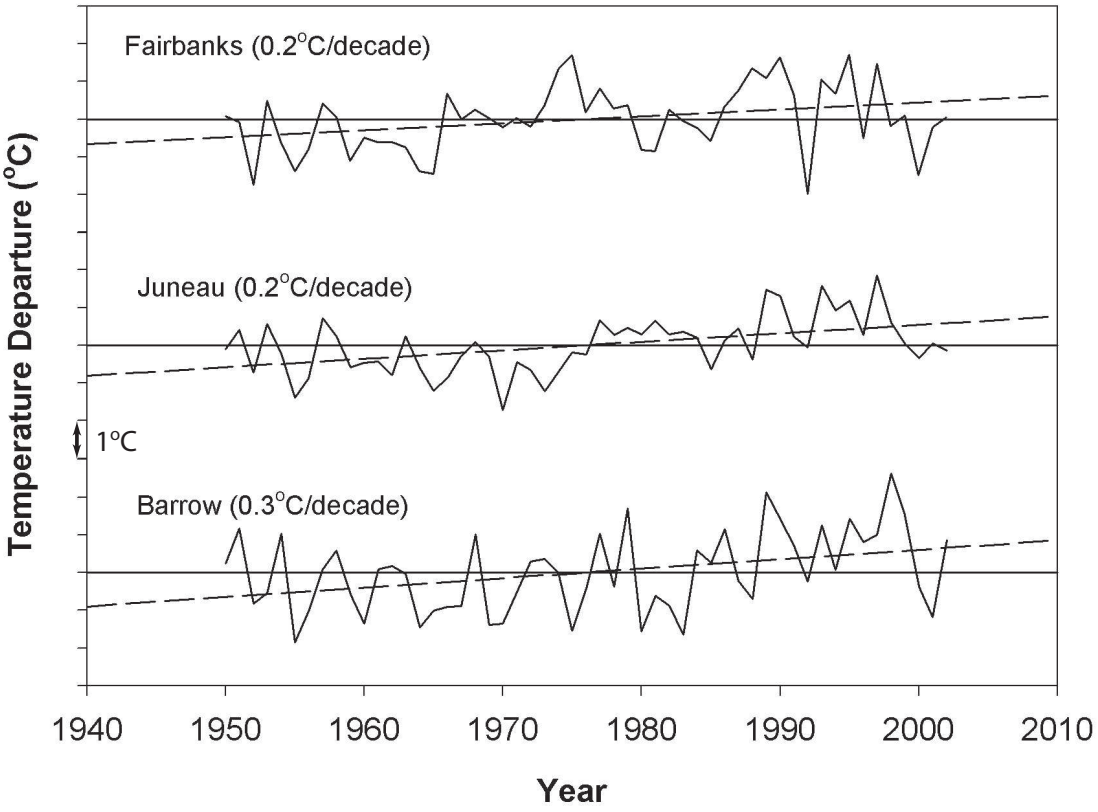

Figure 4.3: Departures from the mean (1950 to 2002) summer (May to September) air temperature at Fairbanks, Juneau and Barrow between 1950 and 2002. Each tick on the y-axis represents 1 °C.

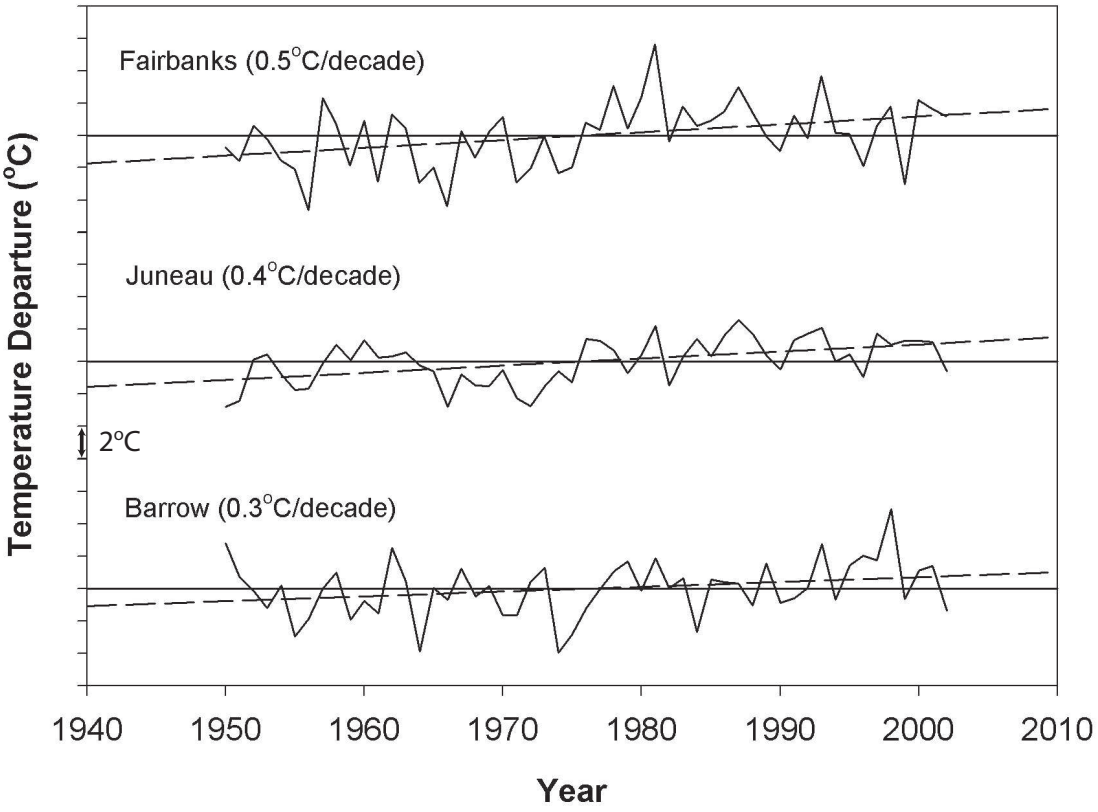

Figure 4.4: Departures from the mean (1950 to 2002) winter (October to April) temperature at Fairbanks, Juneau and Barrow. Each tick on the y-axis represents 2 °C.

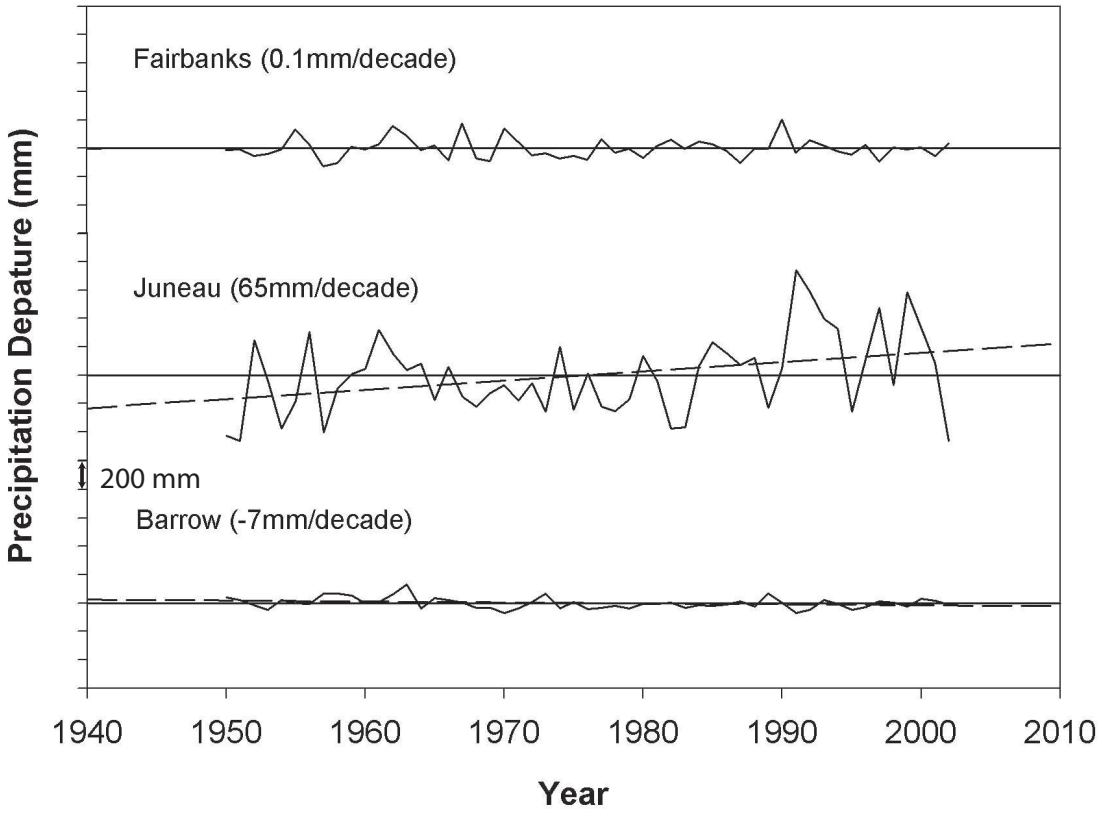

Figure 4.5: Departures from the mean (1950 to 2002) annual precipitation at Fairbanks, Juneau and Barrow. Each tick on the y-axis represents 200 mm.

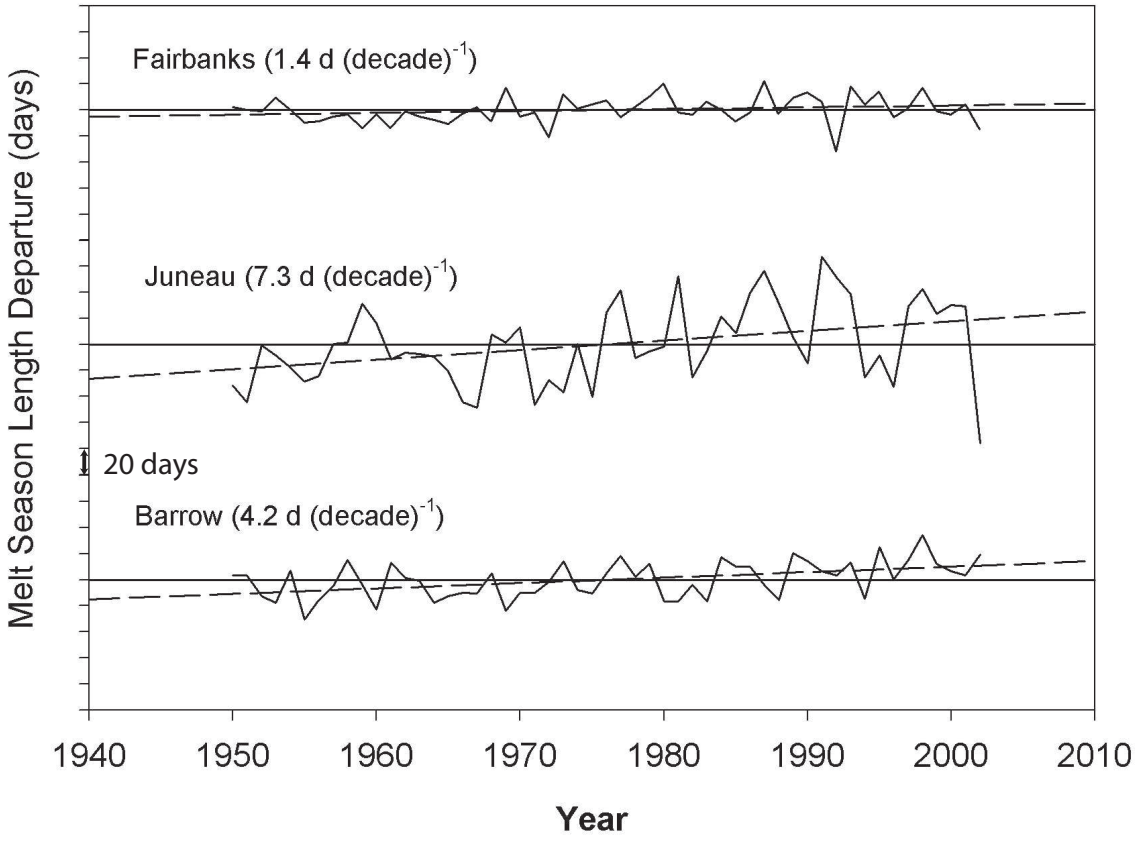

Figure 4.6: Departures from the mean (1950 to 2002) melt season length at Fairbanks, Juneau and Barrow (d (decade) $^{-1}$). Each tick on the y-axis represents 20 days.

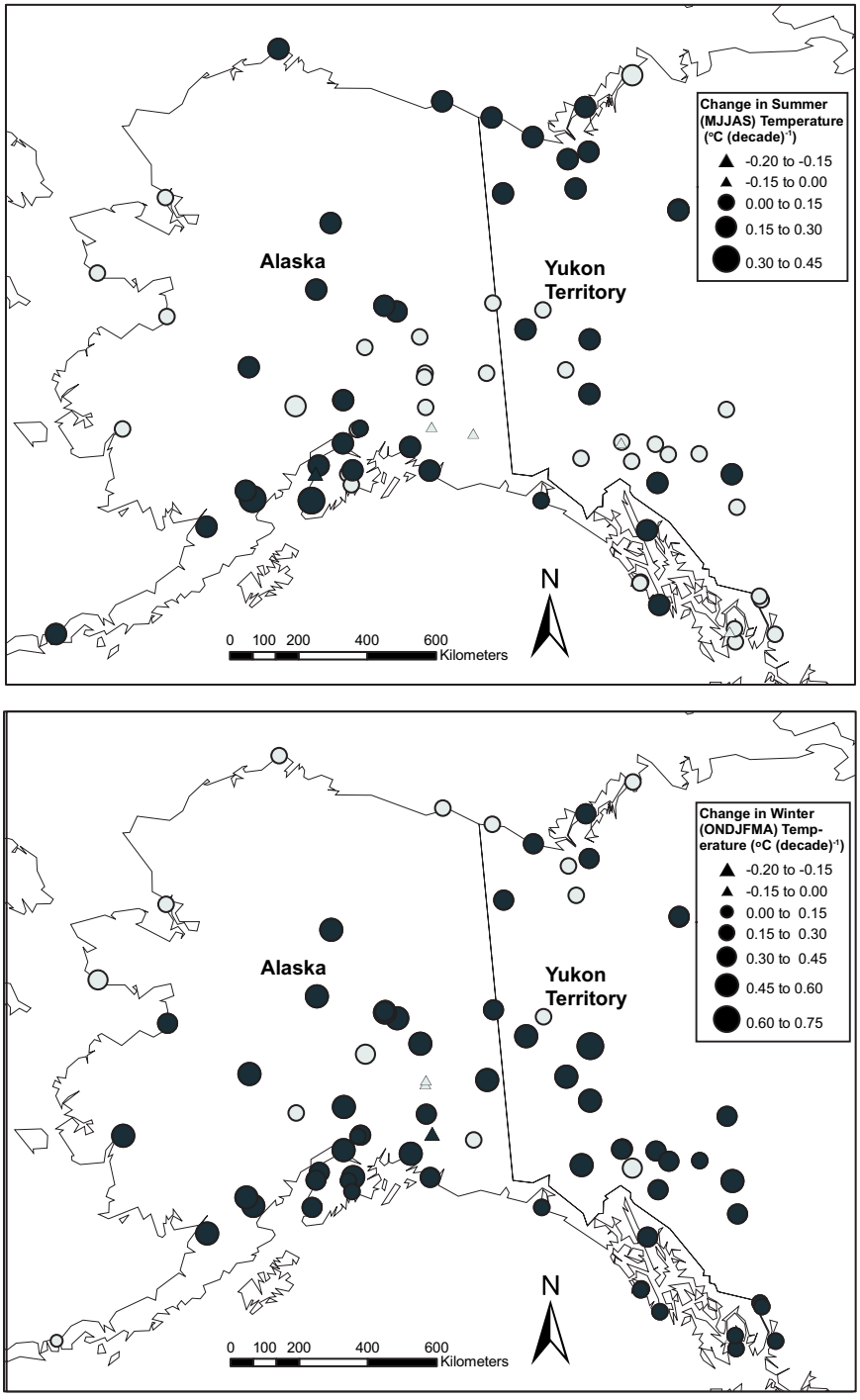

Figure 4.7: Changes in average summer (top panel, May to September) and winter (bottom panel, October to April) air temperature, 1950 to 2002. Black symbols represent changes significant at $p < 0.05$.

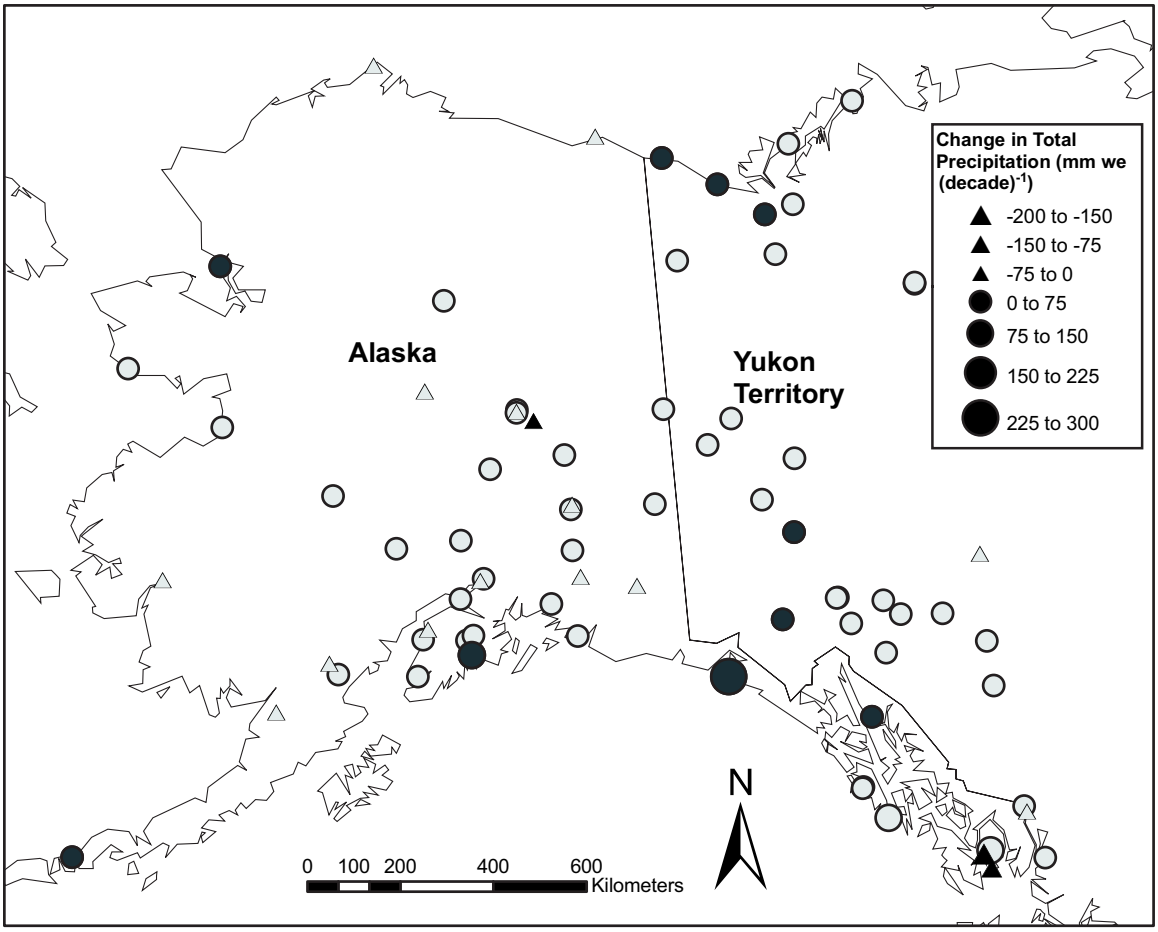

Figure 4.8: Changes in annual total precipitation, 1950 to 2002. Black symbols represent changes significant at $p < 0.05$.

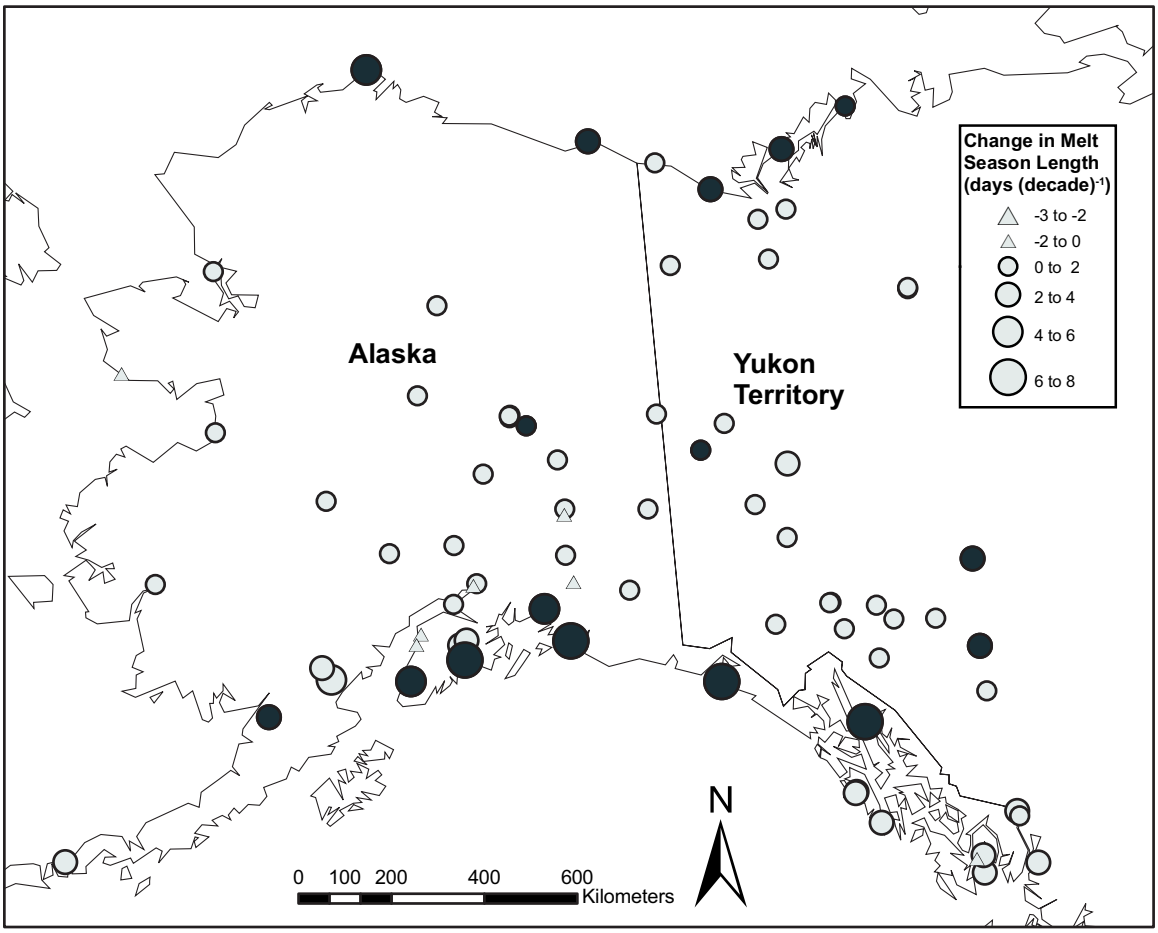

Figure 4.9: Change in melt season length (day (decade)$^{-1}$) in Alaska between 1950 and 2002 at 60 NOAA and 18 Environment Canada climate stations. Black symbols represent changes significant at $p < 0.05$.

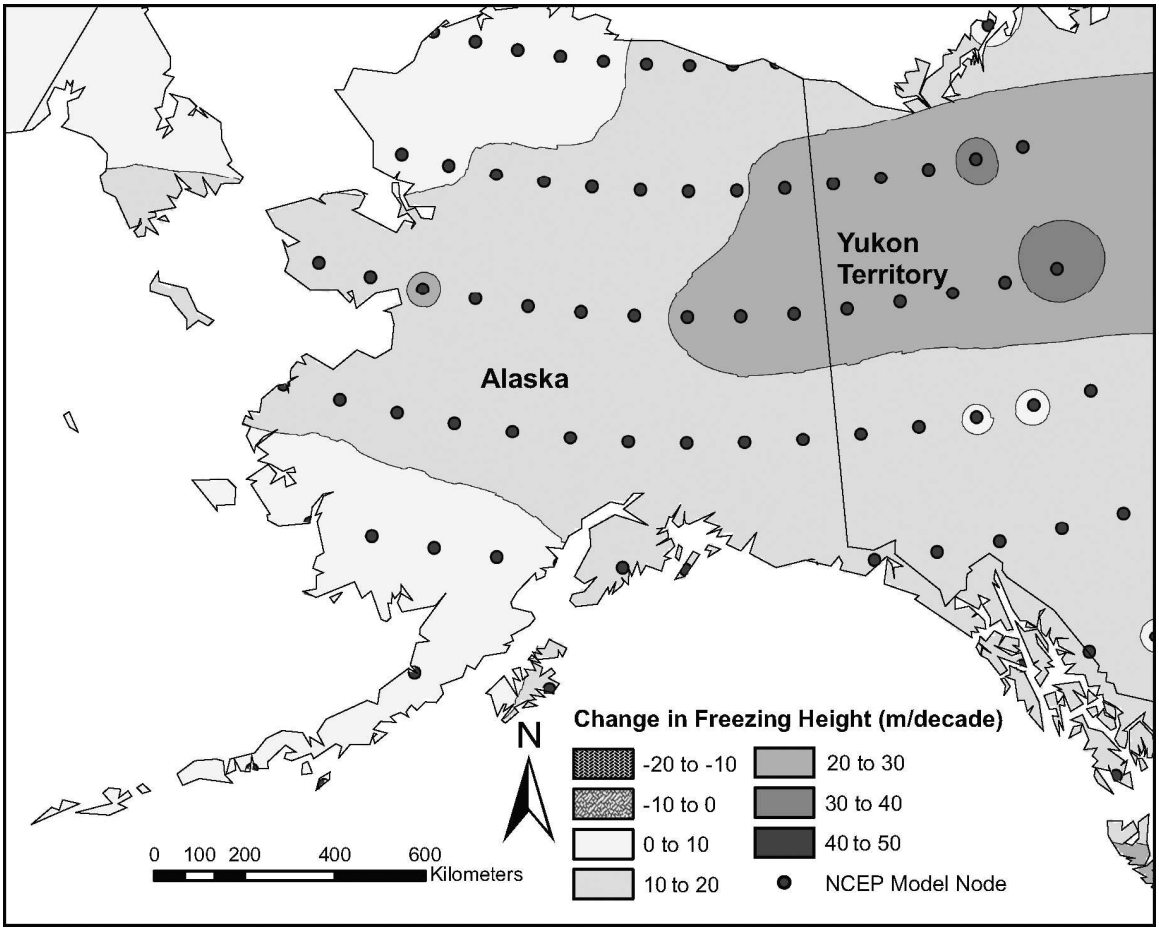

Figure 4.10: Change in annual freezing level height (m (decade)$^{-1}$) in Alaska between 1950 and 2002 as determined by linear interpolation between NCEP upper air temperature and geopotential height fields. Dots represent location of each NCEP node used in the analysis, and grid shading shows interpolation between these nodes using inverse distance weighting.

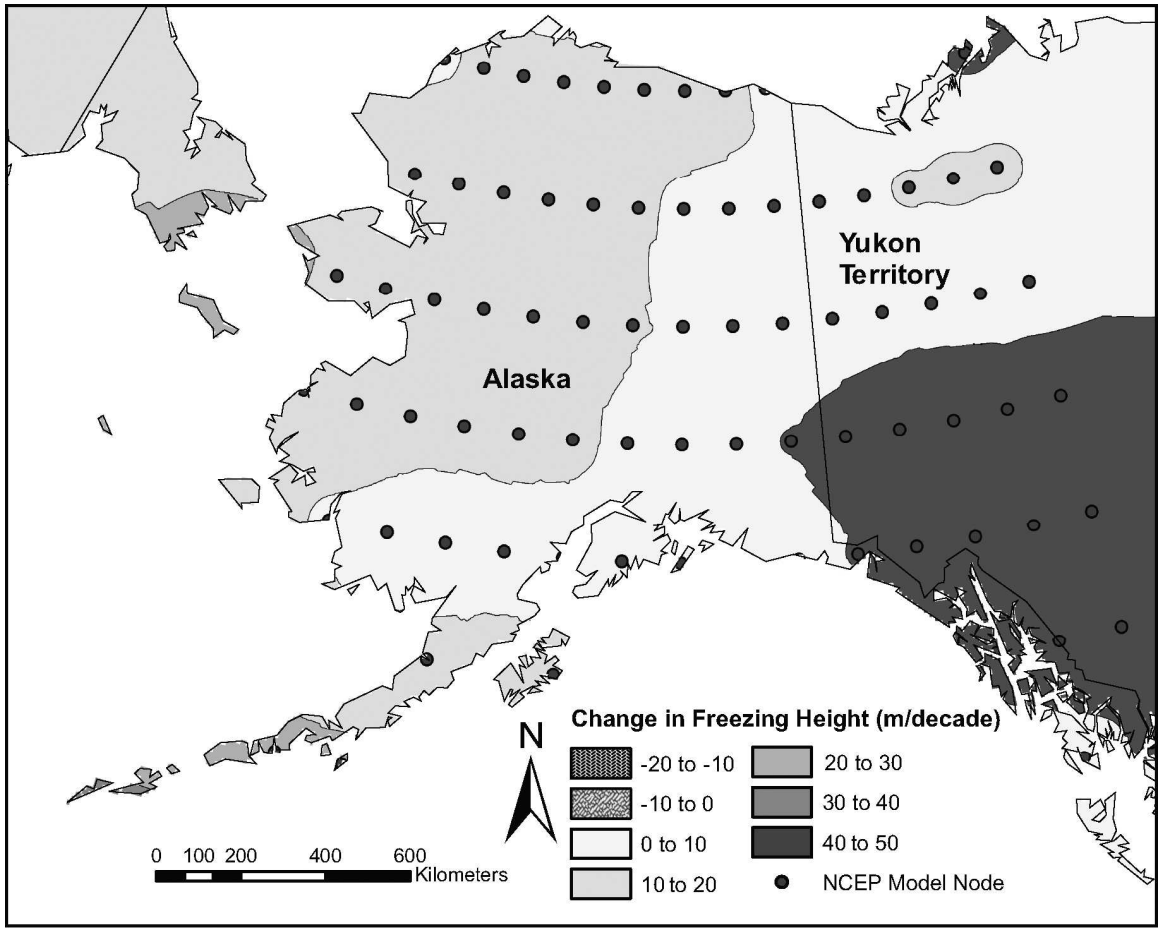

Figure 4.11: Change in summer (May to September) freezing level height (m (decade)$^{-1}$) in Alaska between 1950 and 2002.

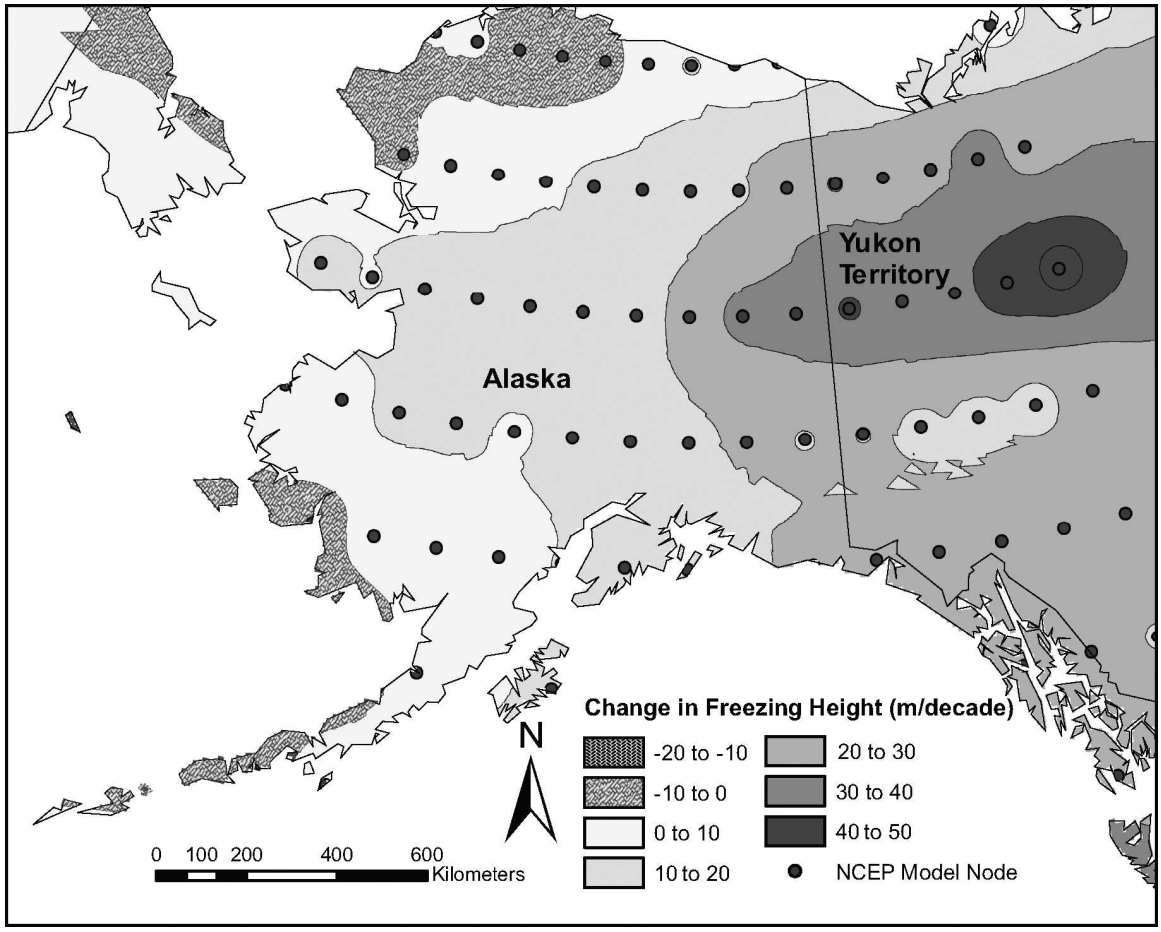

Figure 4.12: Change in winter (October to April) freezing level height (m (decade)$^{-1}$) in Alaska between 1950 and 2002.

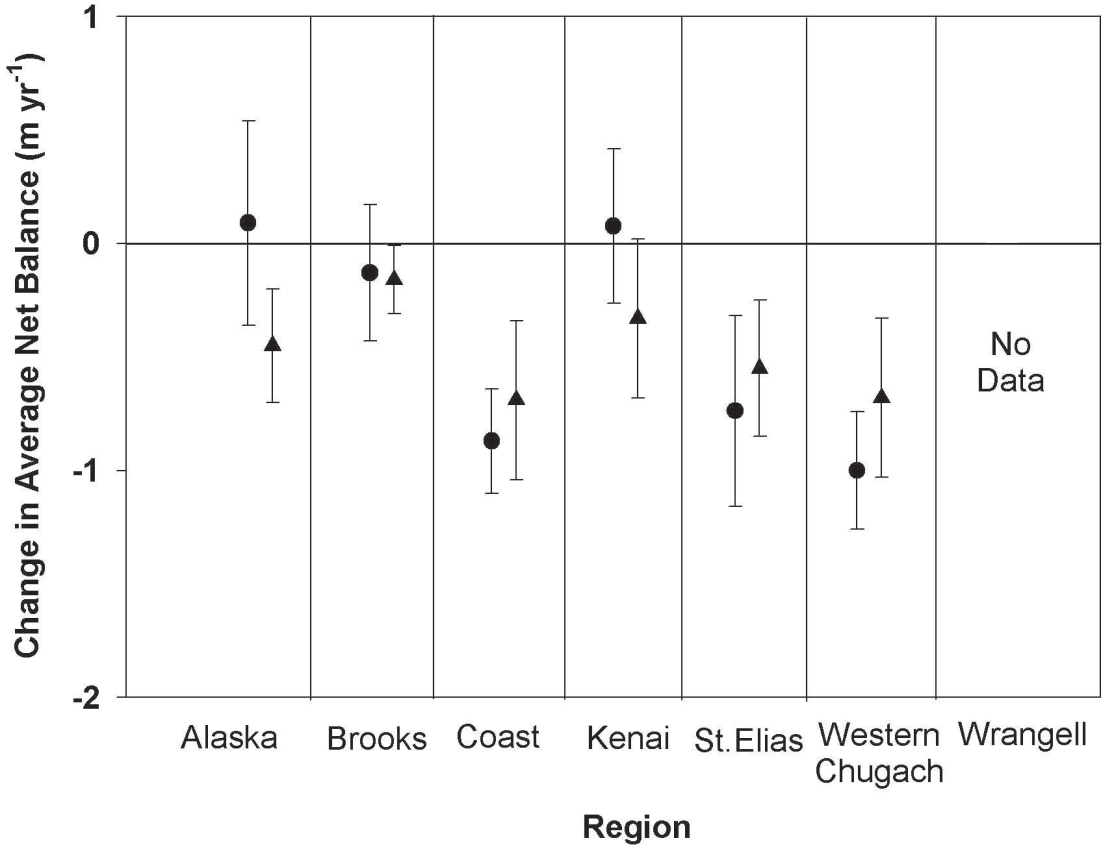

Figure 4.13: Measured (circles) and modeled (triangles) change in average net balance rate in glacier regions of northwestern North America. Modeled balances use regional average changes in temperature and precipitation in each region, and published mass balance sensitivities.

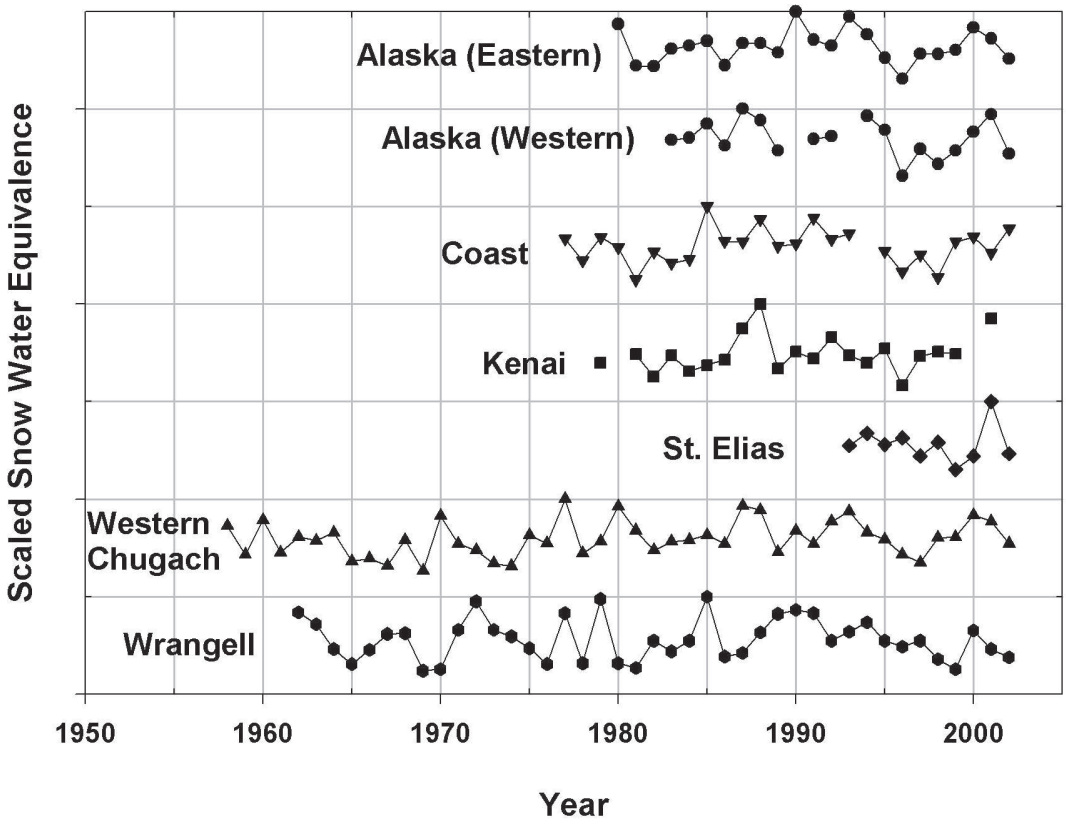

Figure 4.14: Trend in maximum annual winter snow depth measured at snow course stations by the Alaska Natural Resources Conservation Service. For comparison purposes, snow depths are scaled to the largest value in each time series.

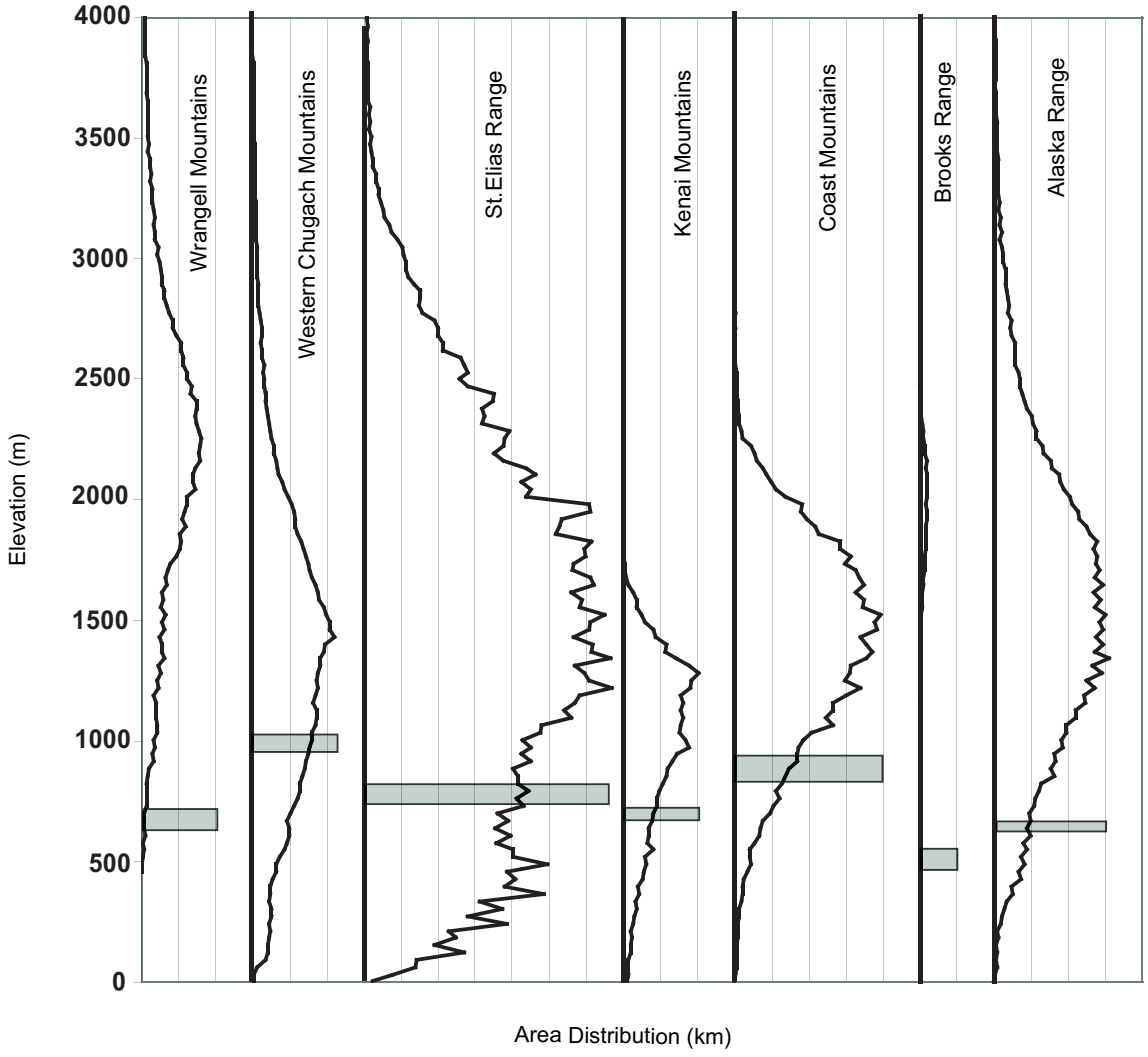

Figure 4.15: Glacier surface area distribution with elevation in each of the seven region in northwestern North America. Gray bars show the mean winter FLH, with the width of the bars representing the shift in FLH between 1950-2002. Dotted lines show the mean elevation of each region. Each horizontal line is 100 km of surface area distribution.

Chapter 5
Conclusion

Glaciers in northwestern North America are rapidly losing mass under present climate conditions. Many tidewater glaciers are in the retreat phase of their cycle and are losing mass catastrophically due to dynamic conditions largely unrelated to climate. The rate of mass loss of most glaciers has increased during the past decade, and our most recent measurements, made during a summer of record warmth in 2004, were the most negative of any in our entire sample.

In Chapter 3 we developed and tested methods to extrapolate from measured to unmeasured glaciers, using data from the Western Chugach Mountains. Extrapolation methods are necessary in order to determine the volume contribution of all glaciers in a region to rising sea level. We found that our extrapolations did a relatively poor job at predicting the area-averaged mass changes of individual glaciers. However, when calculating total volume changes for the entire region of glaciers, several different methods produced similar results. We suggest this was because large, dynamic glaciers were included in our measurement sample. For instance, Columbia Glacier is a retreating tidewater glacier that lost a total of 3.2 $km^3 yr^{-1}$, nearly half the rate of volume change of the entire Western Chugach Mountains. We concluded that over long time periods it is necessary to measure as many glaciers as possible in a region, because of the unique dynamics of individual glaciers. We also showed that simple models relating glacier area and volume changes need further refinement before being applied to the large dynamic glacier systems in Alaska.

The measurements presented here add to the substantial body of evidence of that air temperatures in northwestern North America have increased during the past half-century. In Chapter 4 we compiled and analyzed a database of climate measurements to show that both summer and winter season temperatures have increased (0.2 ± 0.1 and 0.4 ± 0.2 °C respectively). We modeled glacier changes using these climate data and a simple mass balance model, and found a good correspondence between measured and predicted changes. For most regions, trends at low elevation climate stations probably represent the changes that have occurred at high mountain regions. Two regions, the Alaska and Kenai Mountains, had slightly positive changes not predicted by the climate data. More work is necessary to reduce errors in our modeling of glacier changes, which fully account for seasonal

variability in snowfall and the dynamic adjustments of the glacier geometry through time.

Since the publication of Chapter 2, two additional studies have determined glacier volume changes in northwestern North America using methods independent from airborne altimetry. *Larsen et al.* [in preparation] compared the NASA Shuttle Radar Topography Mission Digital Elevation Model (STRM-DEM) with USGS topographic maps. Their calculated volume loss of glaciers in the Coast Mountains of Alaska/Yukon Territory was about double the mass loss predicted in Chapter 2. The difference occurred because the small number of altimetry glaciers did not represent the larger changes occurring on many rapidly thinning glaciers in this region. *Tamisiea et al.* [2005] used gravity anomaly data from the GRACE satellite and calculated a value of -123 km^3 yr^{-1} for the mass loss from all glaciers in northwestern North America from 2002-2004. This is about 30% more mass loss than our estimated 1995-2000/01 value of -96 km^3 yr^{-1}. The results of *Tamisiea et al.* [2005] suggest a continuation, if not acceleration, of glacier mass loss in the last few years. This is consistent with our observations of very high area-averaged thinning rates in the Western Chugach Mountains, determined from measurements in 2004.

Glaciers in northwestern North America show increased rates of glacier mass loss during the past decade, and this is consistent with data from every other major glacier region on Earth including the Canadian Arctic Archipelago [*Abdalati et al.*, 2004], the Patagonian Icefields [*Rignot et al.*, 2003], Greenland [*Krabill et al.*, 2000; *Thomas et al.*, 2001; *Johannessen et al.*, 2005; *Rignot and Kanagaratnam*, 2006] and Antarctica [*Rignot and Thomas*, 2002; *Thomas et al.*, 2004] (Fig. 5.1). In both Greenland and Antarctica, fast-flowing outlet glaciers are important mechanisms for transporting ice at high elevations to the oceans. There is considerable evidence that many ice sheet outlet glaciers are retreating unstably, resulting in larger contributions to rising sea level than previously estimated [*Alley et al.*, 2005].

Airborne altimetry measurements in northwestern North America have provided information important to a wide range of related fields. The increased rate of glacier mass loss means an increase in ocean freshwater discharge, potentially altering salinity-driven ocean circulation patterns [*Royer*, 1982]. As glaciers gain or lose volume they change the load on Earth's crust and are an important driver of crustal uplift or subsidence [*Tamisiea et al.*; *Larsen et al.*, 2004, 2005]. Large changes in glacier mass affect seasonal and multi-annual trends in Earth's gravity field, also affecting Earth tides and rotation [*Munk*, 2003].

Glacier change are driven by climate but also feedback to the climate system via changes in surface albedo [*ACIA*, 2004].

Future altimetry work in northwestern North America should focus on reducing uncertainty in estimates of glacier contribution to rising sea level. The methods developed in Chapter 3 should be tested in other regions, realizing that each region might have unique problems requiring new approaches. For example, there are no tidewater glaciers in the Alaska Range, but there are many surging glaciers which should probably be treated separately when extrapolating altimetry measurements. Concerning glacier/cliamte interactions, future studies should investigate recently available, high resolution reanalysis models. These gridded datasets might be detailed enough to describe spatial patterns in climate necessary to subdivide mountain ranges into smaller sub-regions that are more climatologically homogenous. They might also allow for the development of more sophisticated glacier mass balance models which will help determine the response of glaciers in northwestern North America to future climate change.

Bibliography

Abdalati, W., et al. (2004), Elevation changes of ice caps in the Canadian Arctic Archipelago, *Journal of Geophysical Research*, *109*, 4007–+, doi:10.1029/2003JF000045.

ACIA (2004), Impacts of a warming Arctic, *Tech. rep.*, Arctic Climate Impact Assessment Report, Arctic Council. http://www.acia.uaf.edu.

Alley, R., P. Clark, P. Huybrechts, and I. Joughin (2005), Ice-sheet and sea-level change, *Science*, *310*.

Johannessen, O. M., K. Khvorostovsky, M. W. Miles, and L. P. Bobylev (2005), Recent ice-sheet growth in the interior of Greenland, *Science*, *310*(5750), 1013–1016.

Krabill, W., et al. (2000), Greenland ice sheet: High-elevation balance and peripheral thinning, *Science*, *289*(5478), 428–430, doi:10.1126/science.289.5478.428.

Larsen, C., R. Motyka, J. Freymueller, K. Echelmeyer, and E. Ivins (2004), Rapid uplift of southern alaska caused by recent ice loss, *Geophysical Journal International*, *158*(3), 1118–1133.

Larsen, C., R. Motyka, J. Freymuller, K. Echelmeyer, and E. Ivins (2005), Rapid viscoelastic uplift in southeast Alaska caused by post-Little Ice Age glacial retreat, *Earth and Planetary Science Letters*, *237*, 548–560.

Larsen, C. F., R. J. Motyka, A. A. Arendt, and K. A. Echelmeyer (*in preparation*), Glacier changes in southeast Alaska and contribution to sea level rise.

Munk, W. (2003), Ocean freshening, sea level rising, *Science*, *300*, 2041–2043.

Rignot, E., and P. Kanagaratnam (2006), Changes in the velocity structure of the Greenland ice sheet, *Science*, *311*(5763), 986–990, doi:10.1126/science.1121381.

Rignot, E., and R. H. Thomas (2002), Mass balance of polar ice sheets, *Science*, *297*, 1502–1506.

Rignot, E., A. Rivera, and G. Casassa (2003), Contribution of the Patagonia Icefields of South America to sea level rise, *Science*, *302*, 434–437.

Royer, T. C. (1982), Coastal fresh water discharge in the northeast pacific, *Journal of Geophysical Research*, *87*(C3), 2017–2021.

Tamisiea, M., E. Leuliette, J. Davis, and J. Mitrovica (2005), Constraining hydrological and cryospheric mass flux in southeastern Alaska using space-based gravity measurements, *Geophysical Research Letters*, *32*, 20,501+–.

Tamisiea, M. E., J. X. Mitrovica, and J. L. Davis (2003), A method for detecting rapid mass flux of small glaciers using local sea level variations, *Earth and Planetary Science Letters*, *213*(3), 477–485.

Thomas, R., B. Csatho, C. Davis, C. Kim, W. Krabill, S. Manizade, J. McConnell, and J. Sontag (2001), Mass balance of higher-elevation parts of the Greenland ice sheet, *Journal of Geophysical Research*, *106*, 33,707–33,716, doi:10.1029/2001JD900033.

Thomas, R., et al. (2004), Accelerated sea-level rise from west antarctica, *Science*, *306*, 255–258.

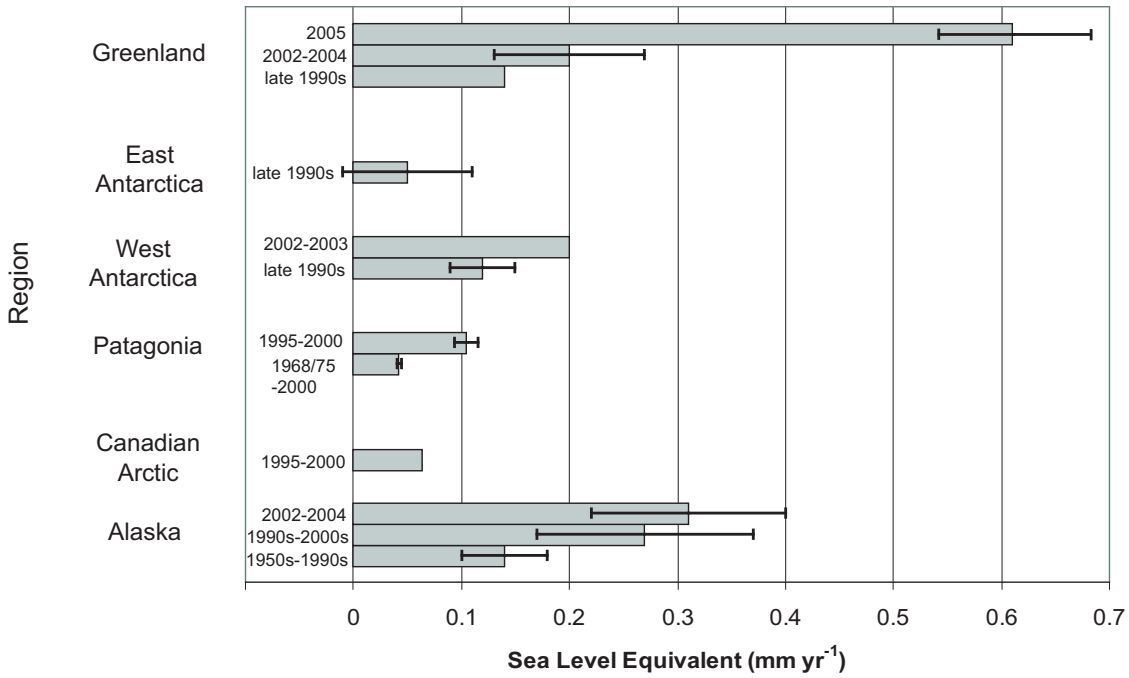

Figure 5.1: Summary of estimated contribution of glaciers and ice sheets to rising sea level.

Appendix A
Error Analysis: Part 1

Early Period:

For early period comparisons, map errors are the dominant random error. For each glacier we assigned random errors of 15 m for the contours in the ablation area, which is the nominal accuracy of the USGS maps (one-half contour interval), and 45 m for the upper accumulation area, based on measurements made on the Harding Icefield, Alaska ([1]), and elsewhere. This higher value in the upper accumulation area accounts for higher random errors in mapping contours over low contrast snow-covered areas. We estimated the equilibrium line altitude for each glacier (delineating the accumulation and ablation areas) by analyzing aerial photographs for some glaciers in our sample, as well as using the change in direction of contour concavity on the topographic maps as a ca. 1950 estimate of the equilibrium line altitude.

Another random (independent) error is associated with assuming that elevation changes from one or a few altimetry profiles can be used to represent changes across the entire glacier. A previous study ([2]) addressed this problem by comparing our volume change calculated on West Gulkana Glacier with that determined by geodetic methods between two (1957 and 1986) high resolution topographic maps, the latter one made near the time of profiling. Taking the geodetic method to be the control, and therefore free of errors, it was found that the mean elevation change from the altimetry profiles was -20.9 m compared to -22.2 m for the geodetic method, a difference of 1.3 m over the 29 year period. We use this value for our areal-extrapolation error, and suggest that it is reasonable for the small glaciers in our sample which probably have small transverse variations in thickness change ([3]). This may not be the case for large glaciers.

Vertical errors in the altimetry system are small, about 0.30 m. In many cases we found these errors to be less, but over steeply sloping terrain they can be larger.

The total estimated random error for early period measurements (as shown in Table S1) is the quadrature sum of all random errors. For early period comparisons, contour errors in the accumulation areas were the largest term in the error budget; for recent period comparisons, areal-extrapolation errors dominated.

Systematic errors are likely to be significant in some cases, but they are difficult to

quantify for every glacier in our dataset. Systematic errors may occur due to poorly defined map photography dates, poorly defined map control and/or the incorrect placement of contours in upper accumulation areas, where snow cover reduces contrast and cartographers tend to "float" contours above their true elevation. Our previous studies on several glaciers generally found small (<2 m) systematic errors in map control by comparing altimetry profiles with mapped proglacial bedrock and nunatak areas. However there are exceptions, such as for glaciers in the Brooks Range, where we measured vertical offsets in map control of up to 45 m. There also may be systematic errors in map control for the large glaciers of the St. Elias Mountains away from the coast. We have corrected for these offsets whenever possible. For example, our calculations for Hubbard Glacier, using an unpublished USGS map with good control that happened to be available, led to about 0.04 m/year more thickening than our calculation which used the published 15-minute USGS map which had poor control. On the Bering Glacier, we observed a transition from thinning to thickening at 1300 m elevation on the glacier. This shift accounts for the unusual positive values on the average thickness change curve between 1300 and 1800 m elevation for the St. Elias Mountains (Figure A.1). In this case, we did not correct for this shift, because it may have been a real feature associated with the 1993-95 surge. To test the effect of this shift as a possible systematic error in our volume change estimates, we set all thickness changes on Bering Glacier above 1300 m to zero, consistent with the thickness change trends of most other sampled glaciers in this region. This test led to 13.5 km^3/year more volume loss for glaciers of the St. Elias Mountains, compared with our reported estimate that included the positive elevation changes on Bering Glacier.

We also tested the sensitivity of our volume change estimates to the potential systematic error produced by floating contours. We assumed all contours 200 m or more above the equilibrium line were originally mapped 15 m (half a contour interval) too high, based on our observation that elevation changes often had increased scatter at these elevations. We then recalculated volume changes and compared these with the original volume change estimates. These calculations led to an increase in the total volume change for a given glacier or, in other words, an overestimation of glacier volume loss. In the unlikely event that all glaciers had floated contours at high elevations, the estimated systematic error in the total annual volume change would be about 3 km^3/year. We incorporate this error, along with

the possible Bering Glacier map errors, in our extrapolated error estimates below.

Early period measurement errors which may occur because we do not know the precise dates at which the aerial photographs, used to create the maps, were acquired. In some cases, more than one set of aerial photographs, acquired at different dates, were used to create the maps. Elevation measurements made at different times of the year introduce seasonal errors, especially when deep snow covers the glacier at the time of profiling. We have corrected for this error on some ([1, 2]), but not all, of the glaciers in our sample.

Recent Period:

Errors in the recent period comparisons on the 28 repeat-measured glaciers are determined by areal-extrapolation and altimetry system errors alone.

Random versus Systematic Error:

There may be additional uncertainty if we have incorrectly designated an error as random, when in reality it is systematic. For instance, in our analysis above, we treat the altimetry system error as random, making it the smallest term in our error budget for both the early and recent measurement periods. If instead the altimetry system error were systematic, it would still be the smallest term in the early period error budget, but it would become the largest term in the recent period error budget (about double the areal-extrapolation error).

Error in Extrapolation to all Alaska Glaciers:

Our extrapolation of the measured changes on 20% of the glacierized area (or 13% for recent period calculations) to all glaciers in Alaska and northwest Canada could be subject to significant uncertainty. We have attempted to quantify this error by considering three factors: (1) the total random error of the measured glaciers, calculated as the quadrature sum of the random errors of each glacier; (2) the scatter of measured elevation changes about their mean value for a given elevation band and region, which, when propagated across the area-altitude distribution of all unmeasured glaciers in that region, gives an estimate of the error in the extrapolated volume change; and (3) the difference between the total regional volume change calculated from area-weighted average thickness changes, and that calculated from non-area weighted average thickness changes. Combining these errors as independent errors (quadrature sum) gives a total error estimate of 7 km^3/year

for the early period and 28 km^3/year for the recent period.

If we incorporate the systematic errors quantified above (including the potential Bering Glacier map error and the floating contours error), our total volume change estimate for the early period is -52^{+10}_{-21} km^3/year. We report a value of -52$\pm$15 km^3/year as a reasonable estimate of this error. There may be additional systematic errors due to poorly defined map control, which should tend to cancel because we consider a large number of glaciers. If they do not cancel, then our early period error estimate would be slightly larger.

Bibliography

1. G. Aðalgeirsdóttir, K. Echelmeyer, W. Harrison, *Journal of Glaciology* **44**, 570 (1998).

2. J. Sapiano, W. Harrison, K. Echelmeyer, *Journal of Glaciology* **44**, 119 (1998).

3. A. G. Fountain, *Geografiska Annaler, Series A: Physical Geography* **81**, 563 (1999).

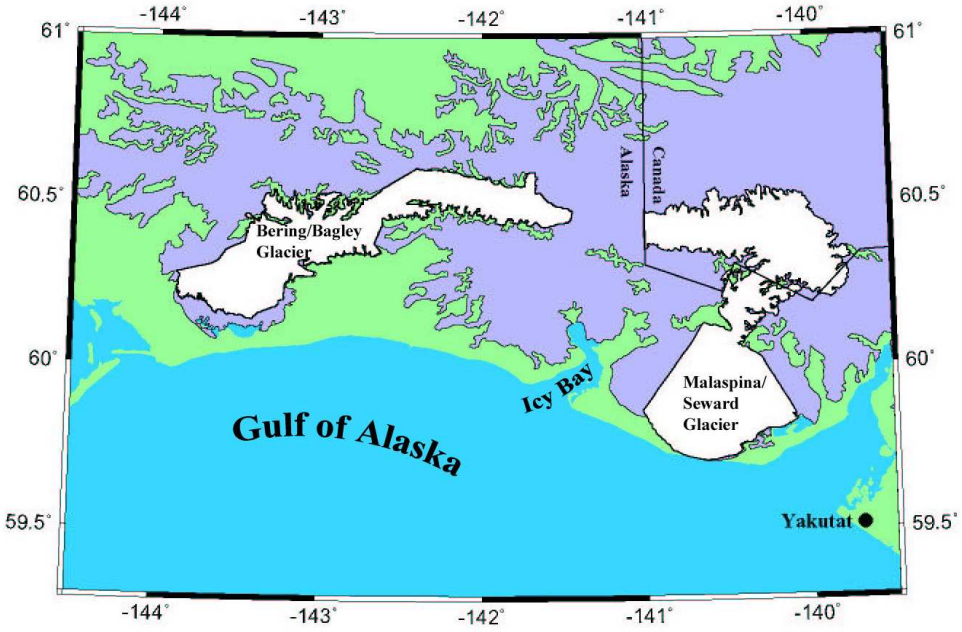

Figure A.1: Detail of the Malaspina/Seward (MAL) and Bering/Bagley (BER) glacier outlines. Our outlined areas for these two glaciers are considerably less than the total area of their glacierized hydrological basins, because we terminated the outlines at the uppermost elevation contours that our profiling sampled (MAL: 2300 m; BER: 1660 m). Note that the uppermost areas of these glaciers are accounted for in the St. Elias regional extrapolation, based on data from nearby glaciers. Portions of the terminal lobes of both glaciers are debris covered, and we would expect this to cause differences in thinning rates due to insulating effects of debris. However, such areas that were profiled on MAL show similar thinning rates as on nearby clean ice areas at the same elevations; therefore, we included the debris-covered ice on the lower lobe of BER in our estimates of its volume change even though we did not adequately sample this area. The included error bounds for BER account for this additional source of uncertainty.

Appendix B
Error Analysis: Part 2

This supplemental material provides details on our methods to estimate random and systematic errors in our measurement of glacier thickness and volume changes.

Map Errors

The 1:63,360 USGS contour maps for Alaska are provided in 0.5° longitude by 0.25° latitude quadrants and were compiled from aerial photographs collected in the early- to mid-1950s. Over each glacier outline we plotted the location of the aerial photo acquisition together with the year of acquisition. We find that in many cases there were multiple photo years for the same location and unfortunately we do not know which particular photo was used to develop the contours. In cases where there was an obvious majority of one photo year over another for a given glacier we chose that photo year. In cases where there was no obvious majority, we selected the average year of all photo years covering the glacier. For glaciers in the Chugach Mountains, photo years were either 1950 or 1957. For simplicity we assigned a photo map date error of $\pm$3.5 yrs. multiplied by the measured average rate of thickness change for each glacier.

The nominal error in contour placement on the USGS maps is half a contour or about 15 m (assumed random), but this error probably increases at high elevations where lack of contrast in the aerial photographs reduced the ability of cartographers to correctly identify map elevations. We assign a value of 45 m for random contour errors in the accumulation zone, based on analysis on the Harding Icefield [*Aðalgeirsdóttir et al.*, 1998]. It is possible that the contour errors in the accumulation zone have a systematic offset which can occur when reduced contrast causes cartographers to "float" contours above their true elevation. We tested the effect of this potential systematic error on our dataset by artificially shifting contour elevations half a contour (15 m) above their true elevation and recalculating the net balance rate. In the unlikely event that all 23 glaciers in our sample had this error, we would have overestimated the regional mass loss by 0.58×10^9 $km^3 yr^{-1}$ or about 12% of the regional net balance rate.

A potentially serious error results from poor map control which may introduce systematic elevation offsets which are difficult to quantify. Our previous studies on several glaciers generally found small (<2 m) systematic errors in map control by comparing al-

timetry profiles with map elevations in proglacial bedrock areas. Here we provide additional estimates of map control errors by comparing altimetry data collected over bedrock near Bench and Tonsina glaciers in 2004 (considered the control elevations) with map elevation contours. This comparison assumes no changes have occurred in bedrock elevations between the time of the USGS map and the laser profile. Also we do not include the viscoelastic response of the solid earth under the changing ice loads, nor the shifting of the Earth's crust due to tectonic events. We were able to extract 9 contour crossing points near Bench Glacier between 750-900 m, and 10 crossing points near Tonsina Glacier between 1640-1740 m. Near Bench the difference between the profile and map elevations ranged between -5 to -24 m, with a mean of -13 m. Near Tonsina the difference ranged between -44 to 21 with a mean of -11 m. The terrain over which these tests were done was steeper near Tonsina than Bench, which might explain the larger range of errors near Tonsina because horizontal mismatch magnifies elevation differences. The mean offsets from these two tests are within the nominal error in contour elevations, but they are not random and suggests a systematic offset of the map above the profile elevations. It is not possible to generalize these results to the entire Chugach Range; our previous studies found different systematic errors even between adjacent map quadrants. Unfortunately we do not have any additional data from bedrock locations in the Chugach Mountains. If we assume every glacier in our sample had a systematic map control error of -13 m, this would have resulted in an underestimation of the regional mass loss by 0.95×10^9 $km^3 yr^{-1}$ or about 20% of the regional net balance rate.

Nolan et al. [in press] recognized an important source of map elevation error not accounted for in our previous work. All USGS maps in Alaska use the NGVD29 vertical datum, and we convert our laser profile elevations collected in the WGS84 datum to the NAVD88 datum which we then assume is equivalent to the NGVD29 datum. In fact NAVD29 is not equal to NAVD88, but to our knowledge at the time of this writing there is no accurate algorithm for transforming the NGVD29 datum into any other datum for regions in Alaska. Based on comparisons of individual USGS benchmarks we found the NAVD88 is higher than the NGVD29 datum by 2.1 m at Valdez and 1.9 m at Anchorage [*Maune*, 2001]. We assume a systematic elevation error of +2.1 m for all glaciers in the Chugach Region. The effect of this offset is small and results in a 3% overestimation of the

regional net balance rate.

Profile-to-Glacier Errors

We define the profile-to-glacier error as the error resulting from using one or a few profiles to represent all areas of the glacier at the measured elevation. We previously termed this an "extrapolation" error, but in order to eliminate confusion with this study in which we are discussing regional extrapolations, we now call it the "profile-to-glacier" error. Our earlier work relied on data from *Sapiano et al.* [1998], who tested their method for constructing a contour map directly from altimetry data with another map made independently through ground-based photogrammetry. When these maps of West Gulkana Glacier, Alaska, were compared with an earlier map, the difference in the resulting average thickness change was 1.3 m.

Here we provide additional estimates of profile-to-glacier errors by calculating the standard deviation of geodetically-derived glacier mass balance [*Cox and March*, 2004]. A geodetic mass balance is the difference between glacier-wide surface elevations measured at different times. The resulting difference map illustrates the variability of surface elevation changes across the width of a glacier, and the standard deviation of elevation differences within an elevation range is a direct measure of the profile-to-glacier error [*Berthier et al.*, 2004]. We calculated the standard deviation (σ) of a digital geodetic mass balance map (1974 to 1993) of Gulkana Glacier, Alaska [*Cox and March*, 2004] and categorized these σ values into 30.48 m elevation bins. We calculated σ = 3-15 m for the terminus region of Gulkana Glacier between 1250 and 1500 m and σ = 1.5-3.8 m between 1500 m and the head of the glacier at 2438 m (Figure B.1). The terminus region of this glacier is very debris-covered which is why σ values were larger there than for the rest of the glacier. Taking an average of the values for debris-covered (d) and clean ice (c) gives σ_d = 8.2 m and σ_c = 2.4 m. One additional study documented cross-glacier variations in surface elevations in the lower ablation area of McCall Glacier, Alaska *Nolan et al.* [in press]. The average standard-deviation of thickness changes over 5 time periods between 1969 and 2003 was 1.7 m.

Based on the three studies listed above we calculate two new estimates for the profile-to-glacier error, one for debris-covered and one for clean glacier ice. For debris-covered ice

we take the value from Gulkana Glacier (σ_d = 8.2 m). The σ values from West Gulkana and McCall glaciers (both primarily clean ice) and Gulkana Glacier range between 1.3 to 2.4 m and we choose the maximum value (σ_c = 2.4 m). Note that Gulkana Glacier is the largest of the three glaciers in these studies and is probably most representative of the even larger glaciers we monitored in the Chugach region. We categorize an elevation bin as debris-covered if over half of that bin has debris, based on visual inspection of the USGS maps and the Landsat satellite images.

Area Mapping Errors

Errors in mapping glacier areas occur due to digital map registration errors and human digitizing mistakes. There is also some subjectivity involved in deciding on the 2002 glacier extent from the Landsat images, especially in areas where the terminus is debris covered. It is difficult to quantify these errors and we assume their effect on volume change estimates is small (note that area errors do not affect average net balance estimates).

Altimetry System Errors

The error in measurement of surface elevations are dominated by GPS-determined aircraft elevations (0.2 m) and those in pitch and roll angles (0.2 m) [*Echelmeyer et al.*, 1996]. Treating these errors as independent, the net error in altimetry system measurements of surface elevation is $\pm$0.3 m.

Seasonal Corrections

Nearly all glaciers reported in this study were measured within a four day period in September. However two glaciers, Harvard and Yale, were measured on May 21. The seasonal mismatch between measurements introduces errors because those glaciers measured in September will have experienced an additional ablation season. We quantify this error using mass balance measurements from Wolverine Glacier, a small 17.2 km^2 land terminating glacier located at 60.4°N, 148.9°W, approximately 150 km from the center of our study area, with an elevation range of 430 to 1680 m *Mayo et al.* [2004]. The average summer balance (March to October) at Wolverine Glacier in 2001 was 3.1 m w.e., and we assume this to be a conservative estimate of the ablation correction between May and September. Averaged over the measurement period, this is a systematic error in $\bar{\dot{b}}$ values for Harvard and Yale glaciers of 0.07 m yr^{-1}.

Errors in Volume Changes of Tidewater Glaciers

Tidewater glaciers displace a quantity of water determined by the depth of the fjord in which they terminate. Glacier ice is less dense than water by about 10%, so a correction to sea level change estimates is required when some portion of ice advance or retreat occurs below water. In the case of a retreating tidewater glacier, 10% of the volume of ice previously below sea level must be subtracted from the contribution of that glacier to sea level rise. Correcting for this systematic error requires information on fjord bathymetry which is rarely available.

We made a rough correction for this error for Columbia Glacier, based on fjord bathymetry data from *O'Neel et al.* [2005]. The correction reduces the contribution of Columbia Glacier to rising sea level by 2.4%. We did not have bathymetric data for Harvard or Yale glaciers but we expect the correction to be very small given their small terminus changes.

Bibliography

Aðalgeirsdóttir, G., K. Echelmeyer, and W. Harrison (1998), Elevation and volume changes on the Harding Icefield, Alaska, *Journal of Glaciology*, *44*(148), 570–582.

Berthier, E., Y. Arnaud, D. Baratoux, C. Vincent, and F. Rémy (2004), Recent rapid thinning of the "Mer de Glace" glacier derived from satellite optical images, *Geophysical Research Letters*, *31*, 17,401–+.

Cox, L. H., and R. S. March (2004), Comparison of geodetic and glaciological mass balance, Gulkana Glacier, Alaska, USA, *Journal of Glaciology*, *50*(170), 363–370.

Echelmeyer, K., W. Harrison, C. Larsen, J. Sapiano, J. Mitchell, J. DeMallie, B. Rabus, G. Aðalgeirsdóttir, and L. Sombardier (1996), Airborne surface profiling of glaciers: A case-study in Alaska, *Journal of Glaciology*, *42*(142), 538–547.

Maune, D. (2001), *Digital elevation model technologies and applications: the DEM users manual.*, ASPRS, Bethesda, MD.

Mayo, L., D. Trabant, and R. March (2004), A 30-year record of surface mass balance (1966-95), and motion and surface altitude (1975-95) at Wolverine Glacier, Alaska, *U.S. Geological Survey open-file report*, *2004-1069*, 105.

Nolan, M., A. Arendt, B. Rabus, and L. Hinzman (in press), Volume change of McCall Glacier, Arctic Alaska, from 1956 to 2003, *Annals of Glaciology*.

O'Neel, S., W. Pfeffer, R. Krimmel, and M. Meier (2005), Evolving force balance at Columbia Glacier, during its rapid retreat, *Journal of Geophysical Research*, *110*(F3), 3012+–, doi:10.1029/2005JF000292.

Sapiano, J., W. Harrison, and K. Echelmeyer (1998), Elevation, volume and terminus changes of nine glaciers in North America, *Journal of Glaciology*, *44*(146), 119–135.

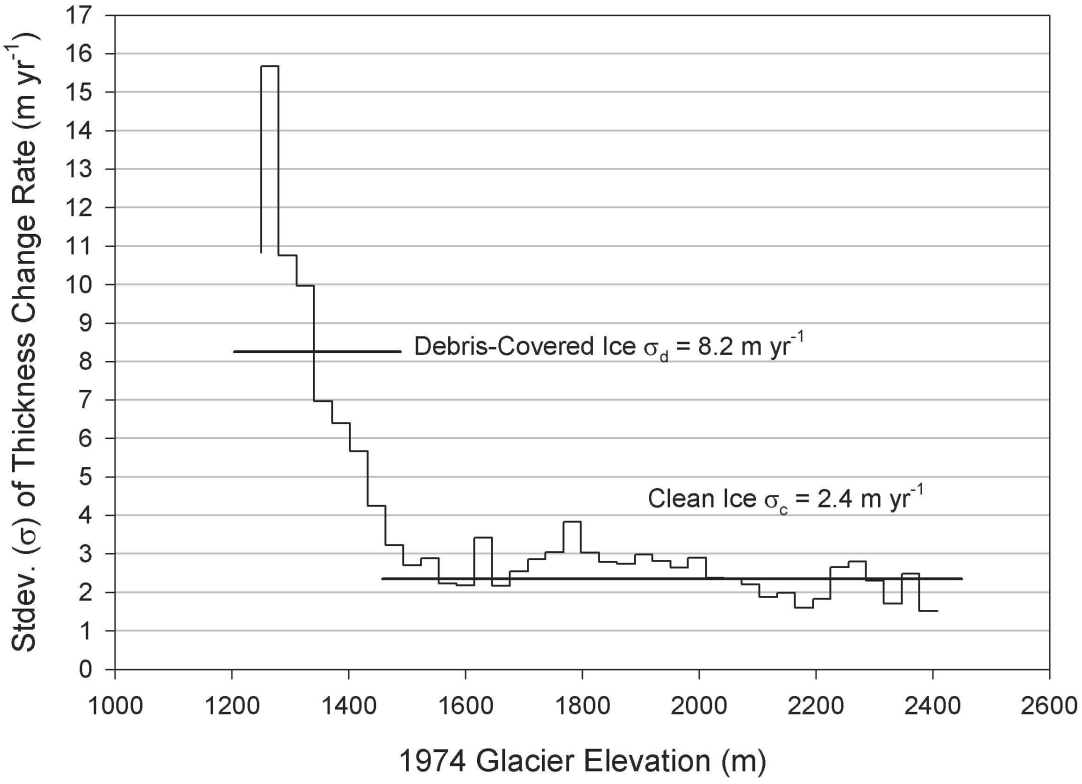

Figure B.1: Standard-deviation (σ) of geodetically-determined glacier thickness change rates (m/yr) on Gulkana Glacier between 1974-1993. σ-values are averaged by 30.48 m elevation bin defined by the 1974 surface. Average values of the debris-covered terminus area (1250-1500 m) and clean glacier ice (1500-2438 m) are shown as σ_d and and σ_c respectively.

Appendix C
Errors in Recent Period Altimetry Measurements

In the error analysis in Appendix A, errors in repeat altimetry measurements were dominated by errors in the elevation measurements. Here we investigate the role of snowcover on the glacier at the time of measurement and estimate its contribution to errors in glacier volume changes.

In general we try to conduct repeat surveys of glaciers during or near the same calendar date as an earlier survey because this is the best way to minimize errors due to snowcover and ice flow. In any given year, however, the total quantity and distribution of snowcover on the glacier will vary, especially for glaciers in maritime environments. This introduces an error in our assumption of a constant density profile near the glacier surface, which dictates that all measured changes in thickness occur due to gains or losses of glacier ice [*Bader*, 1954]. This error is probably small for our early period measurements, but becomes more significant over shorter time periods.

To determine the magnitude of this error we consider area-averaged changes in thickness and snow cover at two different times. We wish to determine the water equivalent average change in thickness ($\bar{b}$) from time 1 to time 2, which occurs as both a change in ice and snow thickness:

$$\bar{b} = \Delta h_i \frac{\rho_i}{\rho_w} + \Delta h_s \frac{\rho_s}{\rho_w} \tag{C.1}$$

where ρ is density and subscripts i, s and w refer to glacier ice, snow and water respectively. Recognizing that:

$$\Delta h_i = \Delta h_{meas} - \Delta h_s \tag{C.2}$$

we substitute into Equation 1 to obtain:

$$\bar{b} = \Delta h_{meas} \frac{\rho_i}{\rho_w} + \Delta h_s \left(\frac{\rho_s - \rho_i}{\rho_w} \right) \tag{C.3}$$

Our previous methods assumed the first term on the RHS in Equation C.3 accounted for all water equivalent thickness changes. We have shown here that the second term on the RHS

is a correction factor required to account for differences in snowcover between the two different years. We assume values of 0.4, 0.9 and 1 kg m^{-3} for ρ_s, ρ_i and ρ_w respectively. Now our error σ_b occurs due to errors in thickness change measurements Δh_{meas} and due to variability in snowcover Δh_s. We calculate Δh_{meas} as in previous publications, and use the standard deviation of winter balances (σ_{z_s}) at benchmark glaciers as estimates of variability in snow cover. We find σ_{z_s} = 0.75 m for continental glaciers (determined from Gulkana Glacier) and σ_{z_s} = 2.5 m for maritime glaciers (determined from Wolverine Glacier). We then add these errors as a quadrature sum, assuming they are random and uncorrelated, to arrive at the total error in average net balance.

Bibliography

Bader, H. (1954), Sorge's law of densification of snow on high polar glaciers, *Journal of Glaciology*, *2*(15), 319–322.